Defining adapter proteins that regulate Fc-epsilon-RI-mediated antigen uptake during IgE-mediated cross-presentation by dendritic cells

Thesis submitted in partial fulfillment of the requirements for the degree of
Master of Science in Engineering at the University of Applied Sciences
Technikum Wien - Degree Program Tissue Engineering and Regenerative Medicine

By: Cornelia Schultz
Student Number: 1210692008

Supervisor 1: Mag. Dr. Wolfgang Holnthoner
Supervisor 2: Edda Fiebiger, PhD

Boston, August 30, 2014

FACHHOCHSCHULE
TECHNIKUM WIEN

Declaration

„I confirm that this thesis is entirely my own work. All sources and quotations have been fully acknowledged in the appropriate places with adequate footnotes and citations. Quotations have been properly acknowledged and marked with appropriate punctuation. The works consulted are listed in the bibliography. This paper has not been submitted to another examination panel in the same or a similar form, and has not been published. I declare that the present paper is identical to the version uploaded."

Boston, August 30, 2014

Place, Date

Signature

Kurzfassung

Ein möglicher, positiver Zusammenhang zwischen erhöhten IgE-Werten und Krebsimmunüberwachung steht bereits seit Jahren zur Diskussion. Wie IgE Antikörper dazu beitragen könnten, ist jedoch nicht bekannt. Ein Hauptziel der Krebsimmuntherapie ist die Zahl der zytotoxischen T Lymphozyten zu erhöhen, deren Funktion die Zerstörung von Krebszellen ist. Neueste Ergebnisse des Gastlabors zeigen, dass der trimere (αγ2), hoch affine, in dendritischen Zellen exprimierte IgE Rezeptor (FcεRI), die Fähigkeit der Kreuzpräsentation besitzt. Vorausetzung dafür ist die Beladung des Rezeptors mit IgE Antikörpern. Dies führt zu einer Induktion von zytotoxischen T Zellen. Ziel dieser Masterarbeit war es, mögliche Mediatoren dieser IgE/FcεRI-vermittelten Kreuzpräsentation von Antigenen zu definieren. Die für IgE-vermittelte Kreuzpräsentation nötigen FcεRI-Signale und die Konsequenzen der Abwesenheit von caveolin, WASP und MyD88 wurden untersucht.

Mäuse, die den humanen FcεRI auf dendritischen Zellen (IgE_R-TG) exprimieren, wurden mit caveolin knockout (KO), WASP KO und MyD88 KO Mäusen gekreuzt. Dendritische Zellen wurden mittels CD11c microbeads aus der Milz isoliert und mit NP-specific IgE beladen. Die Expression des FcεRI und die IgE-Beladung wurden mittels Durchflusszytometrie analysiert. Dendritische Zellen wurden auf deren Fähigkeit getestet exogen aufgenommene Antigene für naive $CD8^+$ T Zellen zu präsentieren. Eine Proliferation von $CD8^+$ T Zellen wurde mittels Durchflusszytometrie detektiert. In den Überständen dieser Kulturen wurden IL-2 und granzyme B Spiegel gemessen, um auf die Proliferation beziehungsweise auf die Induktion von zytotoxischen T Zellen rückzuschliessen. Um Unterschiede in den Signalwegen des FcεRI (ERK, SHP-1, SHIP-1) in dendritische Zellen aus der Milz, oder Mastzellen aus dem Knochenmark zu erforschen, wurden Western Blots durchgeführt.

Es wurde entdeckt, dass bei Fehlen von caveolin die Antigenaufnahme minimal verringert ist, was jedoch keinen Einfluss auf die IgE-vermittelte Kreuzpräsentation hat. Eine gesteigerte Antigenaufnahme wurde bei Abwesenheit von WASP entdeckt. Diese hatte jedoch keine Auswirkung auf die Kreuzpräsentation. Interessanterweise wurde die IgE/FcεRI-vermittelte Kreuzpräsentation durch das Fehlen von MyD88 nicht beeinflusst. Ein bedeutender Unterschied in den FcεRI-Signalwegen wurde zwischen Mastzellen (tetramerer FcεRI) und dendritischen Zellen (trimerer FcεRI) gefunden. Die Aktivierung von ERK1/2 und SHIP-1 war in dendritischen Zellen deutlich geringer als in Mastzellen. Die Gesamtform und aktivierte Form von SHP-1 war in dendritischen Zellen erheblich höher.

Diese Masterarbeit untersucht mechanistische Anforderungen der IgE/FcεRI-vermittelten Kreuzpräsentation, um weitere Einblicke in die Regulation dieses Prozesses zu gewinnen. Dies ist von größter Bedeutung, um Therapien basierend auf dendritischen Zellen zur Krebsbekämpfung im Menschen zu verbessern.

Schlagwörter: hoch affiner IgE Rezeptor, Immunglobulin E, dendritische Zelle, Antigenaufnahme, Kreuzpräsentation

Abstract

Over the recent years, evidences accumulated that elevated IgE levels may have a beneficial effect in cancer immunosurveillance. The functions of IgE antibodies in anti-tumor immunity however are mainly unknown. A major goal of cell-based cancer immunotherapy is to enhance the priming of cytotoxic T lymphocytes (CTLs) to create long-lasting T cell responses that eradicate cancer cells. The host laboratory found that the trimeric (αγ2) high affinity IgE receptor (FcεRI) as expressed by human dendritic cells (DCs) is capable of performing IgE-mediated cross-presentation and subsequent induction of CTLs. The aim of this thesis was to define adapter proteins for IgE/FcεRI-mediated antigen cross-presentation by DCs. Consequences of the absence of caveolin, WASP and MyD88 were investigated and signalling requirements were examined.

For that reason, mice that exhibited a human FcεRI expression pattern on DCs (IgE_R-TG) were crossed with caveolin knockout (KO), WASP KO and MyD88 KO mice. Splenic DCs were isolated using CD11c magnetic microbeads and were loaded with NP-specific IgE. FcεRI expression and IgE-loading was detected by flow cytometric analysis. DCs were analysed in cross-presentation experiments for their ability to present exogenous antigens and to induce $CD8^+$ T cell proliferation. IL-2 and granzyme B levels were measured in DC/T cell co-culture supernatants by ELISA to determine the amount of T cell proliferation and induction of CTLs respectively. Western Blots were performed to detect differences in the signalling pathway down-stream of the FcεRI (ERK, SHP-1, SHIP-1) in splenic DCs and bone marrow-derived mast cells.

We found that caveolin-deficiency only minimally decreases IgE-mediated antigen sampling, and does not influence cross-presentation. WASP-deficiency increases IgE-mediated antigen uptake, but does not affect IgE-mediated cross-presentation. Furthermore, the IgE/FcεRI-mediated cross-presentation pathway remained active in the absence of MyD88 indicating that no additional danger signal is required for this type of cross-presentation. A pronounced difference in the signalling cascade down-stream of the trimeric and tetrameric FcεRI was found. While ERK1/2 and SHIP-1 phosphorylation were significantly decreased in DCs compared to mast cells, elevated levels of total and phosphorylated SHP-1 were detected.

In summary, this thesis addresses a substantial gap in our understanding of IgE-mediated cross-presentation by defining mechanistic requirements of this novel pathway. It is of outmost importance to gain further insight into the regulation of this pathway to improve DC-based therapies to combat cancer in humans.

Keywords: high affinity IgE receptor, Immunoglobulin E, dendritic cell, antigen uptake, cross-presentation

Acknowledgements

I would like to thank my two supervisors, Edda Fiebiger and Wolfgang Holnthoner, for their support and critical comments on my Master thesis.

Especially, I would like to thank Edda for giving me the possibility to be part of her research group and for her guidance during the last months.

A big thank-you to Barbara, whose door was always open and for sharing her theoretical and practical expertise.

My heartfelt thanks to my colleagues Barbara, Ben, Liz, Madeleine, Marion, Shaaji, and Will for the nice atmosphere in the lab and the fun lunch breaks.

I would like to acknowledge the Marshall Plan Foundation and the Industriellenvereinigung Kärnten for their generous financial support.

I would like to thank Eva for supporting me during the last years while working in her research group.

I would like to express my gratitude to my family for all their support. My special thanks to Christian for sharing this adventure with me and much more.

Table of Contents

1 INTRODUCTION

Immunoglobulin E (IgE) is well-known for its detrimental role in allergies and is part of immunological defence mechanisms against helminth infections [1]. An allergic response starts with the sensitization to a commonly harmless antigen (antigen that makes allergy = allergen) which leads to the production of allergen-specific IgE. Generally, antigens are defined as molecules that trigger antibody production. In the context of allergies, it is thought that dendritic cells (DCs), which sample exogenous antigens in peripheral tissues and present them to naive antigen-specific T cells, induce the priming of T helper 2 (Th2) cells. $CD4^+$ Th2 cells stimulate heavy-chain class switching of B cells from IgM to produce IgE antibodies. Upon differentiation into plasma cells antigen-specific IgE antibodies are secreted.

Although IgE levels are commonly increased in allergic individuals, it is important to stress that high amounts of IgE can also be found in healthy non-allergic individuals.

During the past years, there has been increasing evidence of a possible beneficial role of elevated IgE levels and cancer immunosurveillance, leading to the foundation of the field of AllergoOncology. This is in line with epidemiologic studies showing an inverse correlation between allergies and tumor incidences, such as glioma, childhood leukemia and colon and pancreatic cancer, brain cancers and ovarian cancer. [2] Additionally, the presence of tumor antigen-specific IgE antibodies in humans was described by several research groups. [3], [4] These findings strongly suggest tumor-protective properties of IgE. However, the mechanism how IgE antibodies influence tumor immunosurveillance is mainly unknown.

1.1 The IgE network

IgE antibodies in serum are relatively short-lived, but when bound to their Fc receptors such as the high affinity IgE receptor (FcεRI), IgE antibodies reveal an increased half-life. IgE and its receptors comprise a complex protein network that includes transmembrane and soluble IgE receptors, referred to as the IgE network. Basically, three IgE Fc receptors are expressed by human and rodent cells: FcεRI, CD23 which is known as FcεRII and galectin 3. There also exist various co-receptors that do not directly bind the IgE Fc portion. The FcεRI is a key regulator in allergy and its function is addressed in later chapters in more detail. CD23 is a low affinity IgE receptor that is expressed by DCs, B cells and epithelial cells. FcεRI and FcεRII are transmembrane receptors. Galectin 3 is a pentamere that can use other receptors as scaffold to bind to the cell surface. [5] Galectin 3 is another

low affinity IgE receptor and was formerly known as the epsilon binding protein (εBP). There also exist soluble receptor isoforms in the serum that are important regulators of IgE production. Soluble IgE receptors are capable of binding Fc-parts of IgE antibodies and thereby alter the ability of IgE to activate blood or tissue-resident immune cells. [6] The presence of a soluble form of the FcεRI (sFcεRI) was just recently described by the Fiebiger Laboratory. The IgE-binding α-chain circulates in the serum, binds IgE, forms soluble ligand-receptor-complexes and thereby, prevents further binding of IgE to surface Fc receptors. *In vitro* experiments showed that sFcεRI can be generated after IgE-mediated cross-linking of IgE-loaded effector cells. This data show that production of the sFcεRI isoform is coupled to cross-linking-induced receptor activation, resulting in a negative feedback mechanism, which potentially dampens IgE-mediated cell activation. However, detailed mechanistic insight into the generation and function of the sFcεRI is lacking to date. [7]

The soluble isoform of CD23 (sCD23) is a single chain glycoprotein and was described as a positive regulator of IgE-mediated immune responses due to support in B cell differentiation towards plasma cells. The transmembrane receptor isoform on the other hand is known to hamper IgE production via a negative feedback mechanism. [6]

Galectin 3 is found in a large variety of tissues and is expressed by multiple different cell populations. Galectin 3 is capable of cross-linking cell-bound IgE antibodies or initially cross-linking the FcεRI by itself. Furthermore, it plays a crucial role in inflammatory immune responses, but its function in allergic diseases is rather poorly defined. [6]

Extensive research is currently done to reveal insight into the regulation of the IgE network and to identify new participants in its regulation that will allow the generation of novel IgE-target therapies for the treatment of allergic diseases. The recombinant production of sFcεRI would be one of these new treatment options. Capturing IgE antibodies in the serum of severely allergic patients is a well-established therapy. Omalizumab, an anti-IgE specific monoclonal antibody is successfully applied in the clinics. However, this drug may trigger severe adverse events, which could be avoided by using sFcεRI. [6], [8]

1.2 The high affinity IgE receptor

The high affinity Immunoglobulin E receptor, FcεRI, is expressed in two different isoforms on human cells. It is known to assemble as a heterotetrameric complex on mast cells and basophils, consisting of one α-chain (IgE-binding protein), one β-chain and a γ-chain dimer (αβγ2). In contrast to mast cells and basophils, DCs, neutrophils, eosinophils, macrophages, epithelial cells and platelets express the heterotrimeric isoform αγ2. [5], [9], [10] Notably, rodents also express the tetrameric isoform of the FcεRI on basophils and mast cells, but they do not constitutively express the trimeric complex. [10], [11]

1.2.1 Structure of the high affinity IgE receptor

Irrespective of the receptor isoform, the α-chain is responsible for ligand binding and coating the cell surface with IgE antibodies because it contains the extracellular IgE-binding site. One single IgE antibody is bound by two extracellular immunoglobulin-related domains of the α-chain. The α-chain requires N-glycosylation on seven sites for proper folding and to facilitate IgE-binding. Interestingly, the short cytosolic tail of the protein does not have known signalling functions. Signal transduction is conducted by the β- and γ-chains. [12]

An IgE molecule consists of two identical heavy and light chains. The heavy ε-chain comprises four constant domains, in contrast to the architecture of other antibody classes, which only hold three constant domains. This additional domain facilitates substantial conformational flexibility of the IgE molecules and allows them to bind to their ligand, the high affinity IgE receptor. [13] It was described that IgE-binding stabilizes the FcεRI on the cell surface. This is in line with data showing that allergic patients display upregulated FcεRI expression, which is found to be even more pronounced in the trimeric isoform. [14]

The β- and γ-subunits comprise an immunoreceptor tyrosine-based activation motif (ITAM) on the carboxyl (C) terminus of their cytoplasmic tails. The β-chain is a membrane-tetraspanning protein that amplifies ITAM signals for the γ-chain and acts as a regulator of FcεRI surface expression. [15] The disulphide-linked γ-chain dimer is mainly responsible for signal transduction. The ITAM sequences of the β- and the γ-chain can be distinguished by their structure. While the ITAM sequence of the γ-chain contains two tyrosine residues, the ITAM of the β-chain comprises a third tyrosine. The ITAM motif is a conserved sequence of usually two tyrosine residues separated by 6-8 amino acids. Tyrosine residues within ITAM motifs represent phosphorylation targets for receptor-associated Src-family tyrosine kinases. [12] Various different other receptors use ITAM motifs for signal transduction, among them the T cell receptor (TCR), B cell receptor (BCR) and other Fc receptors.

The schematic structure of both the timeric (αγ2) and the tetrameric isoform (αβγ2) of the FcεRI is depicted in Fig.1.

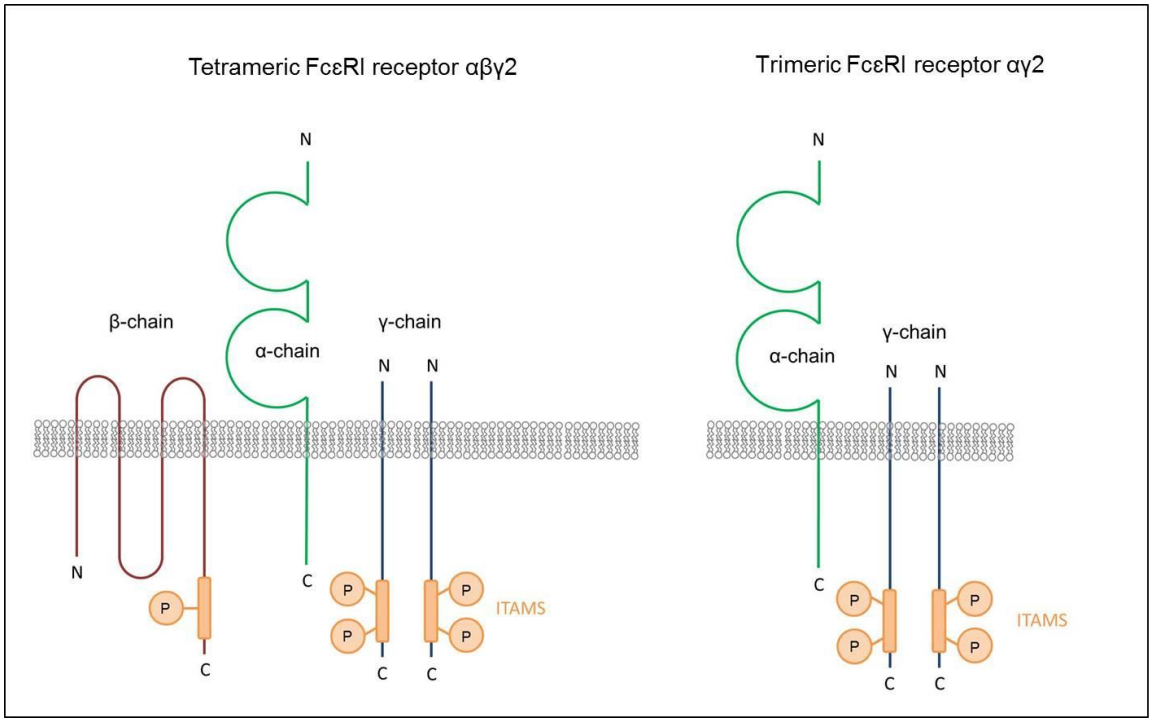

Fig.1: Schematic structure of the tetrameric (αβγ2) and trimeric (αγ2) high affinity IgE receptor.
The fully glycosylated α-chain binds IgE antibodies to the cell surface. The γ-chain dimer comprises four phosphorylation sites on its cytoplasmic tail to facilitate signal transduction. The β-chain of the tetrameric receptor works as a signal amplifier for the γ-chain.

A truncated isoform of the β-chain was discovered by Donnadieu and colleagues as a consequence of alternative splicing. It was described as a negative regulator of the FcεRI surface expression since it prevents maturation of the α-subunit. [16]. Another splice-variant of the β-chain was only recently discovered in human mast cells, which promotes cell degranulation and is important for microtubule formation. [17]

The β- and γ-chains of the FcεRI are additionally used for the assembly of various other Fc receptors. The γ-chain is also called the common Fc receptor γ-chain and associates with the high (FcγRI) and low affinity IgG receptor (FcγRIII) and the IgA Fc receptor (FcαRI). The β-chain can be also part of the FcγRIII. [10]

FcεRI complexes are assembled in the endoplasmic reticulum (ER), which act as a quality control organelle for the formation of multimeric receptors. The production of the α-chain is induced by IL-4 secretion in humans. Retention signals expressed by the cytosolic tail of the α-chain prevent the export of immature subunits form the ER and results in degradation. [18] Only after the non-covalent association of β- and/or γ-chains, the α-chains get N-glycosylated at seven sites. This process facilitates the correct folding of the α-chain and allows the transport of the completely assembled FcεRI complexes to the Golgi apparatus and from there further to the cell surface. It was described that the human

γ-chain alone is able to mask the retention signals on the α-chain and that this might be an explanation why humans, but not rodents, express the heterotrimeric isoform. [12], [19]

1.2.2 Tetrameric FcεRI receptor

The function of the tetrameric FcεRI is well-known. Starting with sensitization to a given allergen and during allergy, IgE antibodies are produced. A part of those antibodies are bound via the FcεRI expressed by effector cells of allergy, such as mast cells or basophils. The antigen-specific cross-linking of IgE-loaded effector cells represents a key event in the pathology of type I allergy. The engagement of FcεRI/IgE complexes triggers the signalling cascade down-stream of the receptor and is responsible for the immediate-type allergic reaction. This causes the release of pre-formed granules including chemical mediators, among them histamine, leukotrienes, prostaglandins and cytokines, resulting in clinical hypersensitivity reactions, such as increased mucus production, bronchoconstriction and increased vascular permeability, or even life-threatening circulatory collapse that occurs in systemic anaphylaxis. The production of chemokines and cytokines during the late-phase allergic reaction upon ongoing antigenic stimulation recruits leukocytes and induces inflammation. [10] A scheme of mast cell degranulation is shown in Fig.2.

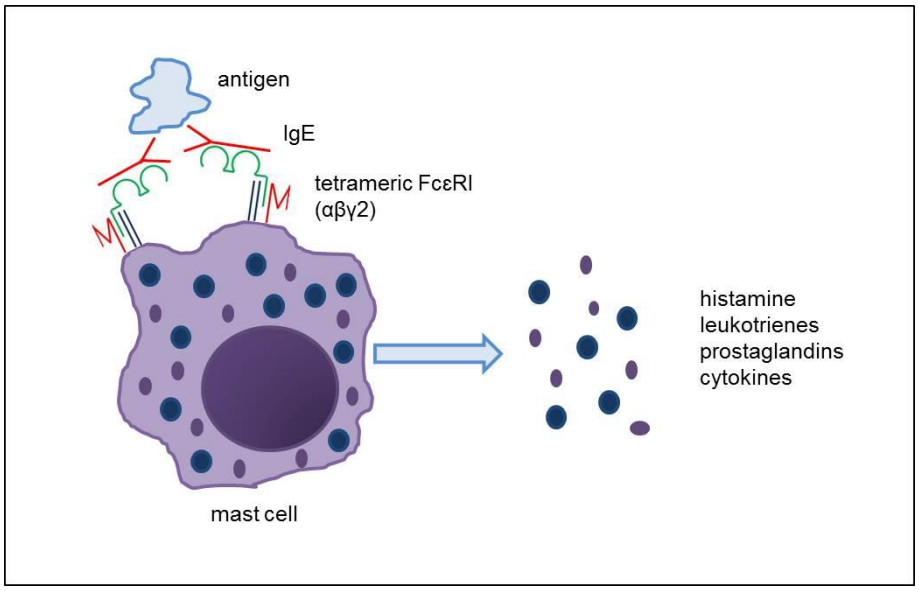

Fig.2: Mast cell degranulation upon FcεRI engagement during an allergic reaction.
IgE antibodies are bound to the α-subunit of the tetrameric FcεRI expressed by mast cells. Antigen-binding facilitates receptor cross-linking, which triggers the intracellular signalling cascade and leads to release of inflammatory mediators.

1.2.3 Trimeric FcεRI receptor

In comparison to the well-defined function of the tetrameric FcεRI complex, the mechanistic insight in biology and function of the trimeric isoform remains mainly unclear to date. The reason behind that is that no cell or animal model for mimicking the human FcεRI expression profile of DCs existed until recently.

Maurer et al. revealed that the trimeric FcεRI/IgE complex on human peripheral blood DCs functions as an antigen sensing and uptake receptor for major histocompatibility complex (MHC) class II-mediated antigen presentation. It was shown that already minor amounts of antigens can be detected and can induce T cell proliferation in the presence of IgE. [11]

The establishment of a transgenic mouse model that mimics human FcεRI expression patterns [20], [21], allows now to elucidate the function and biology of the FcεRI trimer expressed by DCs in more detail.

1.2.4 Signalling down-stream of the high affinity IgE receptor

The signalling pathway triggered by antigen cross-linking of the tetrameric FcεRI/IgE complexes in mast cells and basophils, is well-defined. However, due to the high complexity of this activation pathway, only simplified models exist. The functions of various participants in this signalling cascade, that facilitate FcεRI-mediated degranulation, still remain unclear.

To trigger the FcεRI-mediated signalling cascade, IgE antibodies are bound to the extracellular domains of the α-subunit and get cross-linked upon antigen binding. This causes phosphorylation of the ITAM motifs of the β- and γ-chain by mainly two Src-family kinases, namely Lyn and Fyn. These two kinases activate basically two different pathways, described as the classical and the complementary pathway, initiated by Lyn and Fyn respectively. Both pathways are depicted and shown as a simplified scheme in Fig.3. [12]

In the classical pathway, IgE-mediated cross-linking of the tetrameric FcεRI induces ITAM phosphorylation by Lyn, which initiates spleen tyrosine kinase (Syk) recruitment to the γ-chain. Association with the γ-subunit is mediated by the Src homology domain 2 (SH2) domains of Syk, causing a conformational change in SH2 and subsequent activation of Syk. Syk initiates further tyrosine phosphorylation of down-stream signalling molecules, such as linker for activation of T cells (LAT) and phosphoinositide 3-kinase (PI3K). PI3K causes the formation phosphatidylinositol-3,4,5-trisphosphate (PIP_3), which recruits Bruton´s tyrosine kinase (BTK) to the membrane. LAT phosphorylation recruits various

other mediators to form a complex needed together with BTK for activation of phospholipase Cγ (PLCγ). This complex includes growth-factor-receptor-bound protein 2-related adapter protein (GADS), growth-factor-receptor-bound protein 2 (GRB2), son-of-sevenless homologue (SOS), PLCγ and SH2-domain-containing leukocyte protein of 76k Da (SLP76). Inositol-1,4,5-triphosphate (IP_3) and diacylglycerol (DAG) are generated by hydrolysis of PIP_3 by PLCγ. These two molecules work as second messengers that mobilize Ca^{2+} from the ER and activate protein kinase C (PKC), respectively, which results in mast cell degranulation.

In the complementary pathway, Fyn and Syk activate PI3K via a signalling complex. Activation of PI3K and generation of PIP_3 initiates membrane recruitment of 3-phosphoinositide-dependent protein kinase 1 (PDK1). PDK1 in turn activates PKCδ resulting in degranulation. PDK1 is also known to catalyse the activation of AKT, which then stimulates various other signalling molecules involved in protein synthesis, cell survival, proliferation, cytokine production and metabolism.

Both pathways activate Ras via GRB2 and SOS phosphorylation, which results in signal transduction via the mitogen-activated protein kinase (MAPK)/extracellular signal-regulated kinases (ERK) pathway. Activation of this cascade leads to production of various transcription factors which are involved in cytokine production. Furthermore, the MAPK/ERK pathway induces the release of phospholipase A_2 (PLA_2). PLA_2 causes the production of arachidonic acid that leads to the biosynthesis of eicosanoids. Those signalling molecules are capable of inducing inflammation and vasodilation. [12], [22], [23]

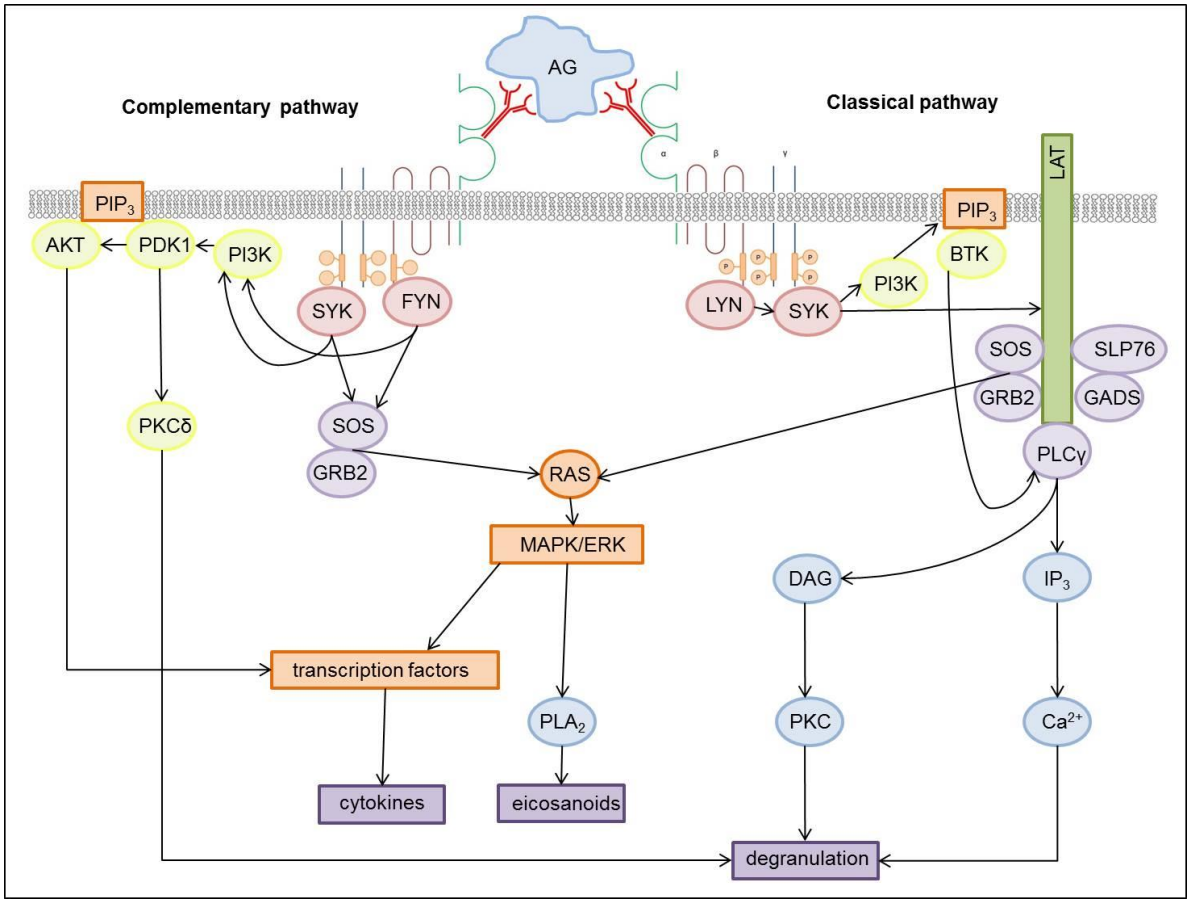

Fig.3: Simplified scheme of the signalling cascade down-stream of the tetrameric high affinity IgE receptor.
Antigens (AG) cross-link receptor-bound IgE antibodies triggering the intracellular signalling cascade. **Classical pathway:** Lyn phosphorylates ITAMs (immunoreceptor tyrosine-based activation motif) and activates Syk (spleen tyrosine kinase). PI3K (phosphoinositide 3-kinase) and LAT (linker for activation of T cells) get activated by Syk. PI3K facilitates the formation of PIP_3 (phosphatidylinositol-3,4,5-trisphosphate), which recruits BTK (Bruton´s tyrosine kinase) to the membrane. LAT recruits many other signalling molecules, among them SOS (son-of-sevenless homologue), GRB2 (growth-factor-receptor-bound protein 2), GADS (growth-factor-receptor-bound protein 2-related adapter protein) and SLP76 (SH2-domain-containing leukocyte protein of 76k Da), to form a complex. BTK is required together with the signalling complex to activate PLCγ (phospholipase Cγ). The production of IP_3 and DAG (diacylglycerol) is catalysed by the hydrolysis of PIP_3 by PLCγ, which induces the release of Ca^{2+} and PKC (protein kinase C), respectively. The release of both mediators results terminates in mast cell degranulation. **Complementary pathway:** ITAM phosphorylation is accomplished by Fyn, which activates Syk. Both mediators activate PI3K, which in turn initiates the synthesis of PIP_3 that lead to membrane recruitment of PDK1. PDK1 activates the AKT pathway and PKCδ. While PKCδ directly promotes degranulation, activation of the AKT pathway leads to cytokine generation. Both pathways stimulate the MAPK/ERK (mitogen-activated protein kinase/extracellular signal-regulated kinases) pathway via activation of SOS and GRB2. This leads to enhanced cytokine production and the release of eicosanoids produced by PLA_2 (phospholipase A_2).

How and whether the signalling cascade of trimeric FcεRI differs from the tetrameric isoform is not known, but has to be anticipated because of the lack of the β-chain and therefore the absence of one ITAM. Furthermore, it has to be noted that DCs do not express LAT [24], a major signal adapter, which must substantially change the classical pathway of activation.

The β-subunit of the FcεRI acts as an amplifier for the γ-chain and results in increased Syk phosphorylation and pronounced Ca^{2+} release. [15] As mentioned beforehand, the β-chain comprises a third phosphorylation site in its ITAM motif. Recently, it was described that this additional phosphorylation site is responsible for the activation of Src homology region 2 domain-containing inositol-5-phosphatase (SHIP). SHIP is a lipid phosphatase that is able to degrade PIP_3 molecules. It was suggested that this might work as a negative feedback mechanism capable of dampening mast cell activation. [25] The Src homology region 2 domain-containing phosphatase 1 (SHP-1) is an important regulator of intracellular signalling events in hematopoietic cells. Recently, it was reported by Nakata et al. that SHP-1 regulates signalling down-stream of the FcεRI negatively and positively in mast cells. The authors hypothesized that SHP-1 dephosphorylates SLP-76 and LAT, which results in negative regulation of the MAPK/ERK pathway. The positive regulation of SHP-1 was found in increased phosphorylation of PLCγ, Ca^{2+} mobilization and degranulation. [26]

1.3 Dendritic cells

DCs are known to be the most potent antigen-presenting cells (APCs) of the human body and possess unique immune regulatory capacity. Additionally, B cells and macrophages are also capable of using the endocytic pathway to present antigenic peptides on their cell surface, however with less efficiency and dependent on the cellular activation status. DCs represent an essential part of the innate immune system and originate from the myeloid progenitor cell in the bone marrow. Immature DCs migrate from the bone marrow to the peripheral blood and tissues were they encounter various different antigens. DCs are highly phagocytic and monitor their antigenic environment, such as mucosal surfaces and the skin, when they are immature. Maturation is induced upon antigen uptake via receptor-mediated endocytosis, phagocytosis or macropinocytosis, which results in generation of highly effective APCs. Engulfed antigens are degraded intracellular and are presented to antigen-specific T lymphocytes in draining lymph nodes to induce an efficient adaptive immune response. However, activation of T cells can only take place upon antigen presentation and expression of co-stimulatory molecules by the APC simultaneously. The expression of co-stimulatory molecules CD80 and CD86, also described as B7.1 and B7.2 respectively, is induced by the activation of the Toll signalling pathway via various Toll-like receptors (TLR). Lipopolysaccharide (LPS) from the cell membrane of gram negative bacteria, nucleic acids derived from viruses or papain found in baculovirus, plants, protozoa, mammals, eubacteria and yeast trigger the activation of this pathway, which leads to subsequent activation of the down-stream transcription factors. Nuclear factor kappa-light-chain-enhancer of activated B cells (NF-κB) is one the most important transcription factors and is responsible for production of cytokines, co-stimulatory molecules and chemokines. DCs upregulate the expression of MHC class II molecules

upon activation and secrete cytokines such as IL-12, IL-16, tumor necrosis factor-α (TNF-α) and CC-chemokine ligand 2 (CCL-2).

1.3.1 Antigen presentation pathways for exogenous antigens: default pathway and cross-presentation

DCs take up exogenous antigens via phagocytosis, macropinocytosis and receptor-mediated endocytosis. [27]

Fig.4 shows two distinct pathways of how DCs can present exogenous antigens and the corresponding T cell responses. Exogenous antigens are engulfed and shuttled into the MHC class II presentation pathway, which is considered the default pathway. Peptides in the MHC class II groove are recognized by the TCR of antigen-specific naïve $CD4^+$ T cells. The CD4 co-receptor of T cells binds to the MHC class II molecule. The co-stimulatory molecule CD28, expressed by T cells, binds to CD80 or CD86, expressed by DCs.

The type of T cells response is mainly dependent on the different pathogens that activate distinct signalling pathways. Immune responses that are typically involved in the killing of intracellular parasites or the perpetuation of autoimmune reactions facilitate the priming of Th1 cells which release IFN-γ, IL-2 and TNF-α to combat pathogens and to attract other immune cells. During allergic reactions and helminth infections, Th2 type responses are induced. Inflammatory Th2 type responses are typified by the secretion of IL-4, IL-5, IL-10 and IL-13 and switch of B cells to plasma cells, which generate antibodies including IgE. Th17 cells are found during extracellular bacterial and fungal infections. IL-17A, IL-17F and IL-22 are produced. T regulatory cells (T regs) can be induced by the presence of TGF-β and are responsible to maintain tolerance against self-antigens. [28] Activated T cells produce IL-2 in an autocrine manner which facilitates proliferation.

Interestingly, exogenous antigens can also be presented via MHC class I molecules to naïve $CD8^+$ T cells. This mechanism is known as cross-presentation and is also depicted in Fig.4. [29]

1.4 Cross-presentation

A major goal of cancer immunotherapy is to enhance the priming of naïve $CD8^+$ effector T cells, also known as cytotoxic T lymphocytes (CTL). CTL are capable of attacking and eradicating target cells with their lytic complex. Priming of CTL is facilitated by a process known as cross-presentation accomplished by DCs. (Platzer et al., unpublished data) There is increasing interest to use DCs as cell-based tumor vaccines to combat cancer via

induction of CTL, which was recently reviewed by Andersen et al. [30] Several ongoing clinical trials currently use DCs as therapeutic tools in cancer immunotherapy. [31], [32]

It is of significant importance to investigate underlying mechanisms of cross-presentation to improve existing therapies and to generate new DC-based vaccination strategies to create long-lasting T cells responses which result in eradicating cancer. [27]

Antigen cross-presentation by DCs results in the induction of $CD8^+$ effector T cells, so-called CTLs, which was described as cross-priming. Cross-priming is thought to occur in the presence of inflammatory conditions or in the context of danger signals. [33] Cross-presentation is facilitated by all APCs in general, however with less efficiency compared to DCs. Importantly only DCs are capable of priming CTL *in vivo*. [34]

This activation pathway requires binding of the CD8 co-receptor to the MHC class I molecule and the TCR to the MHC class I restricted peptide. Furthermore, the co-stimulatory signal from interaction of CD28 with CD80 or CD86 is necessary for the induction of CTL. These cells store various mediators in their granule, such as granzyme B, perforin, TNF-α and IFN-γ. The release of this lytic complex can induce the activation of the caspase cascade and can lead to apoptosis of the target cell.

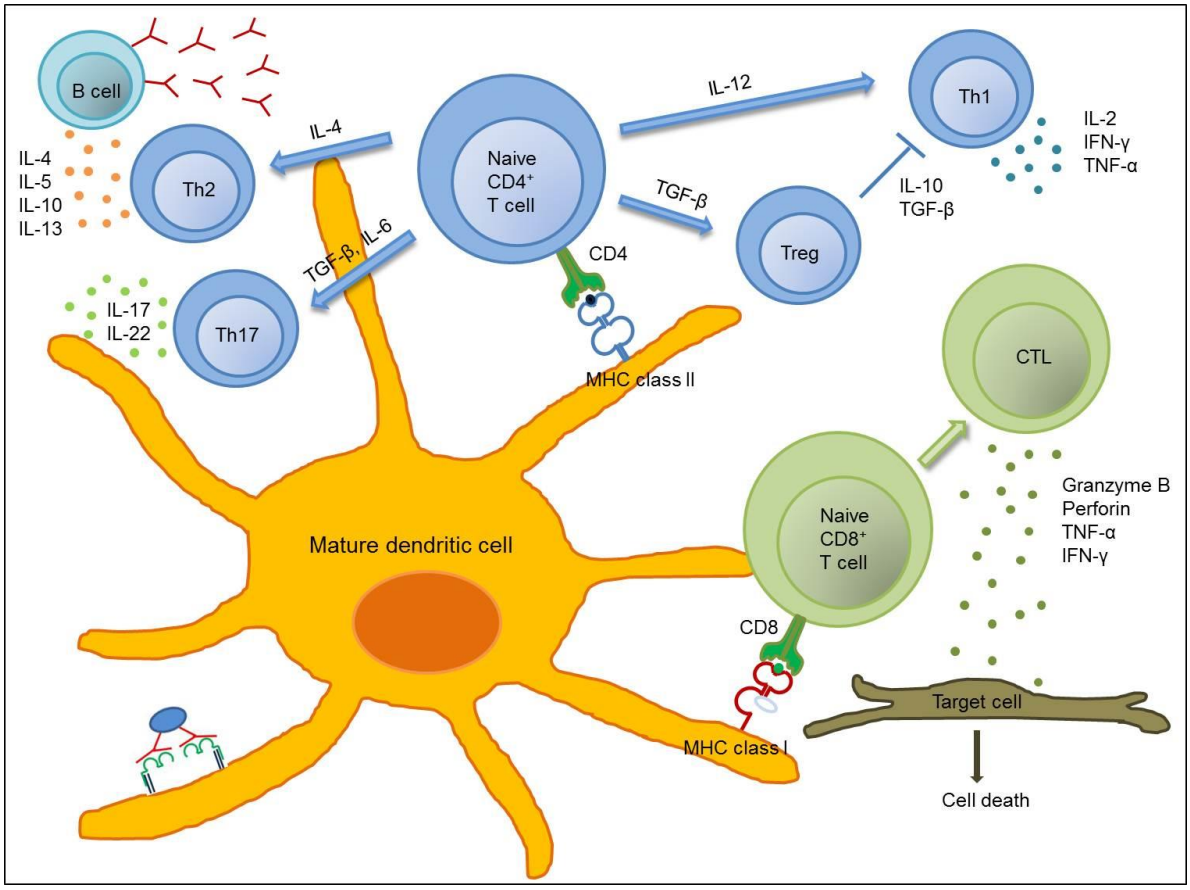

Fig.4: Schematic overview of T cell responses upon dendritic cell activation.
Antigens are engulfed by DCs via macropinocytosis, phagocytosis or receptor-mediated antigen uptake and are presented via MHC class II molecules, described as the default pathway. Different classes of pathogens activate distinct signalling pathways. This results in variable T cell responses. Th2 cells are produced during allergic reactions and to combat helminths. Priming of Th1 cells is induced by intracellular bacteria and viruses. Th17 cells secrete IL-17 and IL-22 to combat extracellular bacteria and fungi. Regulatory T cells (Treg) are induced by the release of TGF-β and play an essential role in maintaining self-tolerance by inhibiting Th1 responses. The cargo presentation of MHC class I molecules to $CD8^+$ T cells is called cross-presentation and leads consequently to cross-priming of cytotoxic T lymphocytes (CTL).

The absence of DC maturation can also result in cross-tolerance during cross-presentation, which is an important process to eliminate self-reactive CTLs. However during cancer immunotherapy it is of highest importance to avoid cross-tolerance. [35], [36]

A distinction is made between cross-presentation of soluble antigens and immune complexes. The latter mechanism is a well-described phenomenon that requires binding of IgG to specific epitopes on soluble antigens. Those complexes associate with Fcγ receptors which promote antigen internalization and shuttling into cross-presentation pathway. [36]

1.4.1 DC subsets and cross-presentation

Human and murine DCs are heterogeneous cell population. Each specific cell subset possesses dedicated features in terms of antigen presentation and initiating T cells responses. Both human and murine DCs can be divided into two major populations, plasmacytoid DCs (pDCs) and conventional or classical DCs. A schematic overview of the human and murine DC subsets is depicted in Fig.5. Murine pDCs were described to be poor APCs and are therefore negligible in terms of cross-presentation. Conventional mouse DCs can be further divided into migratory DCs and lymphoid organ resident DCs. The latter population is found in spleen, lymph nodes and thymus and consists of two subsets: $CD8\alpha^{-}CD11b^{+}$ and $CD8\alpha^{+}CD11b^{-}$ cells. Migratory DCs are separated into $CD103^{+}CD11b^{-}$ and $CD103^{-}CD11b^{+}$ cells. The former subset was described as the most efficient cross-presenting cell type within the migratory DC population. Langerhans cells resident in the skin represent another subset of migratory DCs, however with less relevance in cross-presentation. A third type of DCs that differentiates from monocytes during infections, is known as inflammatory DCs. [34–37]

Recently, the human functional equivalent to the murine $CD8\alpha^{+}$ population was found, namely the blood DC antigen 1 ($BDCA3^{+}$) also known as $CD141^{+}$ subset. These cell types are described to be the most efficient cross-presenters. The human $CD1c^{+}$ DC population is comparable to the murine $CD8\alpha^{-}$ subset, which is able to cross-present ICs via FcγR-mediated AG uptake. Lately, it was reviewed by Segura et al. that all human DC subsets are capable of performing cross-presentation however with distinct efficiency dependent on the antigen modulation and the receptor used for uptake. [34–37]

Interestingly, it was only recently found by Platzer et al. that the human $CD1c^{+}$ and the murine $CD8\alpha^{-}$ subset express the highest levels of the FcεRI. Furthermore, it was determined that the murine $CD8\alpha^{-}$ population is superior in FcεRI/IgE-mediated cross-presentation of soluble antigen and cross-priming of CTL compared to the $CD8\alpha^{+}$ subset. (Platzer et al., unpublished data)

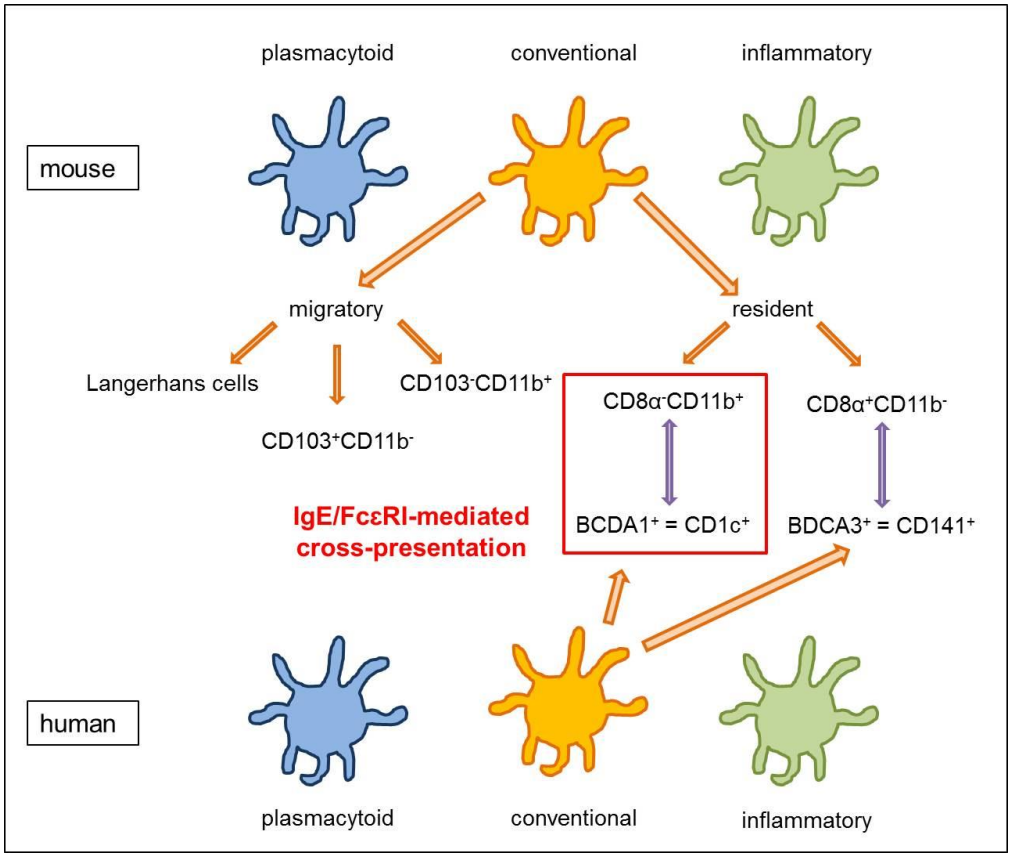

Fig.5: Schematic overview of human and murine dendritic cell subsets.

1.4.2 Cross-presentation requirements

In general, cross-presentation is dependent on the executing DC subset, the antigen formulation, the type of engulfment, the signal transduction and the intracellular trafficking route. [27]

It was just recently discovered by the Fiebiger Laboratory that the IgE/FcεRI complex takes up soluble exogenous antigens and shuttles them efficiently into the cross-presentation pathway. (Platzer et al, unpublished data) Other receptors that are capable of performing cross-presentation are C-type lectin receptors (e.g. mannose receptor, DEC-205 and Clec9a) and other Fc receptors. The mannose receptor is described to preferably shuttle soluble antigens into the cross-presentation pathway. Engulfed antigens traffic into early endosomes where they are loaded onto recycled MHC class I molecules. [34] However, it was found that the required antigen amount for efficient cross-presentation is substantially decreased for IgE/FcεRI-mediated uptake compared to uptake via the mannose-receptor. (Platzer et al, unpublished data)

1.4.3 Internalization of the high affinity IgE receptor

There are two major endocytic pathways described for receptor internalization, namely the clathrin- and the lipid raft-dependent endocytosis. A lot more research has been done on the clathrin-mediated endocytic pathway. [38]

Both pathways require tyrosine-based internalization signals on the cytosolic tail of the β- and the γ-subunit that are recognized by cytoplasmic adapter molecules. Upon receiving internalization signals, the receptor-associated adapter complex recruits clathrin to the cell membrane. This leads to the formation of endocytic vesicles consisting of clathrin as its major component, so-called clathrin-coated vesicles (CCV). Adapter protein complex 2 (AP-2) was described as the major actor of the receptor-associated adapter complex. [39] However, various other adapter molecules exist, that are all thought to recognize specific internalization signals. [40]

Receptor internalization via lipid raft-mediated endocytosis leads to co-localization with lipid raft components, such as flotillins, GM1 gangliosides and caveolin-1. Therefore, this pathway is also known as caveolin-mediated endocytosis. Furthermore, it was described to be dependent on the presence of cholesterol. Caveolin is recruited to the cell membrane and forms caveosomes with the assistance of dynamin. Dynamin is required for both described endocytic pathways. It is a GTPase that facilitates membrane invagination and the vesicle release from the cell membrane. Furthermore, Dynamin communicates with the cytoskeleton to allow actin rearrangement required for receptor internalization. [38]

Caveosomes and CCVs merge with early endosomes, so-called sorting tubular endosomes. The fate of the internalized cargo is determined herein dependent on the signal they carry and their way of internalization. Recently, it was described that ubiquitation may play a key role in receptor uptake and defining the fate of internalized cargo. [39] The cargo either passes along the endosomal-lysosomal system machinery, which terminates in lysosomal degradation, or it gets introduced into recycling endosomes, which transport the cargo back to the cell membrane.

It was described that the cross-linked FcεRI gets mainly internalized by clathrin-mediated endocytosis. [41] However, it was recently shown by Fattakhova et al. that FcεRI internalization still remains intact in the absence of clathrin and AP-2. [38] This provides evidence that there exists another pathway that drives FcεRI uptake. And indeed various contradictory publications exist, that suggest receptor internalization via lipid-raft mediated endocytosis. [42], [43] Additionally, experiments in the host laboratory found that cross-linked FcεRI can be found in caveolin-positive endosomes using live cell microscopy.

Furthermore, siRNA-mediated knockdown of caveolin in a cell line inhibited FcεRI internalization. (Platzer et al., unpublished data) However, it still remains unclear, if the presence of caveolin is essential for shuttling antigen through IgE/FcεRI complexes into the cross-presentation pathway.

1.4.4 FcεRI-mediated antigen uptake and intracellular trafficking

Using live cell imaging microscopy, the host laboratory showed that the cross-linked FcεRI gets internalized within 5 min and can be found in early endosomes after 10 min. After 45 min the presence of the FcεRI dramatically dropped in early endosomes and completely disappeared after 90 min. The vesicle fusion with early endosomes is regulated by the Rab5, an important GTP-binding protein. Twenty minutes after receptor cross-linking, the FcεRI started to traffic into late endosomes, which were detected using an anti-Rab7 antibody. The endocytic pathway terminates with the cargo degradation in lysosomes. The majority of the FcεRI was found in lysosomes 45 min after receptor cross-linking, which were located using an antibody against the lysosomal membrane protein-1 (LAMP-1). (Platzer et al., unpublished data)

MHC class I and II molecules do not only distinguish themselves in their structure, but also in the source of peptide they display and in the way they are loaded. MHC class I molecules are expressed by all nucleated cells. It consists of a large glycoprotein chain that is anchored in the cell membrane (α-chain) and a short non-covalently bound chain (β_2-microglobulin). The α-chain includes three domains, $\alpha_{1\text{-}3}$. The peptide-binding cleft is formed by the α_1- and α_2-domain. MHC class II molecules are mainly expressed by APCs, including B cells, macrophages and DCs. Those molecules comprise two non-covalently associated transmembrane polypeptide chains, the α- and β-chain. Both hold two domains, known as α_1 and α_2, and β_1 and β_2. The peptide-binding groove is formed by the α_1- and the β_1-subunit.

MHC class I molecules are loaded with peptides from the cytosol and present their cargo to naïve $CD8^+$ T cells. The peptides can either be modified self- or foreign proteins to detect infected DCs, or if the DC is not infected itself, it can also present exogenously derived antigens. MHC class II molecules on the other hand, carry peptides derived from intracellular vesicles, which are recognized by naïve $CD4^+$ T cells.

The processing of newly synthesized MHC class II molecules occurs in the ER. To prevent binding of premature peptides, the binding groove is occupied by a specific protein known as invariant chain or CD74. This protein directs MHC class II molecules to endolysosomal compartments where it gets partly degraded by proteases. The remaining fragment, still

sitting in the cleft, is known as class II-associated invariant chain peptide (CLIP). HLA-DM is an intracellular protein that leads to disassociation of CLIP upon binding to MHC class II molecules. Finally, they are loaded with internalized and degraded antigens and are transported to the cell surface to get displayed.

Partly folded MHC class I α-subunits arrive in the ER and associate with the chaperone protein calnexin. The β_2-microglobulin assembles with this complex and calnexin is released. The heterodimer of transporters associated with antigen processing-1 and -2 (TAP1 and TAP2) proteins bind to the MHC class I molecules via tapasin, a TAP-associated protein. Furthermore, protein disulphide isomerase 3 (ERp57) and calreticulin assemble to this complex. Proteins are degraded in the cytosol by a large catalytic protease, the proteasome. Peptides are then transported via TAP into the ER, where they are loaded onto MHC class I molecules with the assistance of the peptide-loading complex (PLC). ER-aminopepidases 1/2 (ERAP1/2) enable further peptide degradation. Peptide loading initiates proper folding and facilitates transportation of the MHC molecule to the Golgi apparatus and consequently to the cell surface. [27]

There are two pathways described that enable cross-presentation in DCs, the vacuolar and the cytosolic pathway. Upon antigen uptake endocytic and phagocytic vesicles fuse with early endosomes in the first place. The acidic pH activates proteases that chop engulfed proteins into small peptides, which can be directly applied to recycled MHC class I molecules in the phagosome. This process is known as the vacuolar pathway.

The cytosolic pathway differentiates between cargo loading in phagosomes or in the ER, which both are dependent on the presence of TAP and the proteasome. Peptides that require further degradation before they can be loaded onto MHC class I molecules in phagosomes, are exported into the cytoplasm, where they undergo proteasomal degradation. Those peptides are then either transported back via TAP into phagosomes or they enter the ER via TAP. Both locations facilitate MHC class I loading and subsequent surface expression to be recognized by naïve $CD8^+$ T cells. [27], [34]

It was recently described that efficient cross-presentation requires slow antigen trafficking and prolonged retention in early endosomes. [44] The low acidic pH prevents rapid antigenic degradation as it is the case in lysosomes. This might be a reason why macrophages are thought to be poor cross-presenters. Antigenic proteins engulfed by macrophages undergo fast endolysosomal degradation which terminates in lysosomal compartments after 20 to 30 min. On the other hand antigen trafficking in DCs was found to be more slowly. [34] This is in line with unpublished data already described beforehand, that reveal FcεRI presence 45 min after cross-linking in lysosomal compartments. (Platzer et al., unpublished data) Antigens that are transported to late endocytic compartments

favour loading onto MHC class II molecules compared to proteins in early endocytic compartments are preferably displayed by MHC class I complexes. [34]

Several different GTP-binding proteins, such as Rab3, Rab14 and Rab27a were associated with cross-presentation compartments. Jancic et al. showed that cross-presentation was impaired in Rab27a-deficient DCs, due to enhanced phagosomal acidification. [34], [45], [46] Furthermore, it was determined that not only newly synthesized MHC class II but also MHC class I molecules are guided by CD74 to endosomal compartments and that this itinerary is preferably used for cross-presentation. [34]

Extensive research was recently done to gain insight into the regulation of cross-presentation and to identify compartments that are associated with cross-presentation. However, how decisions are made to determine the fate of engulfed antigens and which signals are required are largely unknown.

1.4.5 Signalling pathways involved in cross-presentation

Receptors that facilitate cross-presentation are thought to be dependent on the presence of danger signals and the activation of myeloid differentiation primary response gene 88 (MyD88). [47] MyD88 is an important signalling molecule down-stream of TLRs. Its major assignment is the activation of the NF-κB pathway. TLRs are expressed by almost all cells, including DCs. TLR-4 is activated upon binding of LPS complexed with LPS-binding protein (LBP), which causes the activation of the adapter molecule MyD88 by binding with its cytosolic TIR domain. MyD88 associates with serine/threonine innate immunity kinase (SIIK) known as IRAK and results in signal transfer to TRAF6. TRAF6 in turn forwards the signal via Iκκ, which phosphorylates IκB resulting in its degradation. The transcription factor NF-κB is secured in the cytoplasm until IκB is degraded. NF-κB is then released and migrates into the nucleus to activate gene transcription. MyD88-deficient mice are more prone to bacterial infections, as there is no induction of cytokine production via the activation of NF-κB that could combat an ongoing infection.

WASP is a major player of actin rearrangement in the cytoskeleton and was described to be important during cell adhesion, intracellular signal transmission, migration, polarization and vesicular trafficking. Furthermore, it plays a critical role during endocytosis, due to the fact that endocytic vesicle formation requires actin rearrangement. [48] Pivniouk et al. showed that WASP plays an important role during signalling down-stream of the tetrameric FcεRI complex using bone marrow-derived mast cells from WASP-deficient mice. [49] The Wiskott-Aldrich syndrome is a rare, X-linked recessive illness. Absence or defect in the WAS gene, that encodes for the Wiskott-Aldrich syndrome protein (WASP), can lead to

immunodeficiency, bleeding disorder, eczema, autoimmunity including an inflammatory bowel disease (IBD)-like disease, in affected patients. WASP is an intracellular signalling molecule and is primarily expressed in all cells of the hematopoietic system. WASP-deficient mice can be used as a model of human immunodeficiency. They sensitize themselves spontaneously against luminal antigens and, if on the 129 background, develop severe colitis after 4 to 6 months of age. [50] WASP knockout mice are used as a model of IBD. In humans about 5 to 10% of the WASP-deficient patients develop IBD. [51] Using the WASP-deficient mouse strain it was detected that WASP is crucial for T cell development and the function of T regs. [52], [53] Furthermore, it was detected that these cells are impaired in cytoskeletal changes, degranulation ability and cytokine production. [49]

1.5 Aims of this thesis

The research questions are based on an unpublished finding of the Fiebiger Laboratory that IgE-mediated antigen uptake allows for cross-presentation. The overall aim of this thesis was to define requirements for IgE/FcεRI-mediated antigen cross-presentation by DCs.

The first aim was to investigate how the trimeric FcεRI internalizes and shuttles antigen for IgE-mediated cross-presentation, with specific focus on the influences of caveolin and WASP. Preliminary data were already collected demonstrating that the trimeric FcεRI uses the caveolin-mediated endocytosis for receptor internalization. (Platzer et al., unpublished data) Furthermore, it was described that WASP plays a significant role during internalization of the tetrameric FcεRI. [49]

Question 1: Is caveolin-mediated endocytosis necessary for FcεRI-dependent antigen uptake and does this pathway functionally affect IgE-mediated cross-presentation?

Question 2: Are there effects of WASP-deficiency on antigen uptake and cross-presentation?

The second aim was to define cellular activation requirements for DCs. It is known that all other receptors that are capable of performing cross-presentation are MyD88-dependent.

Question 3: Is MyD88 required for cross-presentation as a co-stimulatory signal?

The third aim was to investigate signalling requirements down-stream of the trimeric FcεRI in comparison to the tetrameric complex.

Question 4: Are down-stream FcεRI-signals dependent on the receptor isoform?

It is of outmost importance to investigate which endocytic pathways and cellular activation signals the trimeric FcεRI requires for internalization, activation and signal transduction, to understand how IgE/FcεRI-mediated cross-presentation is regulated in the context of allergy and cancer immunotherapy.

2 Methods and Materials

2.1 Cell lines

The NP-specific IgE secreting cell line Jw 8/5/13 (clone JW8/1) was provided by Dr. D. Maurer from the Medical University of Vienna, Austria. It is a mouse myeloma cell line that grows in suspension. The cells were cultured with RPMI 1640 medium containing 10% FBS, 2 mM glutamine, 100 U/ml penicillin and 100 µg/ml streptomycin. The cell culture supernatant was harvested and concentrated using Amicon centrifugal filter units with a cut-off of 100 kDa.

B16 GM-CSF is a murine melanoma cell line that secretes granulocyte-macrophage colony stimulating factor (GM-CSF). The cell line was provided by Dr. S. Turley from the Dana-Farber Cancer Institute in Boston, MA. Cells were cultured with DMEM medium containing 10% FBS, 2 mM glutamine, 100 U/ml penicillin and 100 µg/ml streptomycin.

2.2 Reagents

To load cells that express the human FcεRI with IgE antibodies, the monomeric hapten-specific chimeric human IgE anti-4-hydroxy-3-nitrophenylacetyl (NP-IgE) was used. It was derived from Jw 8/5/13 cells (clone JW8/1) as recently described. (Singleton, 2009, Dehlink, 2011) The chimeric IgE contains the immunoglobulin heavy chain of human IgE and the variable region genes of a mouse hybridoma. The Fab fragment recognizes 4-hydroxy-3-iodo-5-nitrophenylacetic acid (NIP) and 4-hydroxy-3-nitrophenylacetic acid (NP). While chimeric IgE can be used to load cells expressing the human FcεRI, it is not able to bind to the murine FcεRI.

To cross-link surface-bound NP-specific IgE, Ovalbumin (OVA) haptenized with 4-hydroxy-3-nitrophenylacetyl (NP-OVA) was used.

OVA peptide (OVAp) was used as positive control in antigen presentation experiments. OVAp does not need to be processed by DCs, but can immediately be loaded onto MHC

molecules. The MHC class I-restricted peptide epitope of OVA is also known as SIINFEKL and contains amino acids 257 to 264. The OVAp specific for MHC class II molecules comprises amino acids 323 to 339.

2.3 Mouse strains

All animals were housed under specific pathogen free (SPF) conditions at Boston Children´s Hospital (Boston, MA). Prior to each experiment, mice were genotyped. Age-matched wild-type (WT) mice that had been co-housed after weaning were used in addition to littermates. Several different transgenic mouse strains were used.

CD11c-αTG mice were provided by Dr. D. Maurer from the Medical University of Vienna (Vienna, Austria). This mouse strain is available on C57BL/6N or BALB/c background. Transgenic mice express the human FcεRI α-chain regulated by the DC-specific CD11c promoter. This results in a functional, chimeric FcεRI consisting of a human α-chain and murine γ-chain. Transgenic mice phenocopy the FcεRI expression and IgE-binding pattern of human DCs which are depicted in Fig.6. The human FcεRI α-chain is coupled to an IRES-eGFP reporter gene. Therefore CD11c-αTG mice possess GFP^+ DCs. Mast cells and basophils express the murine FcεRI.

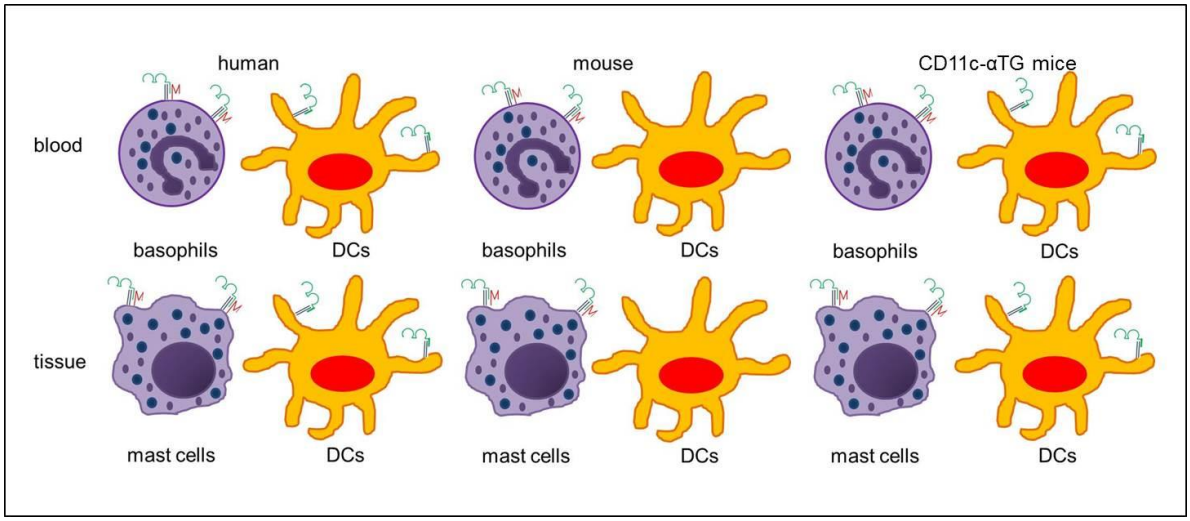

Fig.6: FcεRI expression profile of human and murine cells and CD11c-αTG mice.
While the tetrameric FcεRI is expressed by both human and mouse mast cells and basophils, the trimeric isoform of the FcεRI is only expressed by human dendritic cells (DCs). CD11c-αTG mice are humanized for the FcεRI expression on DCs.

Mu-α knockout (KO) and HP-αTG mice were received from Dr. J.P. Kinet from the Laboratory of Allergy and Immunology at the Beth Israel Deaconess Medical Center (Boston, MA, USA) and are on C57BL/6J background. Animals that are mu-αKO

completely lack the murine FcεRI α-chain on all cells. HP-αTG mice express the human FcεRI α-chain controlled by the human α-chain promoter. This results in expression of the human FcεRI α-chain by DCs, mast cells and basophils. The mu-αKO strain was crossed with CD11c-αTG mice resulting in another mouse strain named DC-αTG. These mice express the humanized FcεRI on DCs, but lack FcεRI expression on mast cells and basophils. DCs isolated from CD11c-αTG and DC-αTG mice are both referred to IgE_R-TG throughout this thesis, as they reveal identical FcεRI expression patterns. Table 1 gives an overview of the FcεRI expression patterns of the described mouse strains.

Mouse strain	Dendritic cells Trimeric FcεRI		Mast cells Tetrameric FcεRI		Basophils Tetrameric FcεRI	
	Human α-chain	Murine α-chain	Human α-chain	Murine α-chain	Human α-chain	Murine α-chain
CD11c-αTG (IgE_R-TG)	+	-	-	+	-	+
Mu-αKO	-	-	-	-	-	-
DC-αTG (IgE_R-TG)	+	-	-	-	-	-
HP-αTG	-*)	-	+	-	+	-

Table 1: Overview of FcεRI expression patterns of used mouse strains.
*) only in plasmacytoid DCs

OT-I and OT-II TCR transgenic mice and caveolin KO mice were purchased from the Jackson Laboratory. $CD8^+$ T cells of OT-I TCR transgenic mice specifically express a TCR that recognizes OVA peptide (aa 257-264) presented by MHC class I molecules. OT-I mice have a C57BL/6 background and are immune-deficient. The transgenic TCR of OT-II mice was designed to recognize OVA peptide (aa 323-339). Those mice show a 4-fold increase of naïve $CD4^+$ T cells in the periphery compared to $CD8^+$ T cells. The latter two mouse strains should not be used after 6 months of age, because there is evidence that the transgene gets lost over time. Caveolin KO mice have a 129 and C57BL/6 background. Hyperproliferative and vascular abnormalities may occur in these mice. Therefore it is advisable to replace breeding pairs after 6 months. The MyD88 KO strain, which has a C57BL/6J background, was provided by the Blumberg Laboratory from the Brigham and Women´s Hospital (Boston, MA, USA). This mouse strain has hematopoietic system defects and is more susceptible to bacterial and viral infections. WASP KO strain on the 129 background is a genetic model of IBD and was provided by the Snapper Laboratory from the Boston Children`s Hospital (Boston, MA, USA). These animals sensitize themselves spontaneously to food allergens and develop spontaneous colitis when they are 4 to 6 months old. Furthermore, WASP deficient mice show elevated serum IgE levels and symptoms of IBD [50].

CD11c-αTG mice were cross-bred with caveolin KO, MyD88 KO and WASP KO mice.

All experiments and procedures were performed according to protocols approved by the Boston Children´s Hospital or the Brigham and Women´s Hospital Institutional Animal Care and Use Committees.

2.3.1 Mouse genotyping by PCR

Twenty-one days after birth the litter was separated from the mother and ear tags and tail clips were taken for genotyping by PCR. The tissue was digested for at least 1 h at 55°C in digestion buffer containing 1 mg/ml proteinase K (ear tags: 20 µl digestion mix, tail clips: 40 µl digestion mix). Next DNase-free water was added (ear tags: 480 µl, tail clips: 960 µl) and the tubes were incubated for 10 min at 92°C. The samples were stored at 4°C until genotyping PCR was performed.

The Master mixes for the different mouse strain were prepared as depicted in Table 2 (volumes are indicated per reaction in µl).

	IgE_R-TG	Mu-αKO	HP-αTG	OT-I	
				Tcra	Tcrb
5x Phire Buffer	4	4	4	4	4
dNTPs 2 mM	2	2	2	2	2
ultrapure H_2O	8.3	11.2	11.7	10.75	10.75
Primer #1	0.5	0.5	0.5	0.5	0.5
Primer #2	0.5	0.5	0.5	0.5	0.5
Primer #3 (optional)	0.5	0.5		0.5	0.5
Primer #4 (optional)	0.5			0.5	0.5
Phire Polymerase	0.3	0.3	0.3	0.25	0.25
Total	19	19	19	19	19

	OT-II	Caveolin KO	MyD88 KO	WASP KO
5x Phire Buffer	5			4
dNTPs 2 mM	5	4	4	2
ultrapure H_2O	7.5	2	2	10.2
Primer #1	0.5	11.2	11.2	0.5
Primer #2	0.5	0.5	0.5	0.5
Primer #3 (optional)		0.5	0.5	0.5
Primer #4 (optional)		0.5	0.5	
Phire Polymerase	0.5	0.3	0.3	0.3
Total	19	19	19	18

Table 2: Overview of the Master mixes used for genotyping of different mouse strains.

Nineteen µl of the Master mix and 1 µl of the DNA was added per PCR tube. With exception of genotyping for WASP KO mice, where 18 µl of the Master mix and 2 µl of the DNA was used. For the different mouse strains distinct genotyping protocols were used. The applied settings on a Bio-Rad C1000 Touch Thermal Cycler are shown in Table 3.

IgE_R-TG		mu_α-KO		HP-αTG	
Temp in °C	Time (30 cycles)	Temp in °C	Time (35 cycles)	Temp in °C	Time (35 cycles)
98	5 min	98	5 min	98	5 min
98	10 sec	98	10 sec	98	10 sec
60	30 sec	60	30 sec	55	1 min
72	25 sec	72	25 sec	72	30 sec
72	1 min	72	1 min	72	1 min
12	hold	12	hold	12	hold
OT-I					
Tcra		Tcrb			
Temp in °C	Time (35 cycles)	Temp in °C	Time (35 cycles)		
98	5 min	98	5 min		
98	10 sec	98	10 sec		
62	1 min	62	1 min		
72	30 sec	72	30 sec		
72	1 min	72	1 min		
12	hold	12	hold		
OT-II		Caveolin KO			
Temp in °C	Time (35 cycles)	Temp in °C	Time (35 cycles)		
98	5 min	94	3 min		
98	10 sec	94	30 sec		
62	1 min	65	1 min		
72	30 sec	72	1 min		
72	1 min	72	2 min		
12	hold	10	hold		
MyD88 KO		WASP KO			
Temp in °C	Time (35 cycles)	Temp in °C	Time (35 cycles)		
98	5 min	94	30 sec		
98	10 sec	94	30 sec		
62	1 min	57	30 sec		
72	30 sec	72	90 sec		
72	1 min	12	hold		
12	hold				

Table 3: Overview of the distinct genotyping protocols used on the Bio-Rad C1000 Touch Thermal Cycler.

A 2% agarose gel (2.4 g agarose, 120 ml 1x TAE buffer) was prepared containing 800 ng/ml Ethidium bromide for all mouse strains except for MyD88 KO. For the latter strain a 3% agarose gel was used to distinguish bands that were in close proximity to each other.

Three µl loading dye was added to all samples and 10 µl were loaded onto the gel. Slots at both edges of the gel were used to apply the DNA standard ladder (3 µl per well). The DNA was separated for approximately 70 min at 100 Volt and analysed on a Bio-Rad Image Lab™.

2.4 Isolation of splenic dendritic cells

Mice were sacrificed with CO_2 and spleens were harvested and transferred into cold RPMI 1640 medium (containing 10% FBS, 2 mM glutamine, 100 U/ml penicillin and 100 µg/ml streptomycin, referred to as complete RPMI medium) in a 6-well suspension culture plate on ice. Next, the spleens were transferred under the hood to a new 6-well suspension culture plate containing 1 ml digestion medium (complete RPMI medium containing 1 mg/ml collagenase D or collagenase type VIII) per well. Using a 5 ml syringe and a 25G 5/8 needle 4 ml pre-warmed digestion medium were injected into the spleen to flush the cells out until the spleen became pale. Thereafter, the spleen was cut with sterile scissors and forceps into very small pieces and incubated for 25 min at 37°C. The whole material was gently passed through a 70 µm cell strainer into a 50 ml tube using a plunger to remove all remaining fat and connective tissue. The well and the cell strainer were washed with 10 ml complete RPMI medium to harvest all cells. Next, the cells were centrifuged for 4 min at 1400 rpm at 8°C and the supernatant was aspirated. Then, red blood cell (RBC) lysis was performed. Splenocytes were resuspended thoroughly with 2 ml 1x RBC lysis buffer using a 1 ml pipette tip and incubated for 5 min on ice. 10 ml cold MACS buffer were added to stop the lysis reaction and cells were spun again for 4 min at 1400 rpm. The cell pellet was first resuspended with 1 ml MACS buffer and filled up to 20 ml MACS buffer before it was filtered through a 70 µm cell strainer into a 50 ml tube. Cells were centrifuged and DCs were isolated using CD11c microbeads following the manufacturer´s protocol (Miltenyi Biotec) which is based on magnetic cell separation (MACS) technology, or using OptiPrep™ density gradient medium.

2.4.1 Magnetic cell separation technology using CD11c microbeads

The magnetic cell separation technology for isolation of DCs is based on positive selection. The whole procedure was performed with ice-cold MACS buffer and all incubation and centrifugation steps were performed at 4°C. This prevented unspecific binding of the microbeads to the cells.

First, cells were counted using the Casy counter and the cell pellet was resuspended with 400 µl MACS buffer per 10^8 total cells. Ten µl Fc Block and 80 µl CD11c microbeads were

added per 10^8 total cells and incubated for 15 min. Then, the cells were washed with 1 ml MACS buffer per 10^7 cells and centrifuged at 250 g for 6 min. The cell pellet was resuspended with 500 µl MACS buffer per 10^8 total cells. Depending on the total cell number the appropriate MACS separation column (MS for up to $2x10^8$, LS for up to $2x10^9$ total cells) was placed into the MACS separator and was washed once with 500 µl MACS buffer to equilibrate the beads. Next, the cell suspension was loaded onto the column followed by 3 washing cycles with 500 µl MACS buffer. The $CD11c^+$ cell population is retained in the column. The column was removed from the MACS separator and placed onto a new 15 ml tube containing 1 ml FBS and 3 ml complete RPMI medium. One ml MACS buffer was added to the column and the magnetically labelled cells, which were $CD11c^+$, were flushed out using the provided plunger.

2.4.2 OptiPrep™ density gradient medium

The cell pellet was resuspended with 3.5 ml solution A (2.5 ml DMEM + 1 ml OptiPrep™) and transferred to a 15 ml tube. Solution B (3.6 ml DC buffer + 1 ml OptiPrep™) was added very gently on top avoiding mixing of those two solutions. At last 2 ml of DMEM was added carefully thereon. The tube was centrifuged using a swing-out rotor for 20 min at 850 g at room temperature (RT) with the brake switched off. DCs were found in the phase between solution B and the DMEM medium. Cells were collected using a 1 ml pipette tip and were washed once with a high volume of DMEM to remove the density gradient medium.

The cells gained from both DCs isolation methods were centrifuged at 350 g for 4 min at 8°C and the pellet was resuspended with RPMI medium depending on the size of the obtained cell pellet. A 6-well suspension culture plate was prepared with 2.5 ml RPMI medium per well. The cell suspension was equally divided between the wells.

2.5 *In vivo* expansion of dendritic cells

B16 GM-CSF tumor cells were grown to a confluency of 50 to 70% to retain the cells in logarithmic phase of proliferation. The cells were detached and harvested from the plate using 0.05% trypsin and were washed twice with ice-cold PBS. The cells were counted and diluted with ice-cold PBS to a concentration of $2x10^7$ cells per ml. The cells were kept on ice until they were injected to avoid cell aggregates.

Mice were anesthetized using an isoflurane machine and were injected subcutaneously with 100 µl cell suspension (= $2x10^6$ cells) into their neck. As soon as the mouse stopped moving and the breathing deepened, a small portion of skin on the back was pinched up

and a 27G needle was inserted superficially to inject the tumor cells. The treated mice were checked daily after injection for tumor growth. Seven to 10 days after tumor cell injection the mice were sacrificed, spleens were harvested and DCs were isolated using CD11c microbeads or the OptiPrep^{TM} density gradient medium or a combination of both techniques.

2.6 Cross-presentation assay and MHC class II antigen presentation experiment

A cross-presentation assay is performed to study the loading efficiency of exogenously derived antigens onto MHC class I molecules and the induction of T cell proliferation. A MHC class II antigen presentation experiment is done to investigate the default pathway of antigen presentation.

On the first day of the experiment DCs were isolated from the murine spleen using magnetically-labelled CD11c microbeads and loaded with NP-specific IgE overnight. On the following day, DCs were incubated with the antigen (NP-OVA), a positive control (OVAp) or a negative control (no AG) and were co-cultured with carboxyfluorescein diacetate succinimidyl ester (CFSE)-labelled $CD4^+$ OT-II or $CD8^+$ OT-I T cells for MHC class II or cross-presentation assay respectively. After approximately 24 h of incubation 100 µl supernatant was harvested to determine IL-2 levels. Two days thereafter, 100 µl supernatant were taken to analyse granzyme B production by CTL in a cross-presentation assay. In a MHC class II antigen presentation assay the production of IL-13 and IFN-γ was determined. Furthermore, flow cytometric analysis was done to determine the amount of proliferated $CD4^+$ (MHC class II) or $CD8^+$ T cells (cross-presentation). The timeline of an antigen presentation experiment is depicted in Fig.7A. Fig.7B gives a schematic overview of an IgE/FcεRI-mediated MHC class II and cross-presentation experiment.

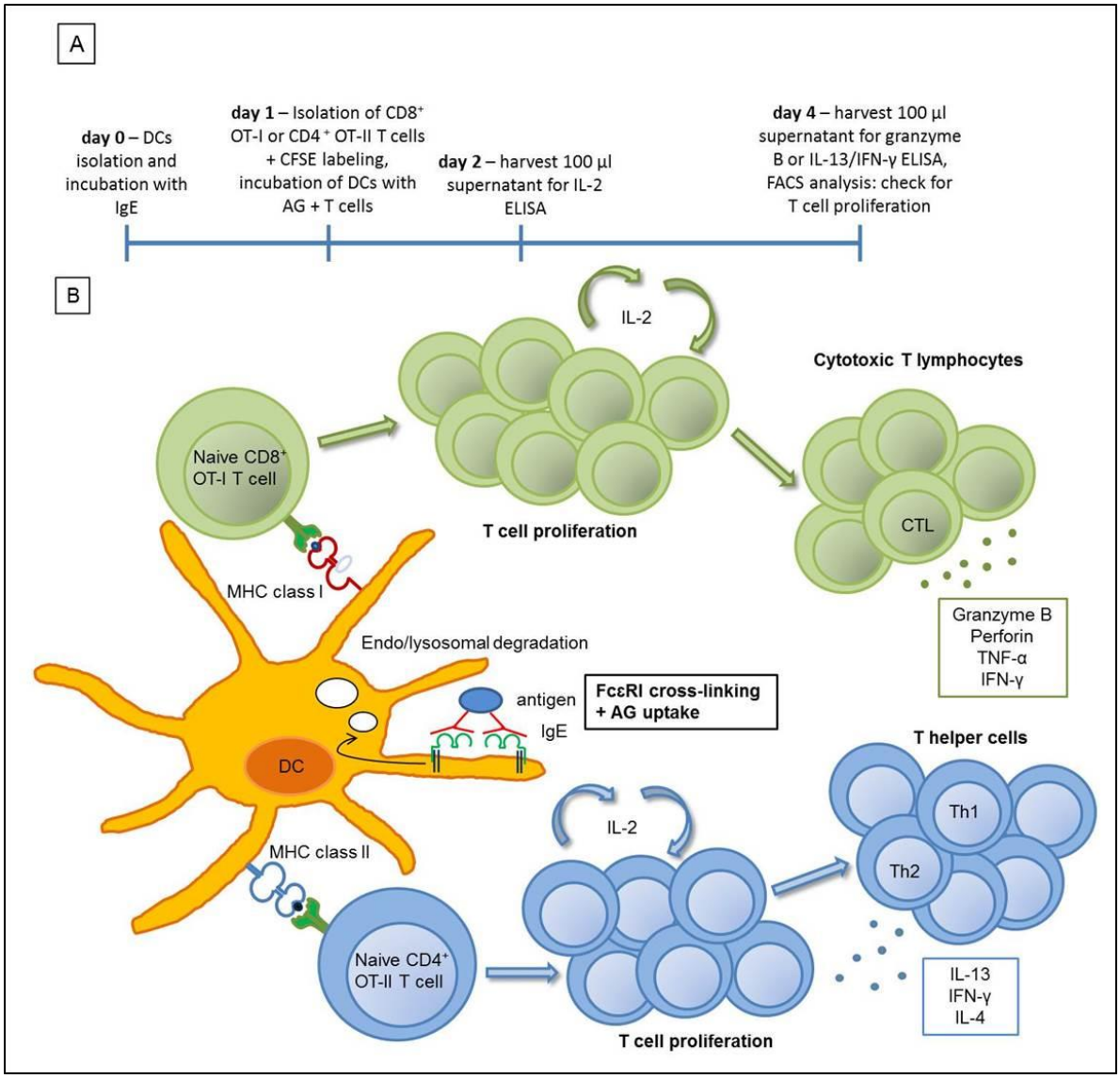

Fig.7: IgE/FcεRI-mediated MHC class II and cross-presentation assay.
(A) Timeline of an antigen presentation assay. **(B)** Schematic overview of an antigen presentation experiment: mouse DCs expressing the humanized IgE_R are sensitized with NP-specific IgE overnight. Incubation with NP-OVA leads to cross-linking of the receptor and subsequent uptake of the antigen. The internalized antigen shuttles into endo/lysosomal compartments and is loaded onto MHC class I or MHC class II molecules. The TCR of $CD8^+$ OT-I or $CD4^+$ OT-II T cells specifically recognizes the presented peptide and proliferates upon antigen binding. Proliferating T cells secrete IL-2 in an autocrine manner. $CD8^+$ effector T cells (cytotoxic T lymphocytes) store granzyme B in their lytic complex, which can be detected after 3 days in the supernatant of the co-culture. $CD4^+$ effector T cells (T helper cells) produce IL-13, IFN-γ and IL-4.

Day 0: Isolation of splenic DCs and incubation with or without NP-IgE

DCs were isolated from the spleen as already previously described.

Day 1: Isolation of $CD8^+$ OT-I and $CD4^+$ OT-II T cells and CFSE-labelling

The protocol for $CD8^+$ and $CD4^+$ T cell isolation is similar to DCs isolation but for omission of the collagenase treatment. The splenocytes were flushed out of the spleen and cut into very small pieces. The whole material was immediately passed through a 70 µm cell strainer using a plunger. Cells were centrifuged for 4 min at 1400 rpm at 8°C and the supernatant was aspirated. Splenocytes were then incubated with 2 ml 1x RBC lysis buffer for 5 min on ice. Ten ml MACS buffer was added to stop the lysis reaction and cells were spun again. The cell pellet was resuspended in 20 ml MACS buffer and filtered through a 70 µm cell strainer into a 50 ml tube. Next, the cells were counted on the Casy counter followed by the MACS protocol for the isolation of $CD8^+$ or $CD4^+$ T cells, which is based on negative depletion.

Cells were spun and resuspended with 40 µl MACS buffer per 10^7 total cells. Ten µl biotin antibody cocktail was added for 10^7 total cells and incubated for 10 min at 4°C. Next, 30 µl MACS buffer and 20 µl anti biotin microbeads were added per 10^7 total cells and incubated for 15 min at 4°C. One ml MACS buffer per 10^7 total cells was added and cells were centrifuged and resuspended in 2 ml MACS buffer. A LS MACS separation column was washed once with 3 ml MACS buffer for equilibration. The cell suspension was added and the flow-through, containing the $CD8^+$ or $CD4^+$ T cell fraction, was collected using a 15 ml tube. The column was washed for 3 times with 3 ml MACS buffer. The cells were spun and the protocol for CFSE-labelling of T cells followed.

A 5 mM CFSE stock was prepared by adding 18 µl cell culture-grade DMSO to 1 vial of 50 µg CFSE. The cell pellet was resuspended in serum-free RPMI and cells were counted. $CD8^+$ T cells were diluted to a concentration of $1x10^6$ cells per ml in serum-free RPMI. One µl of 5 mM CFSE solution was added to 1 ml of cell suspension (final concentration of CFSE was 5 µM) to the side of the tube and was quickly inverted to mix. The cells were incubated for 8 min at RT. The tube was filled with ice-cold complete RPMI medium and cells were spun and washed 2 additional times with ice-cold complete RPMI. Finally, T cells were resuspended in pre-warmed complete RPMI and diluted to a concentration of $1x10^6$ cells per ml in RPMI (100 µl = $1x10^5$ cells).

Day 1: Incubation of DCs with antigen and $CD8^+$ OT-I or $CD4^+$ OT-II T cells

DCs were harvested from the 6-well suspension culture plate and the well was washed once with 1 ml cold MACS buffer to collect all cells. The tube was spun for 5 min at 1400 rpm at 8°C, the supernatant was aspirated and the cell pellet was resuspended with 1 ml cold RPMI. The cell number was determined and cells were diluted to a concentration of 8-$5x10^5$ cells per ml (100 µl = 8-$5x10^4$ cells) depending on the total number of DCs available. DCs were incubated with NP-OVA at 37°C in different concentrations for distinct time

points in appropriate tubes, referred to as antigen pulse. For some experiments, the antigen was present continuously, which mimics the antigen exposure over a longer time period. As negative control DCs were incubated without antigen and for positive control OVAp was used. For the cross-presentation and MHC class II antigen presentation assay OVAp 257-264 and 323-339 was used, respectively. DCs were added to 96-well round bottom plate in triplicates and were incubated together with the antigen and $1x10^5$ CFSE-labelled $CD8^+$ OT-I or $CD4^+$ OT-II T cells per well for 72 h at 37°C.

Day 2: Harvest supernatant for IL-2 ELISA

After approximately 24 h of incubation, 100 µl supernatant per well was transferred using a multichannel pipette to a new 96-well round bottom plate and stored at -80°C to determine IL-2 levels by ELISA. 100 µl fresh RPMI medium was added to the cell containing plate and was incubated again for 2 days at 37°C.

Day 4: Harvest supernatant for granzyme B or IL-13/IFN-γ ELISA and analyse T cell proliferation

After approximately 72 h of co-culturing DCs and T cells, 100 µl supernatant per well was transferred to a new 96-well round bottom plate and stored at -80°C to determine granzyme B levels in a cross-presentation experiment. In a MHC class II antigen presentation experiment IL-13 or IFN-γ levels were determined. The cells were then transferred from the 96-wells into FACS tubes, spun down and the supernatant was aspirated. CFSE-labelled $CD8^+$ OT-I T cells were stained with anti-mouse CD3 and CD8 antibodies (0.5 µl Fc Block, CD3 and CD8 per sample diluted in 100 µl MACS buffer). CFSE-labelled $CD4^+$ OT-II T cells were stained using antibodies against CD4 and CD3 (0.5 µl Fc Block, CD3 and CD4 per sample diluted in 100 µl MACS buffer). Cells were incubated for 15 min at 4°C. The cells were resuspended in 150 µl MACS buffer after one washing cycle and were analysed for $CD8^+$ or $CD4^+$ T cell proliferation.

2.7 Antigen uptake experiment

DCs were isolated from the spleen and were initially enriched using the OptiPrep™ density gradient medium and were then further purified using CD11c microbeads. DCs were loaded overnight with 1 µg/ml murine OVA-specific IgE. Next day, the cells were washed once with medium. $5x10^5$ DCs were incubated at 37°C with increasing concentrations (0, 0.05, 0.5 and 5 µg/ml) of fluorescently-labelled OVA (OVA Alexa Fluor 647) for 20 min. After the incubation the cells were washed once with ice-cold MACS buffer. For cell surface staining an anti-CD11c antibody was used. Acquisitions were done using a BD FACSCanto™ II (BD Biosciences) and analysis was done using FlowJo vX.0.7 or BD

FACSDiva Software. Results are presented as % fluorescent DCs, indicating binding of fluorescently-labelled OVA to cell surface and/or intracellular uptake.

2.8 Mouse CCL-2/granzyme B/IL-2/IL-13/IFN-γ ELISA Ready-SET-Go!

A 96-well plate provided with the kit was coated with 100 µl capture antibody (1:250 diluted in 1x coating buffer for CCL-2, granzyme B, IL-2 and IL-13 ELISA; 1:1000 diluted with 1x coating buffer for IFN-γ ELISA) and incubated overnight at 4°C. Next day, the plate was washed with 300 µl 1x PBS containing 0.05% Tween (PBST) per well for 5 consecutive times. The blocking was done with 200 µl 1x assay diluent for 1 h at RT. Thereafter, 80 µl of the standard or sample was added per well to the plate in duplicates. Ten µl of the CCL-2 standard was diluted with 5 ml 1x assay diluent to prepare the top standard (1000 pg/ml). For granzyme B 100 µl standard was diluted with 400 µl 1x assay diluent (5000 pg/ml), for the IL-2 ELISA 2 µl were diluted with 10 ml 1x assay diluent (200 pg/ml), for the IL-13 ELISA 5 µl were diluted with 10 ml 1x assay diluent (500 pg/ml) and for the IFN-γ ELISA 20 µl were diluted with 10 ml 1x assay diluent (2000 pg/ml). A 2-fold serial dilution was performed to prepare the standard curve for a total of 10 reference points. The plate was incubated at 4°C overnight for maximal sensitivity. The next day, the plate was washed for 5 times with PBST. 100 µl biotin-labelled detection antibody (1:250 in 1x assay diluent for CCL-2, granzyme B, IL-2 and IL-13 ELISA; 1:1000 in 1x assay diluent for IFN-γ ELISA) was added per well and the plate was incubated for 1 h at RT. The plate was washed again for 5 times followed by 100 µl Avidin HRP (1:250 in 1x assay diluent) per well for 30 min at RT. The plate was washed a minimum of 7 times to decrease the background signal. The pre-warmed TMB solution (100 µl/well) was added and plates were incubated for 15 min at RT. To stop the reaction, 50 µl 1 M H_2SO_4 per well was applied. The optical density of the samples was measured at 450 nm using a PerkinElmer 2030 Multilabel Reader Victor^{TM} X3.

2.9 Flow cytometric analysis

For flow cytometric stainings, MACS buffer was used. Cell surface stainings were done for at least 15 min at 4°C. To prevent unspecific binding of Fcγ receptors, 0.5 µl Fc Block was used per sample. Cells were washed once with 600 µl MACS buffer and resuspended in 150 µl thereafter. Cells that were analysed on the next day were fixed using 100 µl Fix&Perm® Medium A per sample for 5 min at RT. After the addition of 500 µl MACS buffer the samples were stored at 4°C. Prior to acquisitions fixed cells were spun down and resuspended in 150 µl MACS buffer. Acquisitions were performed using a BD

FACSCanto™ II (BD Biosciences) and analysis was done using FlowJo vX.0.7 or BD FACSDiva Software.

2.10 Western Blot

For sodium dodecyl sulfate polyacrylamide gel electrophoresis (SDS-Page), a 1 mm thick 10% gel was prepared according to the recipe shown in Table 4. First the resolving gel was poured between two glass plates leaving one 1 cm free at the top. This was covered with isopropanol until the gel was polymerized. The isopropanol was aspirated. The stacking gel was added on top and the comb was gently inserted.

Twenty µl of the sample were loaded. The protein separation was done for 15 min at 80 Volts and was then increased to 120 Volts for 60 min. Thereafter, a wet transfer, using a Polyvinylidenfluorid (PVDF) membrane with a pore size of 0.45 µm, was performed. Due to the membrane`s strong hydrophobicity, it was treated with methanol for 5 min to expose it`s full protein binding capacity and was afterwards equilibrated with cold transfer buffer for 5 min on a shaker. Proteins were transferred onto the membrane for 60 min at 100 Volts using ice-cold transfer buffer. An ice bucket and a stirrer were placed into the transfer chamber to keep the buffer cold. The membrane was blocked with 3% dry milk powder in 1x TBS containing 0.05% Tween (3% DMP/TBST) for at least 30 min at RT. Then, the membrane was probed with the primary antibody overnight at 4°C diluted in 3% DMP/TBST. After 60 min of washing, an appropriate peroxidase-conjugated secondary antibody was added for 60 min at RT diluted in the blocking solution. The membrane was washed again for 60 min and the peroxidase activity was detected using SuperSignal chemiluminescent substrate reagent and a Bio-Rad Image Lab™ or a Kodax X-OMAT 2000A Processor for developing X-ray films. To reprobe the membrane with another primary antibody, it was incubated for 15 min with Restore PLUS Western Blot Stripping Buffer at RT. Before the primary antibody was applied, the membrane was washed for 5 min with TBST and was blocked again with 3% DMP/TBST for 60 min at RT.

Resolving gel	
30% Acrylamide (ml)	1.7
Resolving buffer (ml)	1.25
H_2O (ml)	2
10% Ammonium Persulfate (µl)	50
TEMED (µl)	5
Stacking gel	
30% Acrylamide (ml)	0.3
Stacking buffer (ml)	0.5
H_2O (ml)	1.2
10% Ammonium Persulfate (µl)	20
TEMED (µl)	2

Table 4: SDS-Page recipe for one 10% 1 mm gel.

2.10.1 Sample preparation for Western Blot

The cell lysates used for Western Blot were prepared as follows. Cell pellets ($0.5\text{-}1x10^6$ cells) were kept on dry ice until they were incubated with 50-100 µl RIPA lysis buffer containing 0.5 mg/ml protease inhibitors and 1 mg/ml phosphatase inhibitors for 10 min on ice. After centrifugation for 10 min at 14000 rpm at 4°C, the supernatant was mixed with the same amount of 2-times concentrated Laemmli buffer and cooked for 5 min at 90°C. To provide reducing conditions, β-mercaptoethanol was added to the Laemmli buffer in a ratio of 1:20. Samples were stored at -20°C.

2.11 Generation of bone marrow-derived mast cells

Mice were sacrificed with CO_2. First the whole legs, including femur, tibia and fibia, were isolated and the muscle tissue was removed. The isolated legs were placed into a 50 ml tube filled with ice cold, sterile RPMI 1640 medium (containing 10% FBS, 2 mM glutamine, 100 U/ml penicillin and 100 µg/ml streptomycin) for 10 min. The bones were transferred to sterile paper towels and the remaining muscle tissue was removed by using these towels. Tibia and fibia were then carefully separated from the femur. Only femur and tibia were used for bone marrow isolation and were then transferred to a petri dish filled with cold and sterile RPMI. Next, the bones were transferred into the sterile cell culture hood and placed onto sterile paper towels wetted with 70% ethanol. The bones themselves were sprayed

with 70% ethanol and were then placed into a tissue culture dish containing RPMI. The bones were tightly gripped with sterile forceps while both ends were cut off using scissors. A 5 ml syringe was filled with RPMI and a 25G 5/8 needle was used to flush out the bone marrow from either sides into a new petri dish. The bones turned almost completely white upon thorough flushing. The cell suspension was homogenized thoroughly using a 10 ml pipette and was passed through a 70 µm cell strainer into a 50 ml tube. The petri dish was washed once with 10 ml medium to ensure maximum yield. A plunger of a 5 ml syringe was used to mash the remaining debris through the filter. Thereafter, the filter was washed with 10 ml RPMI and the isolated cells were spun at 300 g at 4°C for 5 min. The supernatant was aspirated and the pellet was resuspended with 2 ml cold RBC lysis buffer. After 5 min the lysis reaction was stopped by addition of 20 ml of complete RPMI medium. The cells were centrifuged again at 300 g at 4°C for 5 min. The cell pellet was resuspended in an appropriate amount of medium depending on the size of the pellet and the cells were counted using the Casy counter. 4-8x10^6 cells were plated in a total volume of 4 ml per well into 6-well culture plates. To generate mast cells IL-3 and stem cell factor was added to the wells in a concentration of 10 ng/ml and 20 ng/ml respectively. A half medium exchange was performed every third day. Complete differentiation into mast cells was achieved after 4 weeks in culture and was confirmed with flow cytometric staining for the mast cell-specific marker c-Kit and the FcεRI. Mast cells were used after 4 to 6 weeks in culture.

2.12 RNA isolation

Dry cell pellets (containing 500.000 cells) were stored at -80°C for short-term. The cells were kept on dry ice until 350 µl RLT Plus Buffer containing β-mercaptoethanol (1:50) was added and the tube was vortexed thoroughly for 30 sec. The whole RNA isolation procedure was done at RT. The solution was transferred to a QIA shredder column which was centrifuged for 2 min at 10.000 g. The flow-through was gently mixed with 350 µl 70% ethanol. The whole solution was loaded onto a RNeasy Mini spin column and was spun for 20 sec at 8000 g. The flow-through was discarded and the column was washed with 700 µl RW1 Buffer (8000 g, 20 sec). Next, 500 µl RPE buffer was added and the column was centrifuged again for 20 sec at 8000 g. The latter step was repeated one more time. Centrifugation was done for 2 min at 8000 g. The RNeasy spin column was then placed into a new 2 ml collection tube and was spun again for 1 min at maximum speed. To collect the RNA, the column was placed onto a 1.5 ml collection tube and 30 µl of RNase-free water was applied directly to the membrane. The column was centrifuged for 1 min at 8000 g. The eluted RNA was immediately stored on ice and RNA levels and purity were determined using the Nanodrop 2000 Spectrophotometer. Isolated RNA was stored at -80°C until cDNA synthesis was done.

2.13 cDNA synthesis

For cDNA synthesis, 600 ng RNA was used. The RNA was diluted with RNase-free water to a total volume of 16 µl in PCR reaction tubes on ice. Four µl 5x iScript reverse transcription supermix was added per sample. The reverse transcription was done using a Bio-Rad C1000 Touch^{TM} Thermal Cycler. cDNA was stored at -20°C.

2.14 Real-time PCR

The cDNA was diluted in a ratio of 1:6 with RNase-free water. Five µl cDNA was added to a 96-well PCR plate on ice in duplicates. The plate was spun down shortly to collect the cDNA on the bottom. Ten µl SYBR® Select Master Mix were mixed with 2.5 µl of both the forward and reverse primers (stock concentrations: 2µM) per sample. 15 µl of this solution was added per reaction. The plate was covered with an adhesive seal and was spun down for 1 min at 1400 rpm at 4°C. The real-time PCR was done using a Bio-Rad CFX96^{TM} Real-Time System.

2.15 Statistical analysis

Statistical analysis was performed using PRISM software (GraphPad Software Inc.). Differences between groups were analysed by two-way ANOVA or Student`s *t*-test. Data are presented as mean +/- standard deviation. Results showing a p-value <0.05 were considered statistically significant. Quantification of Western Blots was done using ImageJ.

3 Results

3.1 Mouse genotyping by PCR

In order to use mice with appropriate genotypes, animals were genotyped by PCR. It is important to note that PCR-based genotyping assays as performed during the study cannot distinguish heterozygous from homozygous transgenic animals. Fig.8 shows representative genotyping pictures of all used mouse strains.

IgE_R-TG mice express the human α-chain of the FcεRI. The human FcεRI α-chain is downstream of the CD11c promoter, resulting in DC-specific expression of the transgene.

Expression of FcεRI α-chain was detected via an IRES-eGFP reporter gene. Additionally, caveolin primers were used as an internal control in order to distinguish from false negative results. Fig.8A shows a representative PCR from genotyping of IgE_R-TG mice. Lane 1 shows a WT mouse with a single band at 690 bp representing the caveolin WT band. An IgE_R-TG mouse is depicted in lane 2 showing both the caveolin WT band and the eGFP band at 400 bp.

Genotyping for mu-αKO mice results in 2 bands for heterozygote animals at 200 and 300 bp (B, lane 1). A knockout mouse for the murine α-chain shows a single band at 200 bp (B, lane 2).

Genotyping PCR from a representative HP-αTG mouse is shown in Fig.8C giving a distinct band at 561 bp. Lane 1 depicts a WT mouse which lacks the transgene.

Genotyping for testing OT-I mice required testing for 2 transgenes (Tcra and Tcrb) in 2 separate PCR reactions. Internal positive controls which show a band at 200 bp are included to avoid false negative results. Fig.8D shows a representative PCR gel from OT-I genotyping. Lane 1 and 2 depict a mouse transgenic for Tcra and for Tcrb respectively with 2 bands at 200 and 300 bp.

OT-II mice also were also genotyped for the Tcra and Tcrb gene but in a single PCR reaction Tcra and Tcrb-positive mice revealed a band at 160 bp and at 500 bp respectively (E, lane 1). Lane 2 shows a WT mouse which lacks both transgenes.

To genotype caveolin KO mice 3 different primers were used. Two forward primers, to either amplify the WT or mutant caveolin, are used together with a common reverse primer. Fig.8H shows in lane 1 a caveolin KO mouse with a single band at 410 bp. A heterozygote mouse for caveolin is shown in lane 2 with bands at both 410 and 690 bp.

Fig.8G shows a mouse that is MyD88 KO with a unique band at 600 bp in lane 1. A heterozygote animal is depicted in lane 2 and represents two bands at 550 and 600 bp. As those bands are in close proximity to each other, it was essential to run the PCR products on a 3% agarose gel.

A representative picture of an agarose gel for genotyping for WASP KO mice is shown in Fig.8H. A heterozygote mouse is shown in lane 1 with 2 bands at 450 bp and 800 bp. Lane 2 depicts a KO mouse with one distinct band at 800 bp.

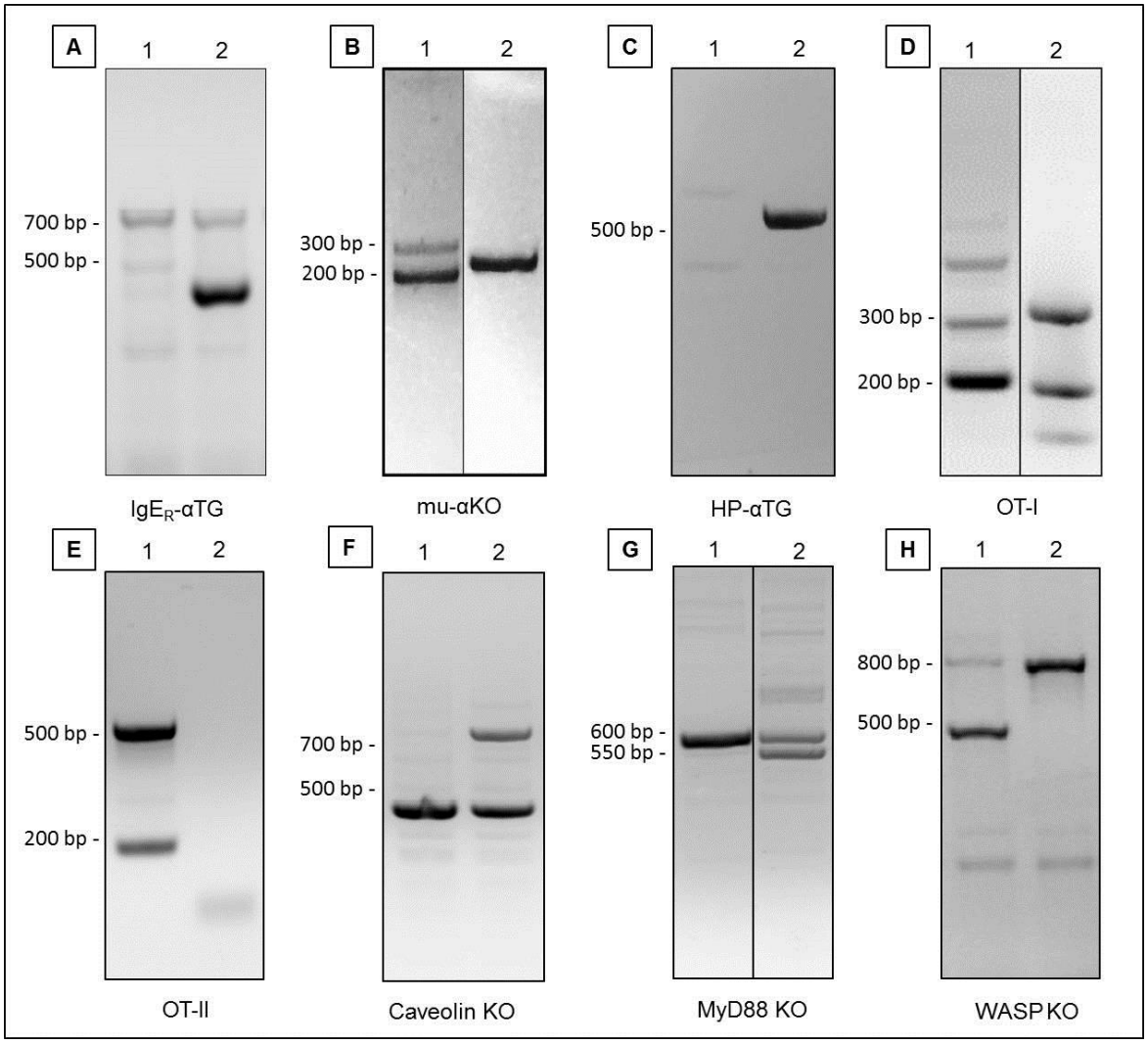

Fig.8: Representative agarose gel pictures from mouse genotyping by PCR. Results are indicated as wild-type (WT), heterozygote (het), knock out (KO), transgenic (TG).
(A) IgE$_R$-TG (1: WT, 2: TG) **(B)** Mu-αKO (1: het, 2: KO) **(C)** HP-αTG (1: WT, 2: TG) **(D)** OT-I (1: TG for Tcra, 2: TG for Tcrb) **(E)** OT-II (1: TG for Tcra and Tcrb, 2: WT) **(F)** Caveolin KO (1: KO, 2: WT) **(G)** MyD88 KO (1: KO, 2: het) **(H)** WASP KO (1: WT, 2: KO)

3.2 Establishment of IgE/FcεRI-mediated cross-presentation assay

3.2.1 CCL-2 secretion of purified splenic CD11c$^+$ dendritic cells

To investigate whether we are able to gain a pure splenic DC population that is capable of responding to stimulation signals, spleens of IgE$_R$-TG mice were harvested, DCs were isolated using CD11c magnetic beads and the cells were stimulated with 500 ng/ml LPS for 20 h.

To determine the purity of the isolated cell population, flow cytometric analysis was performed (Fig.9). GFP^+ DCs from IgE_R-TG mice were detected using antibodies against CD11c and the human FcεRI-alpha (monoclonal antibody (mAb) Cra-1). T cells and B cells were stained with TCR β-chain and CD19 antibodies, respectively. Fig.9 depicts that a high purity of $CD11c^+$ cells can be isolated from the spleen using the magnetic cell sorting technology for DCs. Sixty-three % of the population was positive for CD11c and reveled a GFP signal (Fig.9D). Only 2% T cells (Fig.9B) and 12% B cells (Fig.9C) were found in the isolated cell population.

A remarkable increase of $CD86^+$ expression was found when $CD11c^+$ DCs were stimulated with LPS (Fig.9E), which confirms that LPS stimulation leads to maturation of DCs. Furthermore, a significant induction of CCL-2 secretion was detected by ELISA in supernatants of DCs after stimulation with LPS compared to unstimulated cells. In summary, this set of data indicates that the isolated DCs were functional and were able to respond to stimulation signals (Fig.9F).

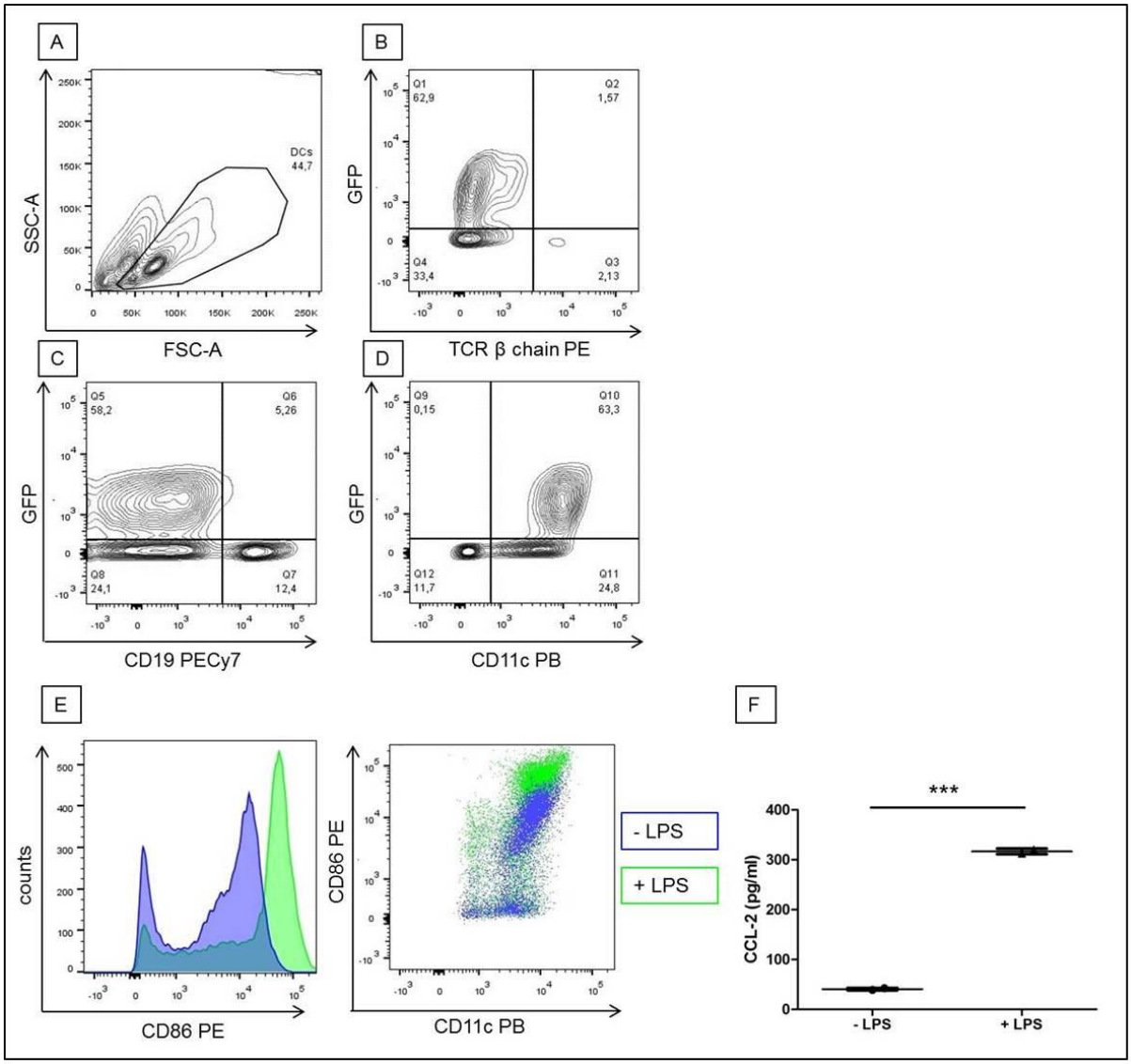

Fig.9: Determination of dendritic cell purity after magnetic cell sorting technology using flow cytometric analysis and CCL-2 measurements upon LPS stimulation.
DCs were isolated using CD11c microbeads. **(A)** FACS blot shows the gating strategy on viable DCs. **(B)** Isolated cells were stained with a TCR β chain antibody to detect T cells and **(C)** a CD19 antibody to detect B cells**. (D**) To identify DCs an antibody against CD11c was used**. (E, F)** $2x10^5$ DCs were stimulated with 500 ng/ml LPS for 20 h. **(E**) A CD86 antibody was used to detect mature DCs before (blue) and after (green) LPS stimulation. **(F)** CCL-2 production of unstimulated and LPS-stimulated DCs was determined by ELISA.

The performed experiments show that, a DC population with a purity of over 60% can be isolated from mouse spleens using CD11c magnetic beads. Furthermore, it was confirmed that these cells are functional and secrete CCL-2 upon LPS stimulation.

3.2.2 Dendritic cells isolated from IgE_R-TG mice can be loaded with NP-specific IgE which results in stabilization and subsequent upregulation of FcεRI expression

To test whether DCs expressing the humanized FcεRI are capable of binding NP-specific IgE, splenic DCs were isolated from IgE_R-TG and WT mice and incubated with NP-IgE overnight. IgE-loading and FcεRI expression was confirmed via flow cytometric analysis. Fluorescently-labelled hapten (NP-PE) was used to detect the surface-binding of NP-specific IgE. DCs from IgE_R-TG mice that were incubated with NP-IgE were found to bind IgE to their cell surface and showed a substantially increased expression of the FcεRI (Fig.10A-C).

In another experiment, FcεRI expression was detected by immunoblotting. Fig.10D depicts DCs isolated from IgE_R-TG and WT mice probed with the mAb 19-1 that specifically detects the properly folded IgE-binding FcεRI α-chain. Upon incubation with NP-IgE, a notable increase in FcεRI expression was observed in DCs from IgE_R-TG mice.

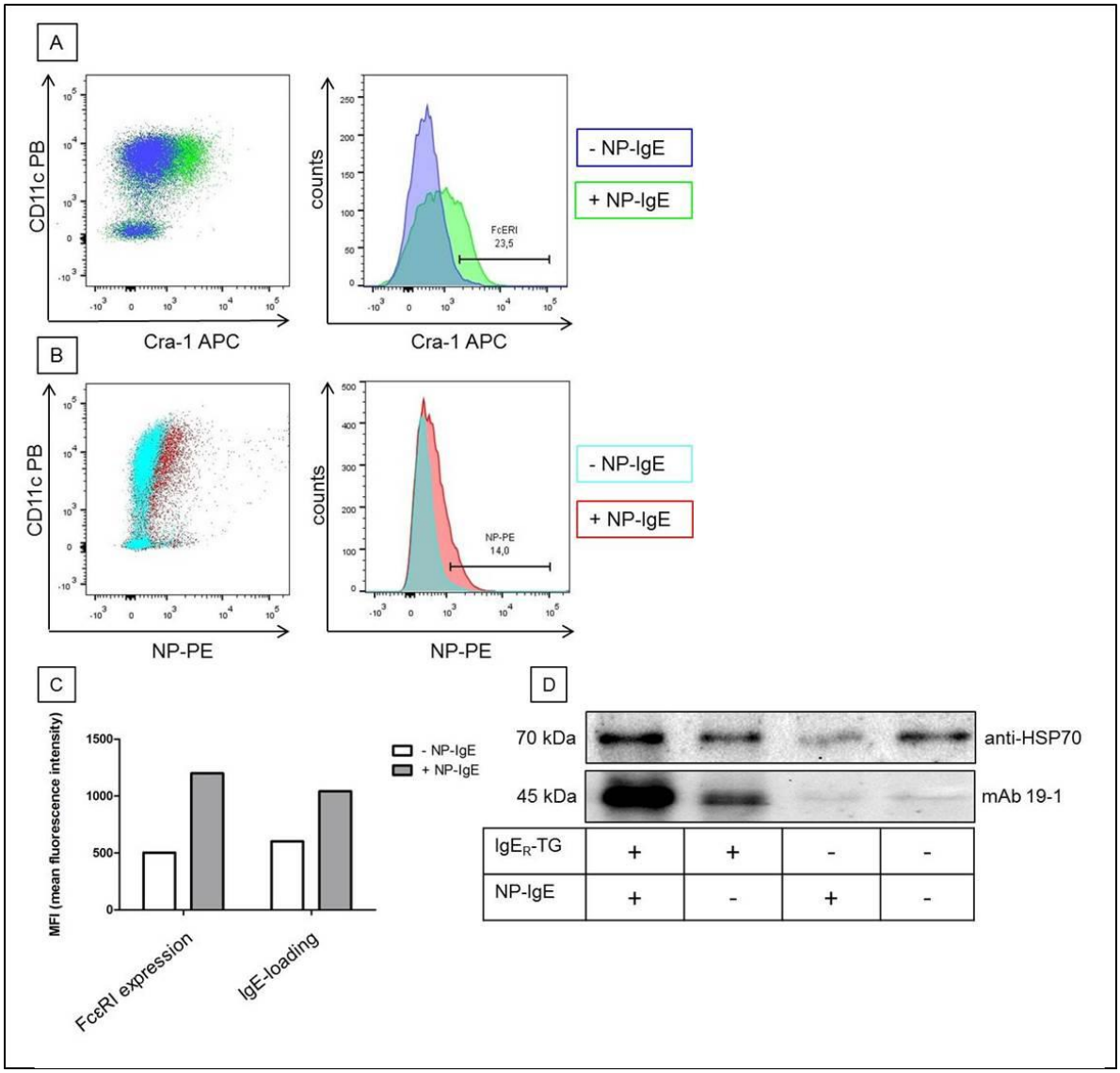

Fig.10: FcεRI expression and IgE-loading of dendritic cells from IgE$_R$-TG and WT mice upon NP-IgE incubation.
(A) FACS plot overlays of IgE-loaded (green) and unloaded DCs (blue) from IgE$_R$-TG mice stained for FcεRI (mAb Cra-1). **(B)** FACS plot overlays of NP-PE staining of IgE-loaded (red) and unloaded DCs (cyan) from IgE$_R$-TG mice. **(C)** Mean fluorescence intensities of FcεRI expression and IgE-loading of loaded and unloaded DCs from IgE$_R$-TG mice. **(D)** Detection of FcεRI of DCs from IgE$_R$-TG and WT mice using the mAb 19-1 -/+ NP-IgE incubation and HSP70 as loading control.

The presented results are in line with already published data that confirm that DCs from IgE$_R$-TG mice can be loaded with NP-specific IgE and that this leads to a stabilization of the FcεRI on the cell surface and subsequent upregulation of its expression.

3.2.3 Splenic dendritic cells numbers increase *in vivo* after subcutaneous injections of GM-CSF secreting tumor cells

Since a high DC number is needed for *in vitro* experiments, we determined whether we can use GM-CSF secreting B16 tumor cells to expand FcεRI-bearing DCs *in vivo* in humanized animals. Therefore IgE_R-TG and WT mice were injected subcutaneously with tumor cells. For control purposes another group of IgE_R-TG mice was left untreated.

Ten days after tumor cell injection, mice were sacrificed and the spleens were harvested. We observed significantly enlarged spleens in mice injected with tumor cells (Fig.11A). A 28-fold increase in DCs numbers was found in IgE_R-TG mice treated with B16 GM-CSF cells compared to untreated TG mice (Fig.11B).

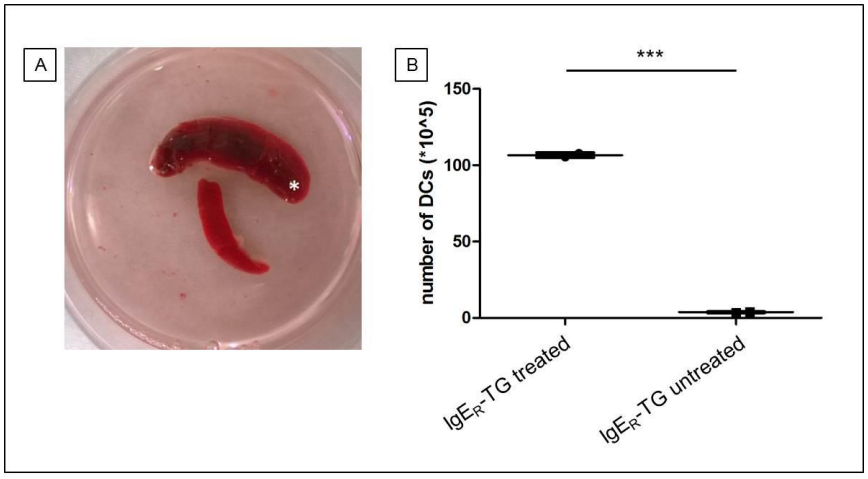

Fig.11: Representative spleens and cell numbers after *in vivo* dendritic cell expansion.
(A) Spleen from IgE_R-TG mouse treated with B16 GM-CSF cells is labelled with an asterisk in comparison to a spleen from an untreated mouse. **(B)** DCs numbers isolated from IgE_R-TG mice treated with tumor cells and untreated.

Flow cytometric analysis showed that the DC $CD8\alpha^-$ subset expresses higher levels of the human FcεRI-α as determined by staining with mAb Cra-1 (Fig.12A). Additionally, a substantial increase in receptor expression was found after overnight incubation with NP-specific IgE in DCs from IgE_R-TG mice treated with B16 GM-CSF cells. Furthermore, it was confirmed that DCs from WT mice do not express the murine FcεRI (Mar-1 was used to stain for murine FcεRI). DCs of IgE_R-TG mice express the human FcεRI and show an elevated expression after IgE incubation (Fig.12B).

Comparable numbers of pDCs, as defined by expression of PDCA1, were found in tumor cell-injected and untreated IgE_R-TG mice but also in injected WT mice. PDCs of IgE_R-TG mice usually do not express the human FcεRI. Interestingly, pDCs of IgE_R-TG mice that were injected with B16 GM-CSF cells showed an upregulation of the human FcεRI expression, but pDCs of uninjected IgE_R-TG mice did not reveal FcεRI expression

(Fig.12C). Furthermore, DCs of IgE_R-TG mice treated with tumor cells showed an elevated IgE surface binding compared to untreated TG mice and treated WT mice (Fig.12D).

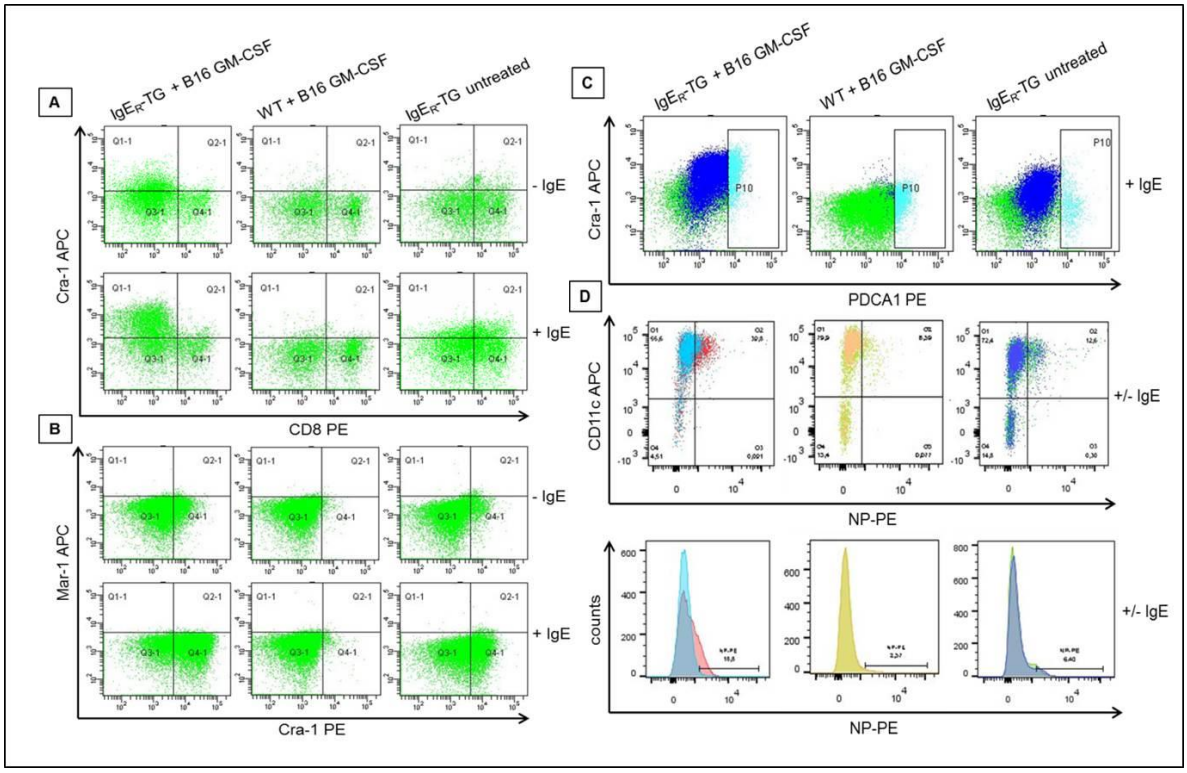

Fig.12: Flow cytometric analysis of dendritic cells isolated from B16 GM-CSF cells injected and not injected IgE_R-TG and from injected WT animals.
(A) $CD11c^+$ gated cells were stained for CD8 and the human FcεRI with or without incubation of NP-specific IgE **(B)** $CD11c^+$ gated cells were stained with mAb Cra-1 and mAb Mar-1 with or without incubation of NP-specific IgE. **(C)** To detect plasmacytoid DCs an anti-$PDCA1^+$ antibody was used. **(D)** IgE-loading was determined using fluorescently-labelled hapten (NP-PE).

In another experiment, DCs were isolated from IgE_R-TG mice that were injected with B16 GM-CSF cells or uninjected mice. The cells were loaded with NP-specific IgE overnight or were left unloaded. Fig.13A shows that the FcεRI expression and IgE-loading was slightly increased in *in vivo* expanded DCs. Both DC populations were compared in a MHC class II antigen-presentation experiment. While a significant difference in $CD4^+$ T cell proliferation was found when non-expanded DCs were loaded with IgE and used as antigen presenting cells, *in vivo* expanded DCs only showed minor differences between IgE-dependent and IgE-independent presentation (Fig.13B).

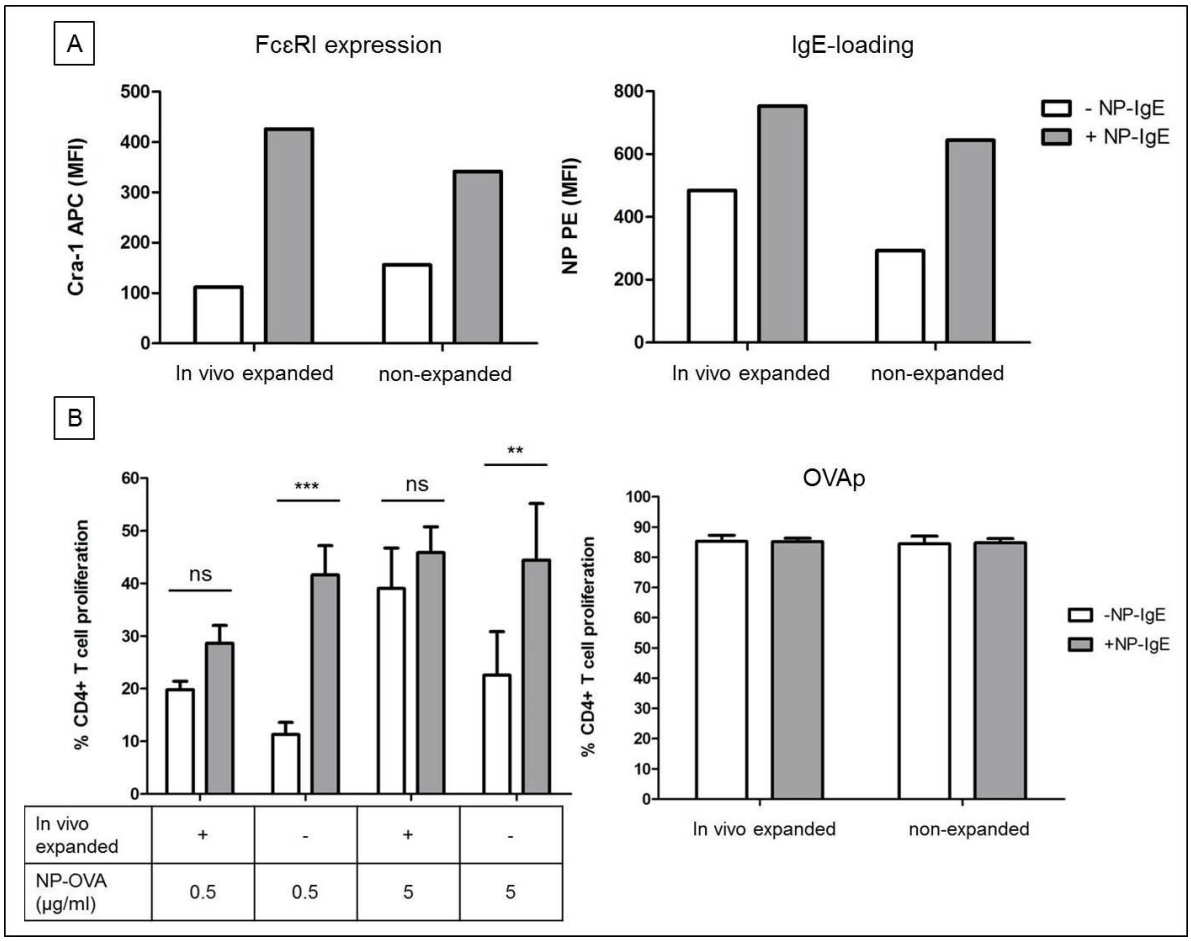

Fig.13: Comparison of *in vivo* expanded and non-expanded dendritic cells in an antigen-presentation experiment.

(A) FcεRI expression was determined using mAb Cra-1. NP-PE was used to detect receptor-bound NP-IgE. **(B)** $CD4^+$ T cell proliferation was determined in a MHC class II antigen presentation assay after 3 days of DC/T cell co-cultures. OVAp was used as positive control.

Based on the presented data, we concluded that *in vivo* expanded DCs reveal unchanged FcεRI expression and IgE-loading, but cannot be recommended for usage in antigen-presentation experiments.

3.2.4 Dendritic cell isolation using OptiPrep™ does not provide similar purity of $CD11c^+$ cells than the magnetic cell separation technique

To investigate whether the OptiPrep™ density gradient medium can be used as a cost-effective alternative to the magnetic cell separation technique, DCs were isolated from mouse spleens from IgE_R-TG animals and both procedures were compared side by side.

Fig.14 shows the flow cytometric analysis of isolated DCs that were unloaded (blue) or loaded (green) with NP-specific IgE. Using the microbeads technology a significantly increased GFP^+CD11c^+ population was found compared to the isolation with the OptiPrep™ density gradient (Fig.14A). While only a minor FcεRI-expressing $CD11c^+$ population (10%) was found when DCs were isolated with the density gradient, an elevated number of FcεRI-expressing DCs (45%) was detected using the microbeads (Fig.14B). Comparable numbers of $CD64^+CD11b^+$ cells indicating monocytes were found for both isolation techniques (Fig.14C). Fourteen % of T cells were detected when OptiPrep™ was used, compared to 3.6% when the magnetic cell separation protocol was performed (Fig.14D). The amount of NP-IgE-loaded $CD11c^+$ cells was substantially increased after overnight IgE incubation in the population that was isolated using the microbeads (Fig.14E). Overall, 29% of $CD11c^+CD86^+$ cells, indicating mature DCs, were detected when DCs were isolated using the density gradient, compared to 68.7% when the CD11c microbeads were used (Fig.14F).

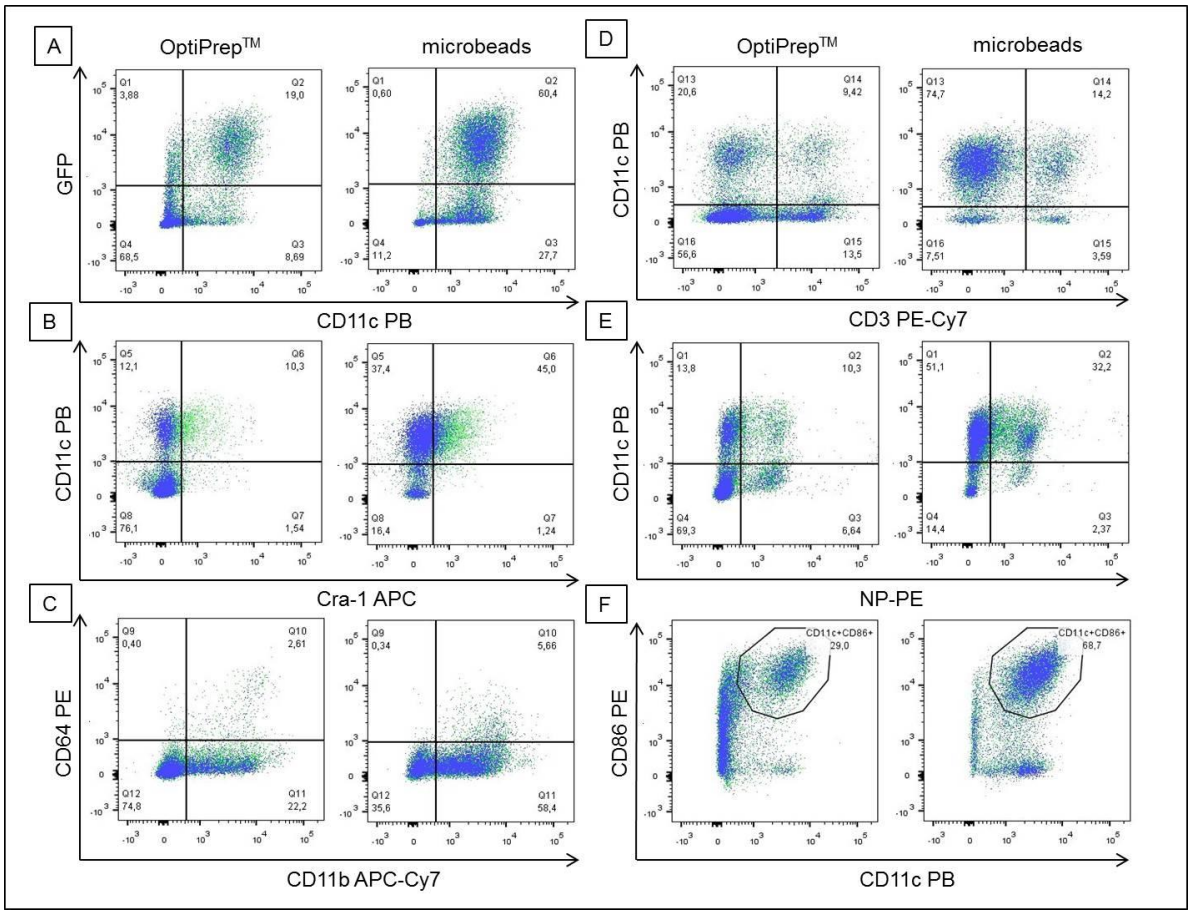

Fig.14: Flow cytometric analysis of dendritic cells isolated using OptiPrep™ density gradient medium compared to magnetically-labelled CD11c microbeads.
(A) Representative FACS blot stained for $CD11c^+$ and GFP^+ cells to detect DCs. **(B)** To determine the human FcεRI expression on DCs, mAb Cra-1 was used. **(C)** CD64 and CD11b antibodies were used to detect monocytes. **(D)** CD3 staining was performed to detect T cells. **(E)** IgE-loading was detected using fluorescently-labelled hapten NP-PE. **(F)** To analyse the amount of mature DCs, CD86 antibody was used.

Based on the presented data, we concluded that DC isolation using magnetically-labelled CD11c microbeads yields a substantially increased $CD11c^+$ population compared to OptiPrep™ density gradient medium.

3.2.5 Dendritic cells of IgE_R-TG mice can be used to study cross-presentation

To investigate whether DCs use the IgE/FcεRI-mediated antigen uptake pathway to present antigens via MHC class I molecules and induce $CD8^+$ T cell responses, a cross-presentation assay was performed *in vitro*.

Prior to the antigen presentation assay, FcεRI expression and IgE-loading of DCs from IgE_R-TG was confirmed via flow cytometric analysis after overnight incubation with NP-specific IgE (data not shown).

In vitro proliferation of CFSE-labelled $CD8^+$ OT-I T cells after IgE/FcεRI-dependent and IgE-independent antigen uptake of DCs was determined after 3 days of co-culture. A remarkable rise in T cell proliferation was found when DCs were loaded with IgE compared to unloaded cells (Fig.15A-C). When no antigen was added to the DCs only background proliferation of around 5% was found. OVAp was used as positive control and induced strong T cell proliferation (Fig.15D).

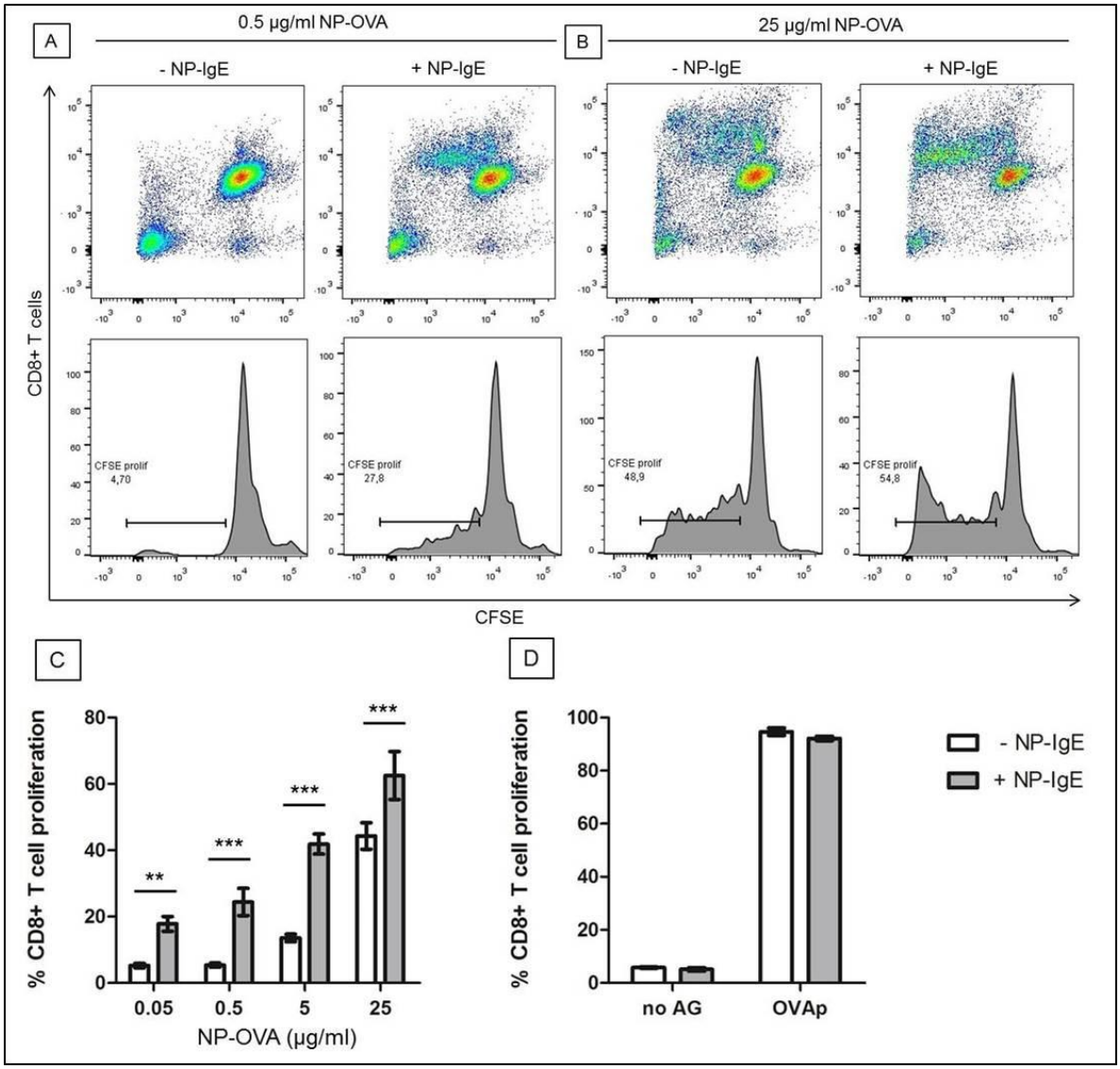

Fig.15: CD8$^+$ T cell proliferation in an IgE/FcεRI-mediated cross-presentation assay.
(A) Proliferation of CFSE-labelled CD8$^+$ T cell at low antigen concentration (0.5 µg/ml NP-OVA) compared to **(B)** CD8$^+$ T cell proliferation at high NP-OVA concentration (25 µg/ml). **(C)** Quantification of CD8$^+$ T cell proliferation for increasing NP-OVA concentrations (0.05 µg/ml, 0.5 µg/ml, 5 µg/ml, 25 µg/ml). **(D)** CD8$^+$ T cell proliferation for negative control (no AG) and positive control (OVAp).

With this data, an unpublished finding of the host laboratory was confirmed, that DC-bound IgE functions as an antigen sensing receptor in the context of cross-presentation. Furthermore, it was found that surface-bound IgE significantly lowers the antigen amount that is required to induce CD8$^+$ T cell responses.

3.3 FcεRI-mediated antigen trafficking and IgE-mediated cross-presentation

Question 1: Is caveolin-mediated endocytosis necessary for FcεRI-dependent antigen uptake and does this pathway functionally affect IgE-mediated cross-presentation?

Preliminary experiments in the Fiebiger Laboratory showed that the trimeric FcεRI utilizes caveolin to get internalized. Therefore, the effect of caveolin deficiency on antigen trafficking and IgE-mediated cross-presentation was examined.

To investigate whether caveolin is required for IgE/FcεRI-mediated antigen sampling, an antigen uptake experiment was performed using DCs isolated from caveolin WT (+/+) or KO (-/-) mice that were transgenic for the FcεRI expression (IgE_R-TG). Comparing those two groups, a decreased difference between IgE-dependent and IgE-independent antigen binding and/or uptake was found in caveolin -/- DCs in high antigen concentration range (0.5 and 5 µg/ml) (Fig.16).

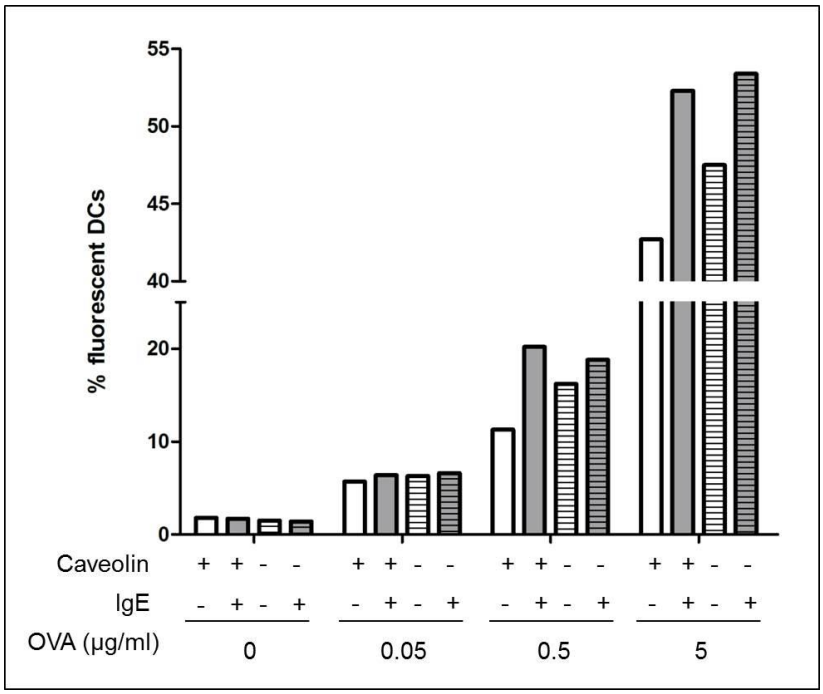

Fig.16: Antigen uptake experiment comparing dendritic cells isolated from IgE_R-TG x caveolin WT (+) or caveolin KO (-) mice.
OVA-specific IgE-loaded DCs were incubated for 20 min with increasing concentrations of fluorescently-labelled OVA (0, 0.05, 0.5, 5 µg/ml). FACS analysis was done to quantify antigen binding and/or uptake.

To further investigate if the slightly impaired antigen uptake of caveolin -/- mice affects cross-presentation, an antigen presentation experiment was performed with caveolin -/- or heterozygote (+/-) mice that were transgenic for the FcεRI expression. The second question we wanted to answer was, if is there is an age-dependent effect on the ability to cross-present in caveolin -/- and +/- mice. Therefore we examined 3 mouse groups with different ages. The first group was 39 weeks old, the second 17 weeks and the third mouse group was 11 weeks old. For each group a caveolin -/- and a caveolin +/- mouse was included.

First, DCs were isolated and sensitized overnight with NP-specific IgE. Fig.17 shows a substantial increase in FcεRI expression (A) as well as IgE-loading (B) upon NP-IgE incubation in a representative sample (blue: no IgE, green: plus IgE). Comparable mean fluorescence intensities (MFI) of FcεRI expression as well as IgE-loading were found in all 3 age groups. Furthermore, no significant differences between the different genotypes were detected (Fig.17C and D).

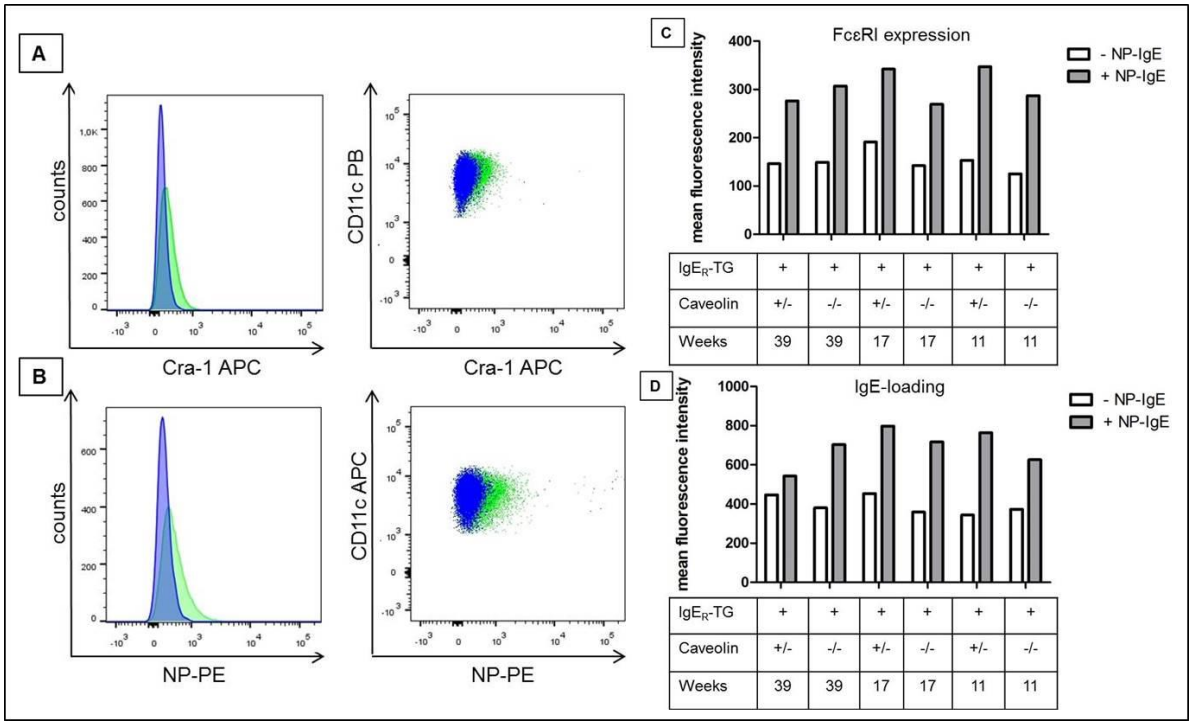

Fig.17: FcεRI expression and IgE-loading of dendritic cells isolated from IgE$_R$-TG x caveolin KO (-/-) and heterozygote (+/-) mice with different ages.
(A, B) Representative FACS plots showing FcεRI expression (A, stained with Cra-1) and IgE-loading (B, stained with NP-PE) of DCs from IgE$_R$-TG x caveolin -/- mice (blue: no NP-IgE, green: plus NP-IgE incubation). **(C, D)** Mean fluorescence intensities (MFI) of FcεRI expression (C) and IgE-loading (D) of DCs isolated from 39, 17 and 11 weeks old IgE$_R$-TG x caveolin -/- and +/- mice.

In another experiment, caveolin expression of DCs was confirmed on the protein level by Western Blot shown in Fig.18. An anti-caveolin-1 antibody was used to detect caveolin

expression and showed a signal at 22 kDa. While a distinct band was found in caveolin +/- mice, no signal was detected in caveolin -/- mice. As loading control a β-actin antibody, that detected a band at 42 kDa, was used.

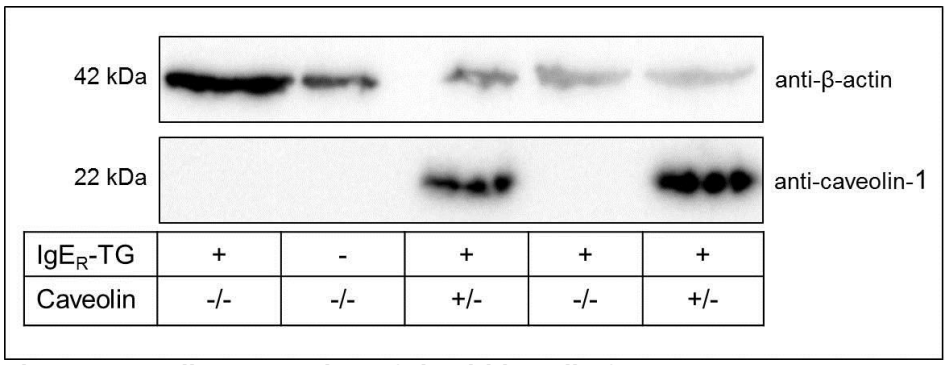

Fig.18: Caveolin expression of dendritic cells from IgE$_R$-TG or WT x caveolin heterozygote (+/-) and KO (-/-) mice detected by Western Blot.
DC lysates were probed with a caveolin-1 and β-actin antibody as loading control.

For the *in vitro* antigen cross-presentation experiment, NP-IgE-loaded or unloaded DCs were pulsed with two different antigen concentrations (0.5 µg/ml and 5 µg/ml NP-OVA) for 60 min. Thereafter, DCs were incubated with CFSE-labelled naïve CD8$^+$ OT-I T cells for 4 days. Proliferation of CD8$^+$ T cells was analysed by flow cytometry.

As shown in Fig.19A and B, the cross-presentation assay showed a strong proliferation of CFSE-labelled CD8$^+$ T cells after NP-IgE-loading (green) and incubation with NP-OVA in caveolin -/- mice. Neither between caveolin -/- and +/- mice, nor between the 3 different age groups an obvious difference in IgE-mediated cross-presentation was found (C).

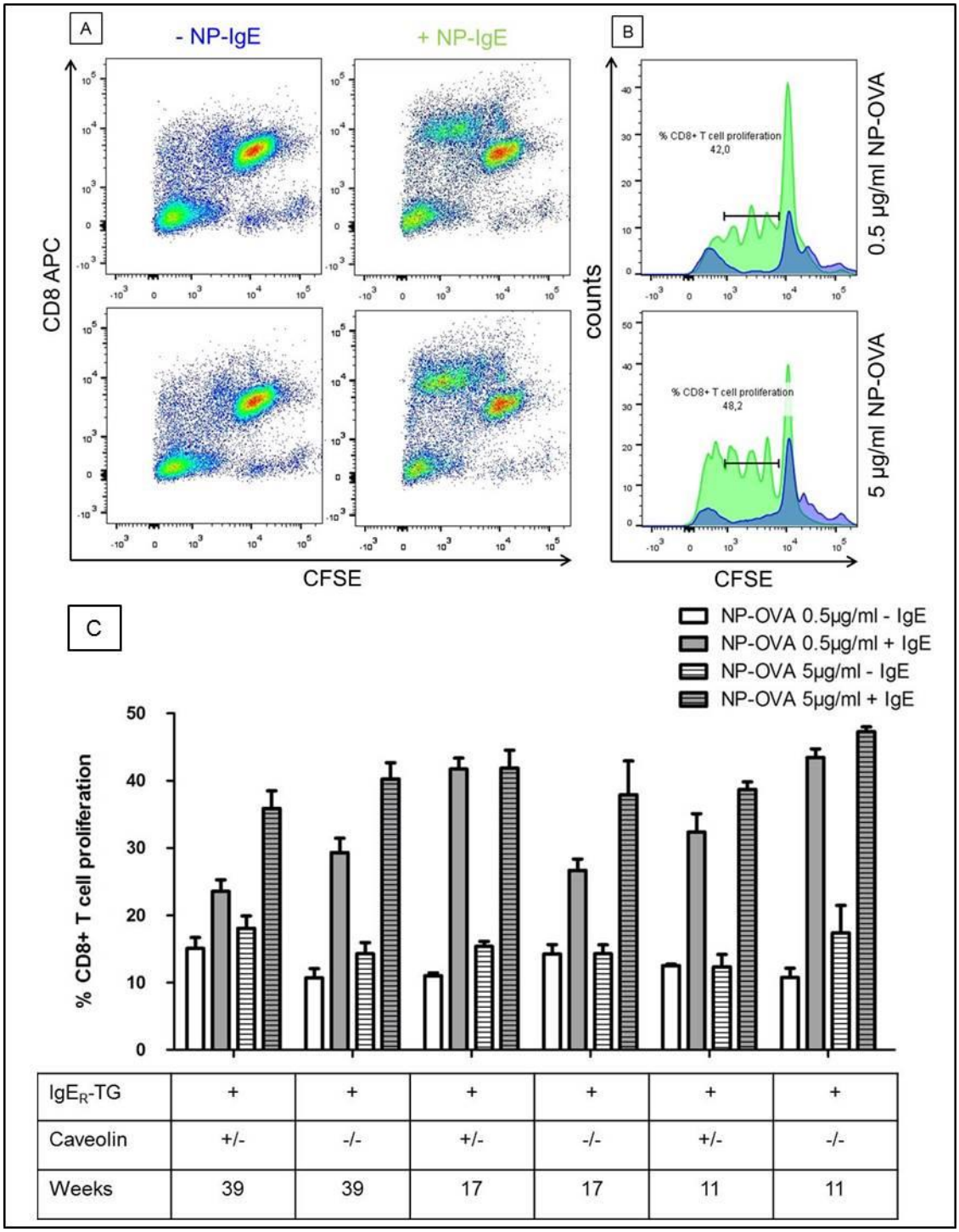

Fig.19: Comparison of the cross-presentation ability of dendritic cells isolated from IgE$_R$-TG x caveolin KO (-/-) and heterozygote (+/-) mice and 3 different age groups.
(A+B) Representative FACS plots of DCs isolated from an IgE$_R$-TG x caveolin -/- mouse incubated with (green) or without NP-IgE (blue) and antigen (NP-OVA) in 2 different concentrations (0.5 µg/ml and 5µg/ml). **(A)** CFSE-labelled T cells stained with CD8 APC with (green) and without NP-IgE (blue) incubation. **(B)** Overlays of mean fluorescence intensities showing CFSE proliferation without (blue) and with NP-IgE incubation (green). **(C)** Quantitative analysis of CD8$^+$ T cells proliferation.

After 24 h of co-culturing DCs and T cells, supernatant was harvested to determine IL-2 levels by ELISA as an indicator of T cell proliferation. Granzyme B, a component of lytic

granules, was measured after 3 days of incubation in cell culture supernatants to confirm cross-priming of CTLs. Variable levels of IL-2 (Fig.20A) as well as granzyme B (Fig.20B) were found in all 3 age groups and no obvious pattern was detected between caveolin -/- and +/- mice.

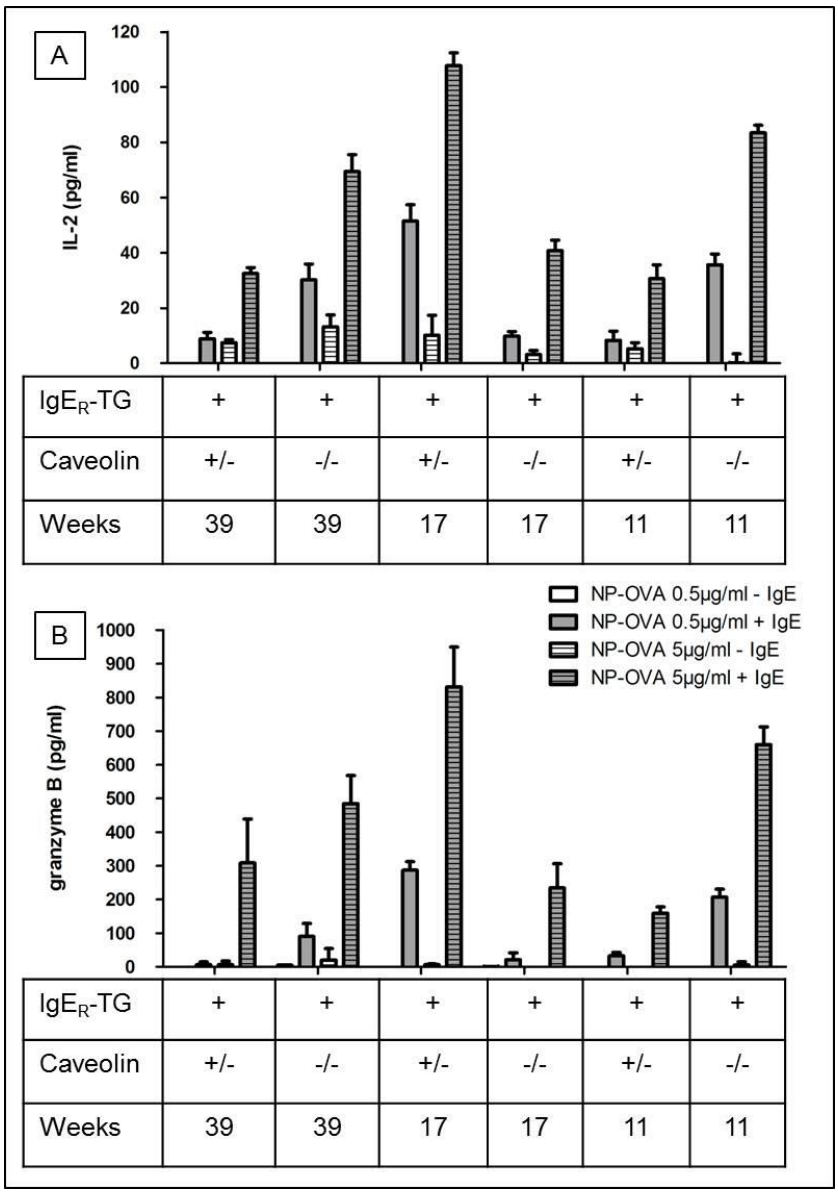

Fig.20: Cytokine levels measured during a cross-presentation experiment to compare dendritic cells of IgE$_R$-TG x caveolin KO (-/-) or heterozygote (+/-) mice and different age groups (11, 17 and 39 weeks).
(A) IL-2 production was determined after 24 h in DC/T cell co-culture supernatants. **(B)** Granzyme B levels were determined after 3 days of co-culture.

The presented results show, that caveolin is not essential for IgE/FcεRI-mediated cross-presentation indicating that the caveolin-mediated FcεRI antigen sampling pathway is functionally substituted in DCs.

Question 2: Are there effects of WASP-deficiency on antigen uptake and cross-presentation?

It has been described that WASP plays an important role in degranulation and inflammatory cytokine production down-stream of IgE-mediated cross-linking of the tetrameric FcεRI. [49] Therefore, the influence of WASP on IgE/FcεRI-mediated antigen shuttling was initially investigated in a cross-presentation assay.

DCs of IgE_R-TG or WT mice that were WASP-deficient (-/-) or WASP-competent (+/+) were isolated from spleens and loaded with NP-specific IgE overnight. FcεRI expression and IgE-loading (not shown) were confirmed by flow cytometric analysis. Interestingly, a pronounced FcεRI expression was found in IgE_R-TG x WASP -/- mice compared to IgE_R-TG x WASP +/+ mice shown in Fig.21.

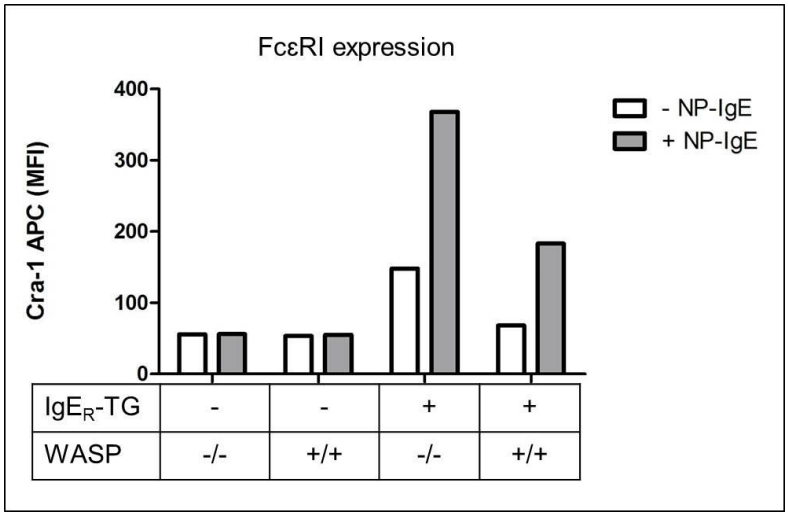

Fig.21: FACS analysis of FcεRI expression of dendritic cells isolated from IgE_R-TG or WT mice that were WASP-deficient (-/-) or WASP-competent (+/+).
FcεRI expression was confirmed after overnight incubation with NP-specific IgE. mAb Cra-1 was used to stain the human α-chain of the FcεRI.

In another experiment FcεRI α-chain expression profiles of *in vivo* expanded DCs isolated from IgE_R-TG and WT mice that were WASP-deficient or WASP-competent were analysed by Western Blot. (Fig.22A and B) IgE_R-TG WASP -/- showed a 1.6-fold increase in expression of the fully glycosylated human FcεRI α-chain (detected with mAb 19-1) compared to IgE_R-TG WASP +/+ mice. mRNA levels were equal in IgE_R-TG WASP -/- and IgE_R-TG WASP +/+ mice (Fig.22C).

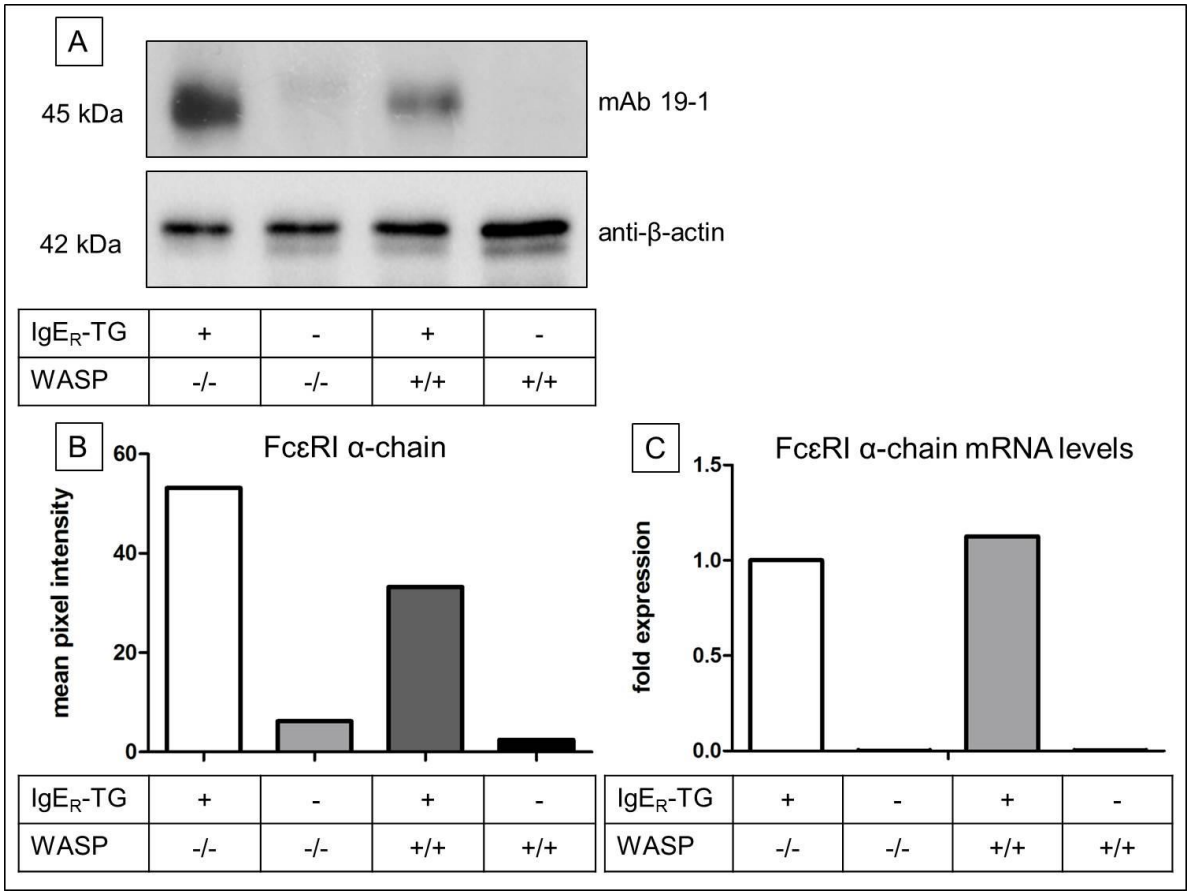

Fig.22: Western Blot of FcεRI expression profile and FcεRI mRNA levels of *in vivo* expanded dendritic cells isolated from IgE$_R$-TG or WT mice that were WASP-deficient (-/-) or WASP-competent (+/+).
(A) The properly folded human FcεRI α-chain was detected using mAb 19-1. For loading control a β-actin antibody was used. **(B)** Quantification of FcεRI α-chain expression was done based on mean pixel intensity. **(C)** mRNA levels of FcεRI α-chain were determined by quantitative real-time PCR.

To investigate the influence of WASP-deficiency on antigen sampling, an antigen uptake experiment was performed using *in vivo* expanded DCs from IgE$_R$-TG x WASP -/- and WASP +/+ mice that were loaded with OVA-specific IgE or unloaded. It was found that WASP-deficient DCs were more efficient in antigen binding and/or uptake than WASP +/+ DCs, even if the cells were not loaded with IgE (Fig.23). 65% of unloaded WASP -/- DCs were fluorescent compared to 79% when the cells were coated with IgE. Sixty-one % of WASP-competent DCs were fluorescent in an IgE-independent setup. When DCs were coated with IgE, antigen sampling increased to 71%.

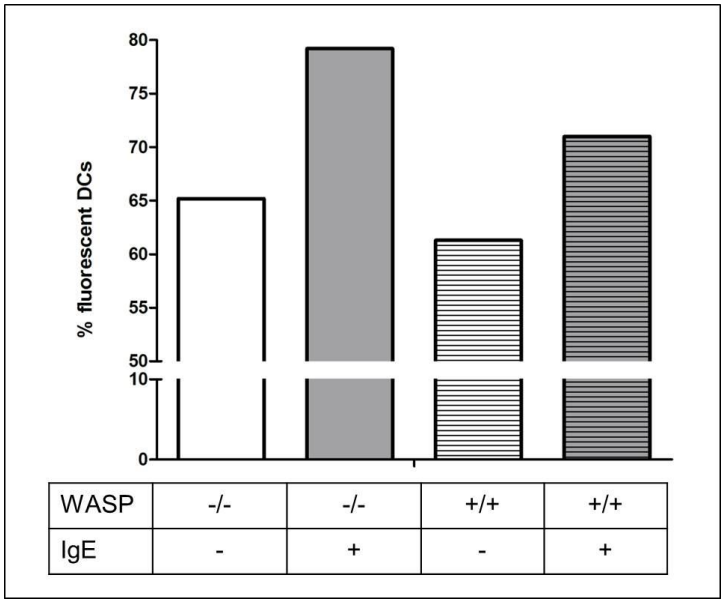

Fig.23: Antigen uptake experiment using *in vivo* expanded dendritic cells from IgE_R-TG x WASP-deficient (-/-) and WASP-competent (+/+) mice.
DCs loaded with OVA-specific IgE were incubated for 20 min with 5 µg/ml fluorescently-labelled OVA. FACS analysis was done to quantify antigen binding and uptake.

To investigate the effect of WASP-deficiency on cross-presentation, increasing NP-OVA concentrations (0.05, 0.5 and 5 µg/ml) were used in an antigen presentation experiment shown in Fig.24. A significant difference in $CD8^+$ T cell proliferation was found between IgE_R-TG WASP -/- and +/+ mice when 0.05 µg/ml NP-OVA was used in the IgE/FcεRI-dependent antigen uptake (Fig.24A). However, the effect of WASP-deficiency on cross-presentation decreased with increasing antigen concentrations. When unloaded DCs were analysed for their cross-presentation ability only background (5-10%) of $CD8^+$ T cell proliferation was found for all mouse groups (Fig.24B). The positive control (OVAp) in the IgE/FcεRI-dependent and -independent antigen uptake showed comparable T cell proliferation (data not shown).

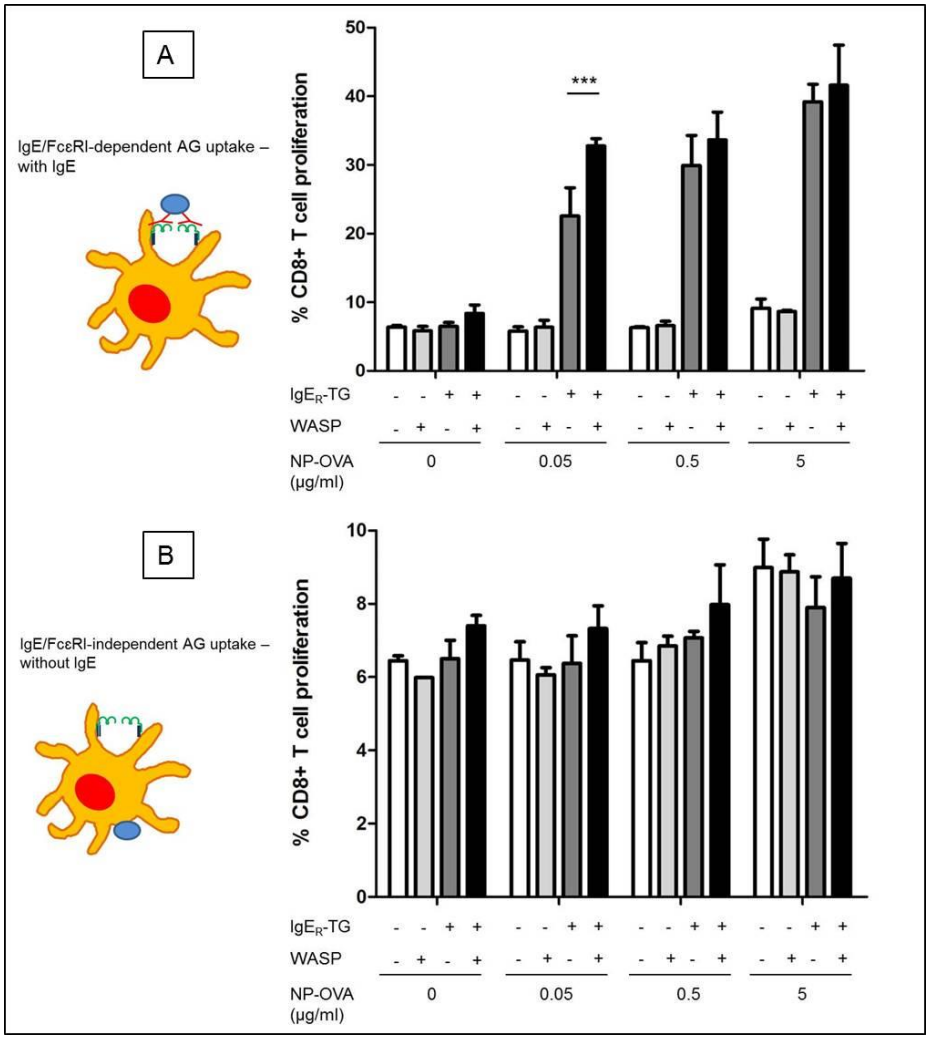

Fig.24: Comparison of the cross-presentation ability of dendritic cells isolated from IgE$_R$-TG or WT x WASP-deficient (-) or WASP-competent (+) mice determined by flow cytometric analysis.
(A) IgE/FcεRI-dependent antigen uptake: Quantification of CD8$^+$ T cell proliferation for increasing NP-OVA concentrations (0 µg/ml, 0.05 µg/ml, 0.5 µg/ml, 5 µg/ml). **(B)** IgE/FcεRI-independent antigen uptake: Quantification of CD8$^+$ T cell proliferation for increasing NP-OVA concentrations (0 µg/ml, 0.05 µg/ml, 0.5 µg/ml, 5 µg/ml).

Based on this data we concluded that WASP alters antigen uptake by DCs but seems to play a minor role in IgE-mediated cross-presentation.

The next step was to investigate the influence of WASP-deficiency on MHC class II-restricted antigen presentation. DCs of IgE$_R$-TG and WT mice that were WASP -/- or +/+ were loaded overnight with NP-specific IgE. NP-OVA was added with increasing concentrations (0.05 µg/ml, 0.5 µg/ml and 5 µg/ml). As negative control no NP-OVA was added and for positive control the MHC class II-restricted OVAp was used. DCs were co-cultured with CFSE-labelled CD4$^+$ T cells for 3 days. CD4$^+$ T cell proliferation was examined by flow cytometric analysis. Fig.25A shows the IgE/FcεRI-dependent T cell proliferation. A significant increase in proliferation was found when T cells were co-cultered

with DCs from IgE_R-TG WASP -/- mice compared to IgE_R-TG WASP +/+ mice at low NP-OVA concentrations (0.05 µg/ml and 0.5 µg/ml). A significant difference in IgE-independent proliferation was found between IgE_R-TG WASP -/- and IgE_R-TG WASP +/+ mice at a concentration of 0.5 µg/ml NP-OVA (Fig.25B).

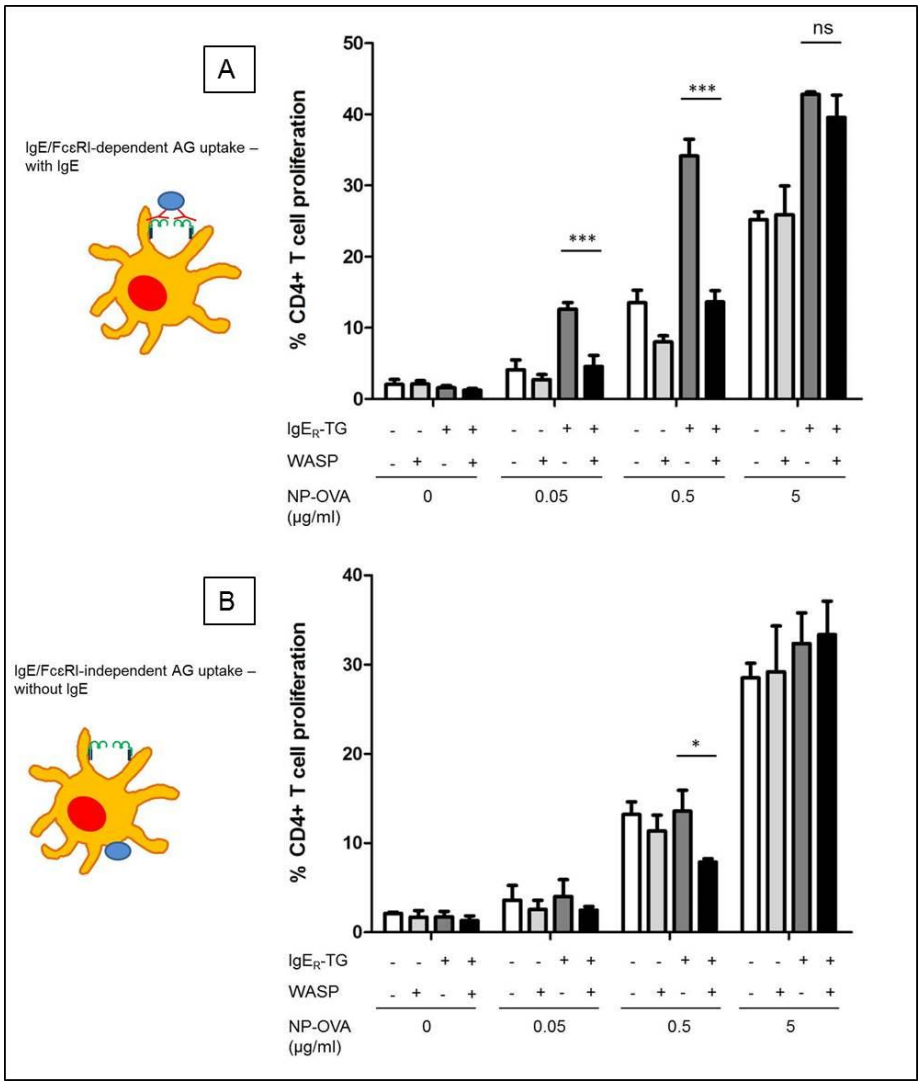

Fig.25: Comparison of the MHC class II antigen presentation ability of dendritic cells isolated from IgE_R-TG or WT x WASP KO (-) and WASP WT (+) mice.
Quantitative analysis of $CD4^+$ T cell proliferation was determined by flow cytometric analysis in an IgE-dependent experiment **(A)** and IgE-independent setup **(B).**

Supernatants were harvested to analyse IL-13 and IFN-γ production by ELISA in co-culture supernatants. While comparable IFN-γ levels were found for all groups in IgE/FcεRI-dependent and independent antigen presentation assay, IL-13 levels were slightly increased for IgE_R-TG WASP -/- mice when DCs were coated with IgE (Fig.26A and B).

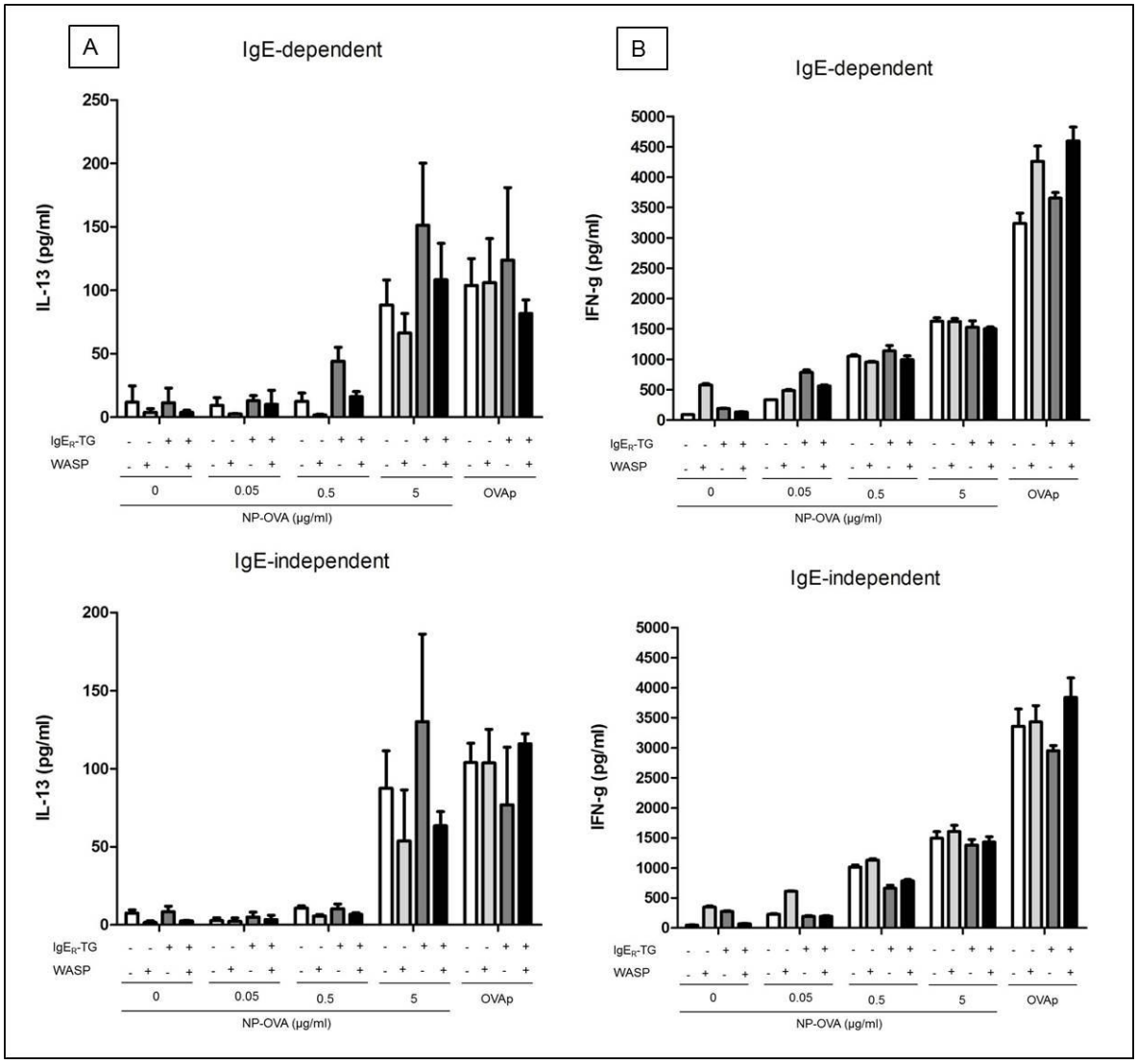

Fig.26: Cytokine levels detected in dendritic cell/T cell co-cultures during a MHC class II antigen presentation assay. Dendritic cells were isolated from IgE$_R$-TG or WT x WASP KO (-/-) or WASP WT (+/+) mice.
(A) IL-13 levels in an IgE/FcεRI-dependent (upper panel) and –independent (lower panel) antigen presentation assay. **(B)** IFN-γ levels determined in an IgE-dependent and –independent setup.

Based on these data, we concluded that WASP-deficiency might promote CD4$^+$ T cell proliferation.

3.4 Cellular activation requirements for IgE-mediated cross-presentation

Question 3: Is MyD88 required for cross-presentation as a co-stimulatory signal?

The next research question of this thesis addressed cellular activation requirements of IgE/FcεRI-mediated cross-presentation. All other known cross-presentation receptors are strictly dependent on the activation of MyD88 in form of a danger signal (e.g. LPS). Therefore we analysed if MyD88 is also essential for the IgE/FcεRI-mediated cross-presentation pathway.

To answer this research question, splenic DCs from IgE_R-TG x MyD88 KO (-/-) and IgE_R-TG x MyD88 WT (+/-) mice were isolated and its cross-presentation ability was tested in an antigen presentation assay. Prior to that, FcεRI and MyD88 expression of DCs was determined by Western Blot. Fig.27 depicts that the FcεRI expression (detected with mAb 19-1) of MyD88 -/- and +/- mice is upregulated upon IgE-incubation. Furthermore, it was confirmed that DCs from MyD88 -/- mice lack MyD88 expression.

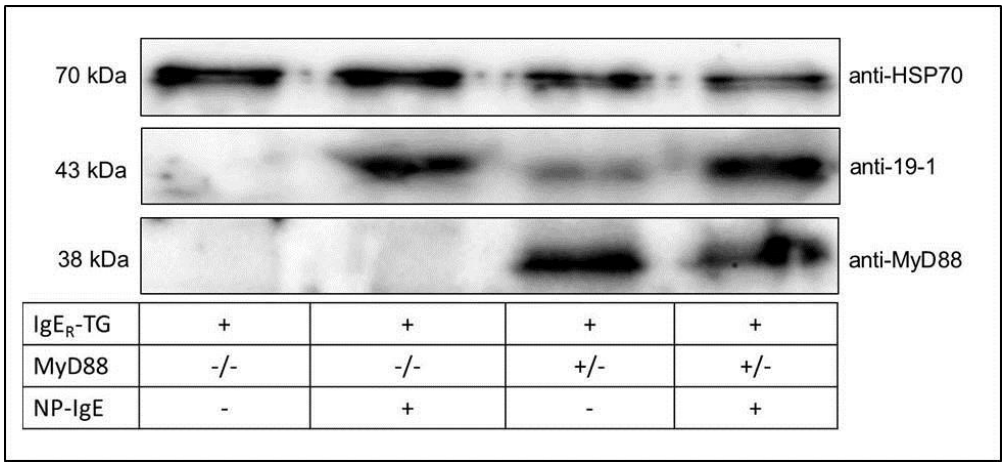

IgE_R-TG	+	+	+	+
MyD88	-/-	-/-	+/-	+/-
NP-IgE	-	+	-	+

Fig.27: Expression profile of FcεRI and MyD88 in dendritic cell lysates from IgE_R-TG x MyD88 KO (-/-) or MyD88 WT (+/-) mice detected by Western Blot.
HSP70 antibody was used as loading control. FcεRI expression was detected using a 19-1 antibody. Absence or presence of MyD88 was confirmed using a MyD88 antibody.

To investigate differences between IgE_R-TG x MyD88 -/- and +/- mice in their FcεRI expression profile or in the ability of DCs to bind IgE to their cell surface, flow cytometric analysis was performed. While the FcεRI expression was comparable in IgE_R-TG x MyD88

-/- and +/- mice (Fig.28A), the IgE-loading was slightly decreased in IgE_R-TG x MyD88 -/- mice (B).

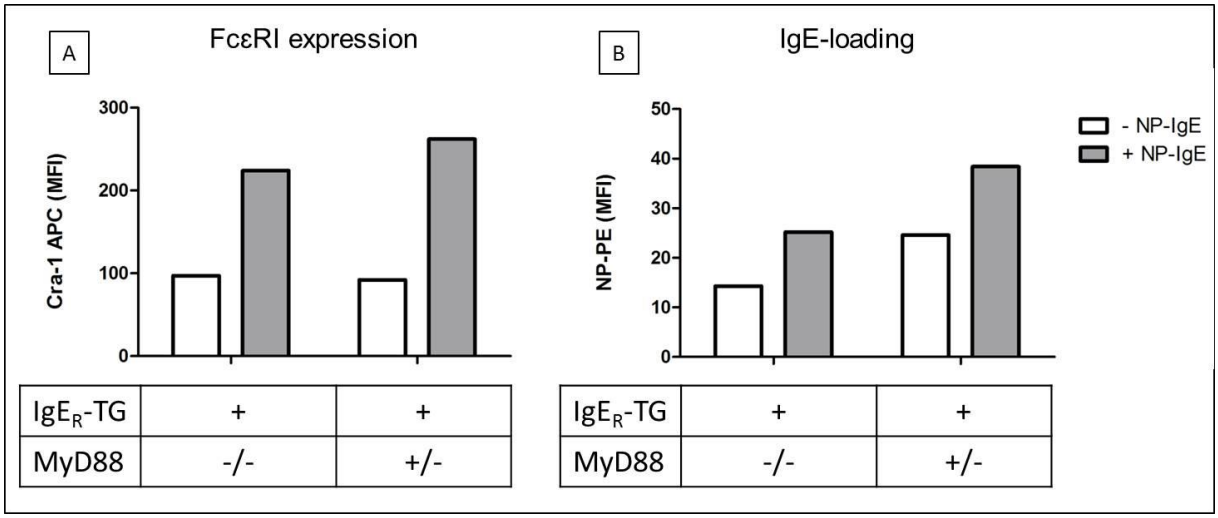

Fig.28: FcεRI expression and IgE-loading of splenic DCs isolated from IgE_R-TG x MyD88 WT (+/-) and KO (-/-) mice determined by flow cytometric analysis.
(A) FcεRI expression was detected using Cra-1 antibody. **(B)** IgE-loading was determined using fluorescently-labelled hapten NP-PE.

To compare the cross-presentation ability of DCs from IgE_R-TG x MyD88 -/- and +/- mice, an antigen cross-presentation assay was performed. DCs were incubated with 2 different NP-OVA concentrations (0.05 and 5 µg/ml) and with or without LPS. Fig.29A depicts the $CD8^+$ T cell proliferation analysed by flow cytometry. A pronounced increase in T cell proliferation was found, when DCs were loaded with NP-specific IgE. However, no differences between IgE_R-TG x MyD88 -/- and +/- animals were detected in both antigen concentrations. Addition of LPS did not enhance $CD8^+$ T cell proliferation. $CD8^+$ T cell proliferation data were confirmed by determination of IL-2 and granzyme B levels (Fig.29B and C). A modest increase in cytokine production was found with DCs from IgE_R-TG x MyD88 +/- mice.

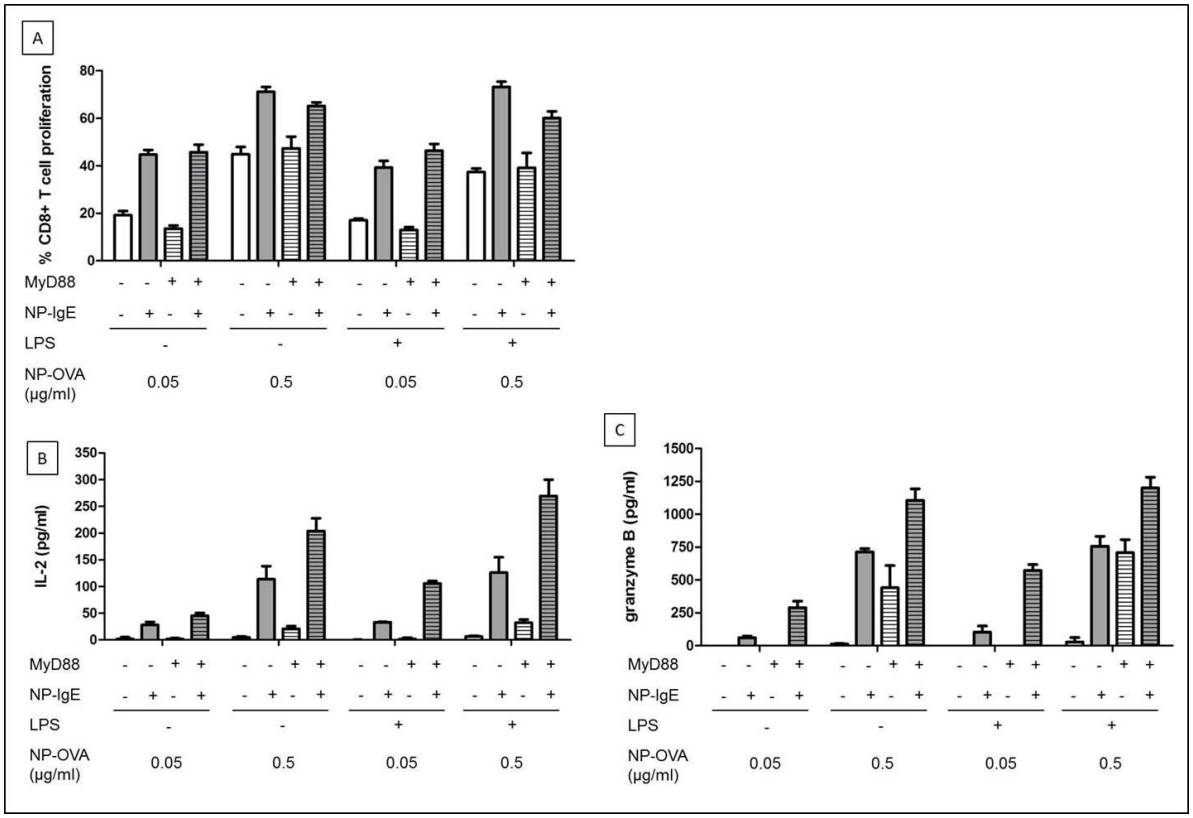

Fig.29: Comparison of the cross-presentation and cross-priming ability of dendritic cells isolated from IgE_R-TG x MyD88 KO (-) and WT (+) mice.
(A) Quantitative analysis of $CD8^+$ T cell proliferation was determined by flow cytometric analysis. **(B)** IL-2 production was determined after 24 h in supernatants of DCs and T cell co-cultures. **(C)** Granzyme B levels were determined after 3 days of co-culture.

The presented data show that the IgE/FcεRI-mediated cross-presentation pathway remained active in the absence of MyD88.

3.5 Signalling requirements for IgE-mediated cross-presentation

Question 4: Are down-stream FcεRI-signals dependent on the receptor isoform?

To investigate if signals down-stream of the trimeric FcεRI are required for cross-presentation, it is important to initially examine the signalling cascade of IgE-mediated DC activation since the trimeric receptor has not been studied in detail on DCs yet. We studied differences in down-stream signalling of the tetrameric and trimeric FcεRI, mast cells and DCs were sensitized with NP-specific IgE and cross-linked with NP-OVA for different time points (0, 5, 10 and 30 min). Mast cells were generated from the bone-marrow of HP-αTG mice. Dendritic cells were isolated from spleens of DC-αTG mice. While DCs revealed

increased levels of total SHIP-1 (Fig.30A) compared to mast cells, the phosphorylated form of SHIP-1 was substantially elevated in mast cells (Fig.30B). Total ERK1/2 levels were comparable in mast cells and DCs (Fig.30A), in contrast the expression of pERK1/2 was significantly enhanced in mast cells (Fig.30B). Degradation of pERK1/2 was found in DCs over time. Fig.30C and D show total and phosphorylated SHP-1 expression in mast cells and DCs. Interestingly, DCs showed substantially increased baseline expression levels of total (Fig.30C) and phosphorylated SHP-1 (Fig.30D) compared to mast cells.

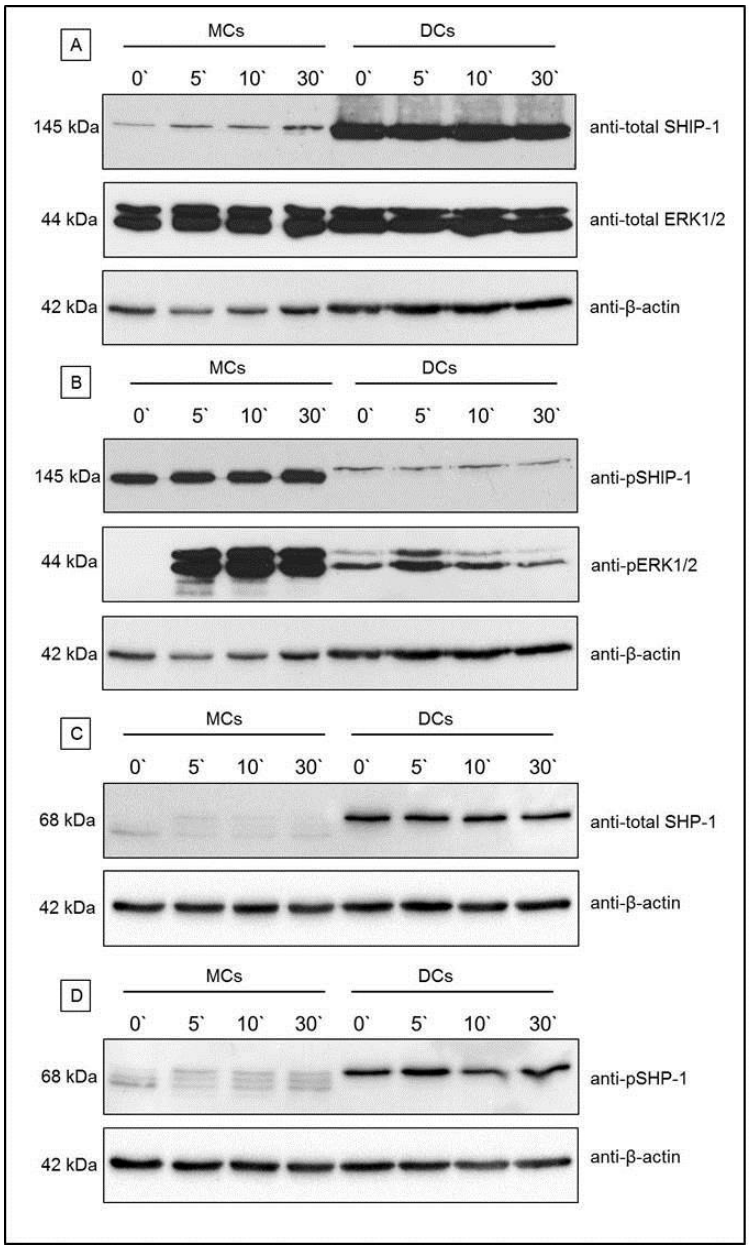

Fig.30: Comparison of down-stream signals of the tetrameric and trimeric FcεRI expressed by mast cells and dendritic cells upon receptor engagement.
Mast cells (MCs) were generated from the bone-marrow of HP-αTG mice. Dendritic cells (DCs) were isolated from spleens of DC-αTG mice. IgE-bearing MCs and DCs were incubated with NP-OVA for increasing time points (0, 5, 10 and 30 min). β-actin antibody was used as loading control. **(A)** Detection of total ERK1/2 and SHIP-1. **(B)** Detection of phosphorylated ERK1/2 (pERK1/2) and SHIP-1 (pSHIP-1). Detection of total **(C)** and phosphorylated SHP-1 (pSHP-1) **(D)**.

The presented data reveal differences in down-stream signals of the two FcεRI isoforms as expressed on mast cells or DCs.

4 Discussion

For a long time IgE antibodies were predominantly considered as key player in allergic diseases. It is important to keep in mind that elevated IgE levels do not necessarily reflect an individual`s allergic status, but can also occur in non-allergic individuals. It was only recently detected that elevated IgE titers may have beneficial effects on the prevalence of certain cancers and other malignant diseases. Significant research is done to use IgE antibodies in active and passive immunotherapeutic settings to combat cancer. [2] DCs are getting more and more in focus of cell-based vaccination strategies to fight tumor. A reason for that is that DCs are highly effective in inducing CTLs via cross-presentation. [27]

The overall aim of this thesis was based on the observation of the Fiebiger Laboratory that IgE-loaded DCs are able to engulf antigens upon FcεRI engagement and perform cross-presentation. We aimed at identifying regulatory steps in the IgE-mediated presentation pathway.

To study IgE/FcεRI-mediated antigen uptake and cross-presentation a large number of DCs is required to perform these assays. The yield of DCs per spleen is with about $1x10^6$ cells relatively small and a large number of transgenic mice would be needed. Therefore, IgE_R-TG mice were injected with B16 tumor cells that secret GM-CSF to expand the DC population *in vivo*. Our results show that *in vivo* expanded DCs express the humanized IgE receptor and can be loaded with NP-specific IgE. A modest increase in FcεRI expression and IgE-loading was detected in *in vivo* expanded DCs. A reason for the increased IgE-loading of expanded DCs that did not express the FcεRI might be an upregulation of various receptors, such as FcγRIV. FcγRIV is highly expressed by macrophages and neutrophils at steady state, but also in lower levels by DCs. It was described that this receptor is capable of binding IgE antibodies to the cell surface. [54] If this receptor also functions as an antigen uptake receptor has not yet been described but it is presumable. Furthermore, it was found that the IgE-mediated antigen presentation is less effective in expanded DCs. When looking into signalling events down-stream of the FcεRI is was found that both *in vivo* expanded and non-expanded DCs showed similar patterns of ERK1/2 phosphorylation (data not shown). Therefore we concluded that *in vivo* expanded DCs might be useful to study the trimeric FcεRI signalling pathway. However, for investigating antigen presentation, *in vivo* expanded DCs should not be used preferably.

For isolation of splenic DCs Optiprep^{TM} density gradient medium was used and compared with magnetic cell separation technology. When Optiprep^{TM} was used for the isolation, only 30% of the isolated cells were CD11c^{+} DCs. Using magnetic cell separation technology over 60% of the isolated cells were confirmed as DCs. However, the density gradient medium was established as a preparatory isolation technique, prior to the magnetic cell separation technology, to attenuate the amount of cost-intensive microbeads. Notably, the density gradient was described to be less cell activating, which might be an important factor for specific research questions.

The effect of caveolin-deficiency on antigen sampling was investigated in an antigen uptake experiment. DCs from caveolin KO mice showed a decreased difference between IgE-dependent and IgE-independent antigen uptake compared to caveolin WT mice. When we examined the absence of caveolin on the cross-presentation pathway, we detected that caveolin is not required for this pathway. On the other hand, it was described by Fattakhova et al. that inhibition of clathrin-mediated endocytosis using siRNA does not affect FcεRI cross-linking and internalization of the tetrameric complex. [38] This strongly suggests that endocytic pathways are capable of compensating and taking over the task of inhibited pathways. Furthermore, it is possible that there are other endocytic pathways for IgE/FcεRI-mediated antigen uptake that haven´t been described yet, such as flotillin-mediated endocytosis. Flotillins are small membrane proteins that can be found in lipid rafts. Flotillins participate in endocytosis, signal transduction and regulation of the cytoskeleton. However, their various functions are poorly understood. [55] It was shown by Kato and colleagues that flotillin-1 is involved in the signal transduction cascade of the tetrameric FcεRI. [56] Whether flotillin-1 plays also a role in FcεRI-mediated endocytosis by DC and or signalling of the trimeric isoform expressed by this cell type is not known.

To further define antigen uptake requirements for IgE/FcεRI-mediated cross-presentation, the influence of WASP was investigated. WASP is known to be a major player in actin rearrangement and therefore crucial for the formation of endocytic vesicles. DCs of IgE_R-TG mice that were WASP-deficient expressed substantially increased levels of the FcεRI. To address the question of elevated FcεRI expression, mRNA levels of the FcεRI were determined in these mice to investigate if this elevated expression is regulated pre- or posttranslational. FcεRI mRNA levels were similar in WASP-deficient and WASP-competent DCs, which suggests that there is a posttranslational regulation that leads to receptor stabilization on the cell surface. It might also be a consequence of impaired receptor outside-in trafficking. It could also be possible that the recycling of unbound receptors from the cell surface is affected. Usually unbound FcεRI are recycled after 24 h on the surface of mast cells.[57] WASP-deficiency might decelerate this recycling pathway.

In an antigen uptake experiment, WASP-deficient DCs showed to be more efficient in antigen sampling. A possible explanation for this finding is that an elevated FcεRI expression can translate to enhanced antigenic uptake.

When we examined the MHC class I antigen presentation assay a modest reduction of $CD8^+$ T cell proliferation was found in IgE_R-TG WASP KO mice compared to IgE_R-TG WASP-competent mice. Therefore, we concluded that WASP is not a critical regulator of IgE-mediated cross-presentation. But when we analysed MHC class II antigen presentation, a substantially increased $CD4^+$ T cell proliferation was found in IgE_R-TG WASP KO mice. An obvious reason for the enhanced proliferation might be the elevated FcεRI expression levels that were found in DCs isolated from IgE_R-TG WASP KO mice.

WASP-deficient patients suffer from various defects and show severe immune deficiencies. The reason was thought to be due to the incapability of T cells to get activated by DCs. This prevents the induction of an efficient immune response since the actin rearrangement machinery is impaired which is required for the formation of an immune synapse. [58] It was just recently discovered that WASP-deficient mice sensitize themselves spontaneously against food antigens (Lexmond et al., unpublished data) Lexmond et al. hypothesized that T cells of WASP-deficient patients are capable of inducing immune responses, however the balance between immunity and protection from immunopathology is impaired. While an ineffective Th1 population is found, the Th2 subset is overactive in these patients. This is in line with cytokine levels found during an MHC class II antigen presentation experiment. Increased levels of IL-13, but not elevated IFN-γ levels were found when T cells were co-cultures with IgE-loaded DCs from IgE_R-TG WASP KO mice. Interestingly, IFN-γ levels are usually in line with T cell proliferation, but they did not correlate in the presented MHC class II antigen presentation experiment. These results suggest that also DCs of WASP-deficient mice are more susceptible in guiding Th2 responses inducing a pro-inflammatory environment. However, this is only speculation and has to be confirmed in future experiments.

It was described that cross-presentation receptors are dependent on the presence of danger signals that activate cells via TLRs. This thesis reveals a unique feature within cross-presentation receptors which shows that IgE/FcεRI-mediated cross-presentation remains active in the absence of MyD88. Due to this finding it is hypothesized that IgE/FcεRI-mediated cross-presentation contributes to tumor-antigen surveillance at steady state. (Platzer et al., unpublished data) This is also an important aspect for the development of DC-based cancer vaccines. It was shown that IgE significantly lowers the antigenic threshold that is needed by the FcεRI to induce efficient immune responses. This is crucial, because tumor antigens usually occur in low amounts and other receptors are known to require high antigen amounts. An advantage for clinical applications would be that there is efficient cross-priming of CTLs in the absence of TLR-mediated danger

signals. The administration of further adjuvants could be avoided and would decrease risking induction of cross-tolerance. [34]

To elucidate signalling requirements for IgE/FcεRI-mediated cross-presentation, we initially investigated down-stream FcεRI signals in DCs in comparison to mast cells. Distinct signalling patterns were found in those two cell populations. A mechanistic explanation for the differences found in the signalling pathway down-stream of the tetrameric and the trimeric FcεRI might be that the trimeric FcεRI receptor lacks the β-chain. It is described that the β-chain amplifies signal for the γ-chain and therefore increases the down-stream signal. This might be the reason why a substantial increased expression of pERK1/2 was found in mast cells compared to DCs upon receptor engagement. However, it was described that mast cell express higher levels of the tetrameric FcεRI than APCs express the trimeric FcεRI. This might also explain the increased phosphorylation of ERK1/2 in mast cells. [57] Unpublished data of the host laboratory showed that there are distinct functional outcomes between mast cells and DCs. While mast cells are known as the effector cells in allergy producing allergy-promoting inflammatory cytokines, it was detected that antigen-specific FcεRI/IgE cross-linking of DCs does neither trigger maturation nor does it promote a Th2 immune response associated with the production of pro-inflammatory cytokines. These results were unexpected, but they strongly suggest that IgE and DCs might play a substantial immune regulatory role in attenuating the severity of allergic diseases. It was hypothesized that DCs comprise an alternative signalling cascade that might elucidate these differential cell properties compared to mast cells. (Platzer et al., article in press, Mucosal Immunology) Within this thesis it was detected that DCs express higher levels of total SHIP-1, but the activated form of SHIP-1 (pSHIP-1) is elevated in mast cells. SHIP-1 is known as a regulatory phosphatase and was described to associate with a phosphorylation site on the β-chain. This might be an explanation why considerable levels of pSHIP-1 were only found in mast cells. Apart from that, total and phosphorylated SHP-1 were both elevated in DCs.

Various different negative and positive regulatory mechanisms contribute to provide balanced immune responses at homeostasis throughout immune cells. On the one hand immunoreceptors can contain ITAM-motifs for cell activation, but on the other hand they can also comprise immunoreceptor tyrosine-based inhibitory motif (ITIM)-motifs that counteract cell activation. However, cell surface receptors that do not comprise ITIM-motifs are still capable of inhibiting FcεRI-signalling. [12] Recently, it was described that ITAMs are also able to transduce inhibitory signal and were therefore described at inhibitory ITAMs (ITAMi). They can activate regulatory phosphatases such as SHP-1. [59] However, this signalling molecule was only recently described as positive and negative regulator of FcεRI-signalling in mast cells. [26]

Since the FcεRI-mediated signalling casacade is clearly very complex, further research is necessary to identify signals that are required for the trimeric FcεRI complex to perform cross-presentation.

In summary, this thesis shows that the presence of caveolin is not required for IgE-mediated cross-presentation. Furthermore, it was detected that WASP is not a critical regulator of IgE-mediated cross-presentation but it induced pronounced Th cell responses in a MHC class II antigen presentation assay. It was elucidated that IgE-mediated cross-presentation is not dependent on the activation of MyD88. We could confirm that DCs and mast cells strongly differ in their down-stream FcεRI-signalling pathways.

This thesis provides significant data that define adapter proteins for IgE/FcεRI-mediated antigen presentation by DCs. However, it is beyond question that only further experiments will provide detailed insight into the regulation of IgE/FcεRI-mediated cross-presentation to improve DC-based therapies to combat cancer in humans.

Bibliography

[1] S. J. Galli and M. Tsai, “IgE and mast cells in allergic disease.,” *Nature medicine*, vol. 18, no. 5, pp. 693–704, May 2012.

[2] E. Jensen-Jarolim, G. Achatz, M. C. Turner, S. Karagiannis, F. Legrand, and M. Capron, “AllergoOncology : the role of IgE-mediated allergy in cancer,” *Allergy*, vol. 63, no. 10, pp. 1255–1266, 2008.

[3] C. Staff, C. G. M. Magnusson, M. Hojjat-Farsangi, S. Mosolits, M. Liljefors, J.-E. Frödin, B. Wahrén, H. Mellstedt, and G. J. Ullenhag, “Induction of IgM, IgA and IgE antibodies in colorectal cancer patients vaccinated with a recombinant CEA protein.,” *Journal of clinical immunology*, vol. 32, no. 4, pp. 855–65, Aug. 2012.

[4] S. L. Fu, J. Pierre, T. A. Smith-Norowitz, M. Hagler, W. Bowne, M. R. Pincus, C. M. Mueller, M. E. Zenilman, and M. H. Bluth, “Immunoglobulin E antibodies from pancreatic cancer patients mediate antibody-dependent cell-mediated cytotoxicity against pancreatic cancer cells.,” *Clinical and experimental immunology*, vol. 153, no. 3, pp. 401–9, Sep. 2008.

[5] B. Platzer, E. Dehlink, S. J. Turley, and E. Fiebiger, “How to connect an IgE-driven response with CTL activity?,” *Cancer immunology, immunotherapy : CII*, vol. 61, no. 9, pp. 1521–5, Sep. 2012.

[6] B. Platzer, F. Ruiter, J. van der Mee, and E. Fiebiger, “Soluble IgE receptors--elements of the IgE network.,” *Immunology letters*, vol. 141, no. 1, pp. 36–44, Dec. 2011.

[7] E. Dehlink, B. Platzer, A. H. Baker, J. Larosa, M. Pardo, P. Dwyer, E. H. Yen, Z. Szépfalusi, S. Nurko, and E. Fiebiger, “A soluble form of the high affinity IgE receptor, Fc-epsilon-RI, circulates in human serum.,” *PloS one*, vol. 6, no. 4, p. e19098, Jan. 2011.

[8] M. V. Kopp, “Omalizumab: Anti-IgE therapy in allergy.,” *Current allergy and asthma reports*, vol. 11, no. 2, pp. 101–6, Apr. 2011.

[9] E. Untersmayr, G. Bises, P. Starkl, C. L. Bevins, O. Scheiner, G. Boltz-Nitulescu, F. Wrba, and E. Jensen-Jarolim, “The high affinity IgE receptor Fc epsilonRI is expressed by human intestinal epithelial cells.,” *PloS one*, vol. 5, no. 2, p. e9023, Jan. 2010.

[10] J. P. Kinet, “The high-affinity IgE receptor (Fc epsilon RI): from physiology to pathology.,” *Annual review of immunology*, vol. 17, pp. 931–72, Jan. 1999.

[11] D. Maurer, C. Ebner, B. Reininger, E. Fiebiger, D. Kraft, J. P. Kinet, and G. Stingl, “The high affinity IgE receptor (Fc epsilon RI) mediates IgE-dependent allergen presentation.,” *Journal of immunology (Baltimore, Md. : 1950)*, vol. 154, no. 12, pp. 6285–90, Jun. 1995.

[12] S. Kraft and J.-P. Kinet, “New developments in FcepsilonRI regulation, function and inhibition.,” *Nature reviews. Immunology*, vol. 7, no. 5, pp. 365–78, May 2007.

[13] H. J. Gould and B. J. Sutton, “IgE in allergy and asthma today.,” *Nature reviews. Immunology*, vol. 8, no. 3, pp. 205–17, Mar. 2008.

[14] D. Maurer, C. Ebner, B. Reininger, E. Fiebiger, D. Kraft, J. P. Kinet, and G. Stingl, “The high affinity IgE receptor (Fc epsilon RI) mediates IgE-dependent allergen presentation.,” *Journal of immunology (Baltimore, Md. : 1950)*, vol. 154, no. 12, pp. 6285–90, Jun. 1995.

[15] S. Lin, C. Cicala, A. M. Scharenberg, and J. Kinet, “The Fc ♪ RI ␋ Subunit Functions as an Amplifier of Fc ♪ RI □ -Mediated Cell Activation Signals,” *Cell*, vol. 85, pp. 985–995, 1996.

[16] E. Donnadieu, S. Rana, M. F. Moffatt, E. H. Mockford, W. O. Cookson, J. Kinet, R. Drive, and O. Ox, “Competing Functions Encoded in the Allergy-Associated Fc ♪ RI ␋ Gene,” *Immunity*, vol. 18, pp. 665–674, 2003.

[17] G. Cruse, M. A. Beaven, I. Ashmole, P. Bradding, A. M. Gilfillan, and D. D. Metcalfe, “A truncated splice-variant of the FcεRIβ receptor subunit is critical for microtubule formation and degranulation in mast cells.,” *Immunity*, vol. 38, no. 5, pp. 906–17, May 2013.

[18] D. M. Cauvi, X. Tian, K. von Loehneysen, and M. W. Robertson, “Transport of the IgE receptor alpha-chain is controlled by a multicomponent intracellular retention signal.,” *The Journal of biological chemistry*, vol. 281, no. 15, pp. 10448–60, Apr. 2006.

[19] E. Fiebiger, D. Tortorella, M.-H. Jouvin, J.-P. Kinet, and H. L. Ploegh, “Cotranslational endoplasmic reticulum assembly of FcepsilonRI controls the formation of functional IgE-binding receptors.,” *The Journal of experimental medicine*, vol. 201, no. 2, pp. 267–77, Jan. 2005.

[20] E. Sallmann, B. Reininger, S. Brandt, N. Duschek, E. Hoflehner, E. Garner-Spitzer, B. Platzer, E. Dehlink, M. Hammer, M. Holcmann, H. C. Oettgen, U. Wiedermann, M. Sibilia, E. Fiebiger, A. Rot, and D. Maurer, “High-affinity IgE receptors on dendritic cells exacerbate Th2-dependent inflammation.,” *Journal of immunology (Baltimore, Md. : 1950)*, vol. 187, no. 1, pp. 164–71, Jul. 2011.

[21] D. Dombrowicz, A. T. Brini, V. Flamand, E. Hicks, J. N. Snouwaert, J. P. Kinet, and B. H. Koller, “Anaphylaxis mediated through a humanized high affinity IgE receptor.,” *Journal of immunology (Baltimore, Md. : 1950)*, vol. 157, no. 4, pp. 1645–51, Aug. 1996.

[22] J. Kalesnikoff and S. J. Galli, “New developments in mast cell biology.,” *Nature immunology*, vol. 9, no. 11, pp. 1215–23, Nov. 2008.

[23] R. P. Siraganian, “Mast cell signal transduction from the high-affinity IgE receptor.,” *Current opinion in immunology*, vol. 15, no. 6, pp. 639–46, Dec. 2003.

[24] F. Facchetti, J. K. Chan, W. Zhang, A. Tironi, M. Chilosi, S. Parolini, L. D. Notarangelo, and L. E. Samelson, “Linker for activation of T cells (LAT), a novel immunohistochemical marker for T cells, NK cells, mast cells, and megakaryocytes: evaluation in normal and pathological conditions.,” *The American journal of pathology*, vol. 154, no. 4, pp. 1037–46, Apr. 1999.

[25] M. Huber and B. F. Gibbs, “SHIP1 and the negative control of mast cell/basophil activation by supra-optimal antigen concentrations.,” *Molecular immunology*, pp. 1–6, Mar. 2014.

[26] K. Nakata, T. Yoshimaru, Y. Suzuki, T. Inoue, C. Ra, H. Yakura, and K. Mizuno, “Positive and Negative Regulation of High Affinity IgE Receptor Signaling by Src Homology Region 2 Domain-Containing Phosphatase 1,” *The Journal of Immunology*, vol. 181, no. 8, pp. 5414–5424, Oct. 2008.

[27] C. M. Fehres, W. W. J. Unger, J. J. Garcia-Vallejo, and Y. van Kooyk, “Understanding the Biology of Antigen Cross-Presentation for the Design of Vaccines Against Cancer.,” *Frontiers in immunology*, vol. 5, no. April, p. 149, Jan. 2014.

[28] B. Pulendran, H. Tang, and S. Manicassamy, “Programming dendritic cells to induce T(H)2 and tolerogenic responses.,” *Nature immunology*, vol. 11, no. 8, pp. 647–55, Aug. 2010.

[29] I. Mellman and R. M. Steinman, “Dendritic cells: specialized and regulated antigen processing machines.,” *Cell*, vol. 106, no. 3, pp. 255–8, Aug. 2001.

[30] B. M. Andersen and J. R. Ohlfest, “Increasing the efficacy of tumor cell vaccines by enhancing cross priming.,” *Cancer letters*, vol. 325, no. 2, pp. 155–64, Dec. 2012.

[31] M. V Dhodapkar, M. Sznol, B. Zhao, D. Wang, R. D. Carvajal, M. L. Keohan, E. Chuang, R. E. Sanborn, J. Lutzky, J. Powderly, H. Kluger, S. Tejwani, J. Green, V. Ramakrishna, A. Crocker, L. Vitale, M. Yellin, T. Davis, and T. Keler, “Induction of antigen-specific immunity with a vaccine targeting NY-ESO-1 to the dendritic cell receptor DEC-205.,” *Science translational medicine*, vol. 6, no. 232, p. 232ra51, Apr. 2014.

[32] B. Chatterjee, A. Smed-Sörensen, L. Cohn, C. Chalouni, R. Vandlen, B.-C. Lee, J. Widger, T. Keler, L. Delamarre, and I. Mellman, “Internalization and endosomal degradation of receptor-bound antigens regulate the efficiency of cross presentation by human dendritic cells.,” *Blood*, vol. 120, no. 10, pp. 2011–20, Sep. 2012.

[33] P. Brossart and M. J. Bevan, “Presentation of exogenous protein antigens on major histocompatibility complex class I molecules by dendritic cells: pathway of presentation and regulation by cytokines.,” *Blood*, vol. 90, no. 4, pp. 1594–9, Aug. 1997.

[34] O. P. Joffre, E. Segura, A. Savina, and S. Amigorena, “Cross-presentation by dendritic cells.,” *Nature reviews. Immunology*, vol. 12, no. 8, pp. 557–69, Aug. 2012.

[35] M.-L. Lin, Y. Zhan, J. a Villadangos, and A. M. Lew, “The cell biology of cross-presentation and the role of dendritic cell subsets.,” *Immunology and cell biology*, vol. 86, no. 4, pp. 353–62, 2008.

[36] B. Platzer, M. Stout, and E. Fiebiger, “Antigen cross-presentation of immune complexes.,” *Frontiers in immunology*, vol. 5, p. 140, Jan. 2014.

[37] E. Segura and S. Amigorena, “Cross-presentation by human dendritic cell subsets.,” *Immunology letters*, vol. 158, no. 1–2, pp. 73–78, Dec. 2013.

[38] G. Fattakhova, M. Masilamani, F. Borrego, A. M. Gilfillan, D. D. Metcalfe, and J. E. Coligan, “The high-affinity immunoglobulin-E receptor (FcepsilonRI) is endocytosed by an AP-2/clathrin-independent, dynamin-dependent mechanism.,” *Traffic (Copenhagen, Denmark)*, vol. 7, no. 6, pp. 673–85, Jun. 2006.

[39] R. Molfetta, F. Gasparrini, A. Santoni, and R. Paolini, “Ubiquitination and endocytosis of the high affinity receptor for IgE.,” *Molecular immunology*, vol. 47, no. 15, pp. 2427–34, Sep. 2010.

[40] J. S. Bonifacino and L. M. Traub, “Signals for sorting of transmembrane proteins to endosomes and lysosomes.,” *Annual review of biochemistry*, vol. 72, pp. 395–447, Jan. 2003.

[41] B. S. Wilson, J. R. Pfeiffer, and J. M. Oliver, “Observing FcepsilonRI signaling from the inside of the mast cell membrane.,” *The Journal of cell biology*, vol. 149, no. 5, pp. 1131–42, May 2000.

[42] R. Molfetta, F. Gasparrini, G. Peruzzi, L. Vian, M. Piccoli, L. Frati, A. Santoni, and R. Paolini, “Lipid raft-dependent FcepsilonRI ubiquitination regulates receptor endocytosis through the action of ubiquitin binding adaptors.,” *PloS one*, vol. 4, no. 5, p. e5604, Jan. 2009.

[43] C. Oliver, A. Fujimura, A. M. M. Silveira E Souza, R. Orlandini de Castro, R. P. Siraganian, and M. C. Jamur, “Mast cell-specific gangliosides and FcepsilonRI follow the same endocytic pathway from lipid rafts in RBL-2H3 cells.,” *The journal of histochemistry and cytochemistry : official journal of the Histochemistry Society*, vol. 55, no. 4, pp. 315–25, Apr. 2007.

[44] L. Delamarre, M. Pack, H. Chang, I. Mellman, and E. S. Trombetta, “Differential lysosomal proteolysis in antigen-presenting cells determines antigen fate.,” *Science (New York, N.Y.)*, vol. 307, no. 5715, pp. 1630–4, Mar. 2005.

[45] C. Jancic, A. Savina, C. Wasmeier, T. Tolmachova, J. El-Benna, P. M.-C. Dang, S. Pascolo, M.-A. Gougerot-Pocidalo, G. Raposo, M. C. Seabra, and S. Amigorena, “Rab27a regulates phagosomal pH and NADPH oxidase recruitment to dendritic cell phagosomes.,” *Nature cell biology*, vol. 9, no. 4, pp. 367–78, Apr. 2007.

[46] M. Weimershaus, S. Maschalidi, F. Sepulveda, B. Manoury, P. van Endert, and L. Saveanu, “Conventional dendritic cells require IRAP-Rab14 endosomes for efficient cross-presentation.,” *Journal of immunology (Baltimore, Md. : 1950)*, vol. 188, no. 4, pp. 1840–6, Feb. 2012.

[47] S. Burgdorf, C. Schölz, A. Kautz, R. Tampé, and C. Kurts, “Spatial and mechanistic separation of cross-presentation and endogenous antigen presentation.,” *Nature immunology*, vol. 9, no. 5, pp. 558–66, May 2008.

[48] J. Zhang, B. Dong, and K. a Siminovitch, “Contributions of Wiskott-Aldrich syndrome family cytoskeletal regulatory adapters to immune regulation.,” *Immunological reviews*, vol. 232, no. 1, pp. 175–94, Nov. 2009.

[49] V. I. Pivniouk, “Impaired signaling via the high-affinity IgE receptor in Wiskott-Aldrich syndrome protein-deficient mast cells,” *International Immunology*, vol. 15, no. 12, pp. 1431–1440, Dec. 2003.

[50] S. B. Snapper, F. S. Rosen, E. Mizoguchi, P. Cohen, W. Khan, C. H. Liu, T. L. Hagemann, S. P. Kwan, R. Ferrini, L. Davidson, a K. Bhan, and F. W. Alt, “Wiskott-Aldrich syndrome protein-deficient mice reveal a role for WASP in T but not B cell activation.,” *Immunity*, vol. 9, no. 1, pp. 81–91, Jul. 1998.

[51] D. D. Nguyen, M. Wurbel, J. A. Goettel, M. A. Eston, O. S. Ahmed, R. Marin, E. K. Boden, E. J. Villablanca, H. Paidassi, V. Ahuja, H.-C. Reinecker, E. Fiebiger, A. Lacy-Hulbert, B. H. Horwitz, J. R. Mora, and S. B. Snapper, “Wiskott-Aldrich syndrome protein deficiency in innate immune cells leads to mucosal immune dysregulation and colitis in mice.,” *Gastroenterology*, vol. 143, no. 3, pp. 719–29.e1–2, Sep. 2012.

[52] M. H. Maillard, V. Cotta-de-Almeida, F. Takeshima, D. D. Nguyen, P. Michetti, C. Nagler, A. K. Bhan, and S. B. Snapper, “The Wiskott-Aldrich syndrome protein is required for the function of CD4(+)CD25(+)Foxp3(+) regulatory T cells.,” *The Journal of experimental medicine*, vol. 204, no. 2, pp. 381–91, Feb. 2007.

[53] V. Cotta-de-Almeida, L. Westerberg, M. H. Maillard, D. Onaldi, H. Wachtel, P. Meelu, U. Chung, R. Xavier, F. W. Alt, and S. B. Snapper, “Wiskott Aldrich syndrome protein (WASP) and N-WASP are critical for T cell development.,” *Proceedings of the National Academy of Sciences of the United States of America*, vol. 104, no. 39, pp. 15424–9, Sep. 2007.

[54] D. A. Mancardi, B. Iannascoli, S. Hoos, P. England, M. Daëron, and P. Bruhns, “FcgammaRIV is a mouse IgE receptor that resembles macrophage FcepsilonRI in humans and promotes IgE-induced lung inflammation.,” *The Journal of clinical investigation*, vol. 118, no. 11, pp. 3738–50, Nov. 2008.

[55] G. P. Otto and B. J. Nichols, “The roles of flotillin microdomains--endocytosis and beyond.,” *Journal of cell science*, vol. 124, no. Pt 23, pp. 3933–40, Dec. 2011.

[56] N. Kato, M. Nakanishi, and N. Hirashima, “Flotillin-1 regulates IgE receptor-mediated signaling in rat basophilic leukemia (RBL-2H3) cells.,” *Journal of immunology (Baltimore, Md. : 1950)*, vol. 177, no. 1, pp. 147–54, Jul. 2006.

[57] K. D. Stone, C. Prussin, and D. D. Metcalfe, “IgE, mast cells, basophils, and eosinophils.,” *The Journal of allergy and clinical immunology*, vol. 125, no. 2 Suppl 2, pp. S73–80, Mar. 2010.

[58] O. Matalon, B. Reicher, and M. Barda-Saad, “Wiskott-Aldrich syndrome protein--dynamic regulation of actin homeostasis: from activation through function and signal termination in T lymphocytes.,” *Immunological reviews*, vol. 256, no. 1, pp. 10–29, Nov. 2013.

[59] U. Blank, P. Launay, M. Benhamou, and R. C. Monteiro, “Inhibitory ITAMs as novel regulators of immunity.,” *Immunological reviews*, vol. 232, no. 1, pp. 59–71, Nov. 2009.

List of Figures

List of Tables

List of Abbreviations

FcεRI	high affinity IgE receptor
WT	wild-type
TG	transgenic
i.v.	intravenously
RT	room temperature
DCs	dendritic cells
OVA	Ovalbumin
KO	knockout
cIgE	chimeric IgE = NP-IgE
TCR	T cell receptor
bp	base pair
h	hours
min	minutes
IBD	inflammatory bowel disease
PBMCs	peripheral blood mononuclear cells
FBS	fetal bovine serum
MHC	major histocompatibility complex
ER	endoplasmatic reticulum
mAb	monoclonal antibody

A: List of Materials

Materials	Company	Productnumber
6-well Suspension cell culture plate	Greiner bio-one	657185
5 ml syringe Luer-Lok Tip	BD	309646
1 ml syringe Luer-Lok Tip	BD	309659
Precision Glide Needle 25G 5/8	BD	303010
Precision Glide Needle 27G 1/2	BD	305109
Cell strainer 70µm	BD Falcon	352350
Manual cell separation columns MS	Miltenyi Biotec	130-042-201
Manual cell separation columns LS	Miltenyi Biotec	130-042-401
PVDF membrane, 0.45 µm	Thermo Scientific	88518
Gel Blot Paper 7x10 cm	Whatman	GB004
Thermal cycling tubes, 0.2 ml cap strips, 0.2 ml tubes	Denville Scientific Inc	C18098-7
96 Well Clear Round Bottom TC-Treated Microplate	Corning	3799
EIA/RIA plate, 96-well, flat bottom	Corning Incorporated	9018
SealPlate	Excel Scientific	12-167
RNeasy Plus Mini Kit	Qiagen	74136
QIAshredder	Qiagen	79656
Multiplate™ PCR Plates, 96-well, clear	Bio-Rad	MLP 9601
Microseal ® ´B`Adhesive Seals	Bio-Rad	MSB 2001
Petri dishes, 100x200mm Style	BD Falcon	353003
Antibodies		
NP-IgE (hapten-specific chimeric human IgE anti- 4-hydroxy-3-nitrophenylacetyl)	derived from Jw 8/5/13 cells	
WB antibodies	**Company**	**Productnumber**
β-Actin Antibody	Cell Signaling Technology	4967
caveolin-1 (clone N-20)	Santa Cruz Biotechnology	sc-894
goat anti rabbit HRP-conjugated (10µg/ml)	Pierce	1858415
goat anti mouse HRP-conjugated (10µg/ml)	Pierce	1858413
Mitochondrial Heat Shock Protein 70 (Hsp 70)	Thermo Scientific	MA3-028
Mouse/Rat MyD88 Affinity purified polyclonal antibody	R&D Systems	AF3109
mAb 19-1	provided by Dr. JP Kinet (Laboratory of Allergy and Immunology, Beth Israel Deaconess Medical Center, Boston,	

	MA)	
Phospho-p44/42 MAPK (Erk1/2) (Thr202/Tyr204) Antibody	Cell Signaling Technology	9101
p44/42 MAPK (Erk1/2) (137F5) Rabbit mAb	Cell Signaling Technology	4695
Phospho-SHP-1 (Tyr564) (D11G5) Rabbit mAb	Cell Signaling Technology	8849
SHP-1 (C14H6) Rabbit mAb	Cell Signaling Technology	3759
Phospho-SHIP1 (Tyr1020) Antibody	Cell Signaling Technology	3941
SHIP1 (D1163)	Cell Signaling Technology	2728
FACS antibodies	**Company**	**Productnumber**
rat anti mouse CD86 PE	BD Pharmingen	553692
anti hu FcERIa Alexa Fluor 647	BioLegend	334614
anti mouse CD11c Pacific Blue	BioLegend	117322
anti mouse CD11c APC	BioLegend	117310
purified rat anti mouse CD16/32 Fc-Block	BD Pharmingen	553142
NP(7)-PE	Bioresearch Technologies	N-5070-1
PE/Cy7 anti mouse CD3ε	BioLegend	100320
anti mouse CD8a Alexa Fluor 647	BioLegend	100724
CellTrace CFSE Cell Proliferation Kit	Life Technologies	C34554
PE/Cy7 anti mouse CD8a	BioLegend	100722
APC/Cy7 anti mouse I-A/I-E (MHC II)	BioLegend	107627
PE anti mouse IgE	BioLegend	406908
anti mouse FcERI APC (Mar-1)	eBioscience	17-5898-22
PE/Cy7 anti human FcERIα (Cra-1)	BioLegend	334619
PE anti mouse CD64 (FcγRI)	BioLegend	139303
APC/Cy7 anti mouse/human CD11b	BioLegend	101225
PE anti mouse PDCA-1 (CD317)	eBioscience	12-3172-82
anti mouse CD19 PE/Cy7	eBioscience	25-0193-81
ELISA antibodies/kits	**Company**	**Productnumber**
EIA/RIA plate, 96 well, flat bottom	Corning Incorporated	9018
Mouse IL-2 ELISA Ready-SET-Go!	eBioscience	88-7024-88
Mouse Granzyme B ELISA Ready-SET-Go!	eBioscience	88-8022-88
Mouse IL-13 ELISA Ready-SET-Go!	eBioscience	88-7137-88
Mouse IFN-γ ELISA Ready-SET-Go!	eBioscience	88-7314-86
Mouse CCL-2 (MCP-1) ELISA Ready-SET-Go!	eBioscience	88-7391-86
Reagents	**Company**	**Productnumber**
SuperSignal West Femto Maximum	Thermo Scientific	34095

Sensitivity Substrate		
SuperSignal West Pico Chemiluminescent Substrate	Thermo Scientific	34077
ProtoGel 30% (w/v) acrylamide/methylene bisacrylamide solution	National Diagnostics	EC-890
ProtoGel Stacking Buffer	National Diagnostics	EC-893
4x ProtoGel Resolving Buffer	National Diagnostics	EC-892
TEMED	Bio-Rad	161-0800
PageRuler Plus Prestained Protein Ladder 10-250K	Thermo Scientific	26619
2x Laemmli sample buffer	Bio-Rad	161-0737
2-mercaptoethanol	Sigma-Aldrich	M6250
1x RBC Lysis Buffer	eBioscience	00-4333-57
Collagenase D	Roche	11088882001
Collagenase VIII	Sigma	C2139
5x Phire Reaction Buffer	Thermo Scientific	F-524
Ultrapure Distilled Water	Invitrogen	10977-015
dNTP Mix 2mM	Thermo Scientific	RO241
Phire Hot Start II DNA Polymerase	Thermo Scientific	F-122S
Proteinase K	Thermo Scientific	EOO491
Agarose GPG/LE	American Bioanalytical	AB00972-00500
100bp DNA ladder	New England Biolabs	N3231L
Gel Loading Dye Blue (6x)	New England Biolabs	B7021S
UltraPure 10mg/ml Ethidium Bromide	Invitrogen	15585-011
Trypsin-EDTA 0.05%	Life Technologies	25300
RPMI	Life Technologies	11875-093
DMEM	Life Technologies	11965-092
PBS pH7.2 (1x)	Life Technologies	20012-027
Casy Ton	Roche	5651808001
HI FBS	Invitrogen	10438-026
Penicillin Streptomycin	Invitrogen	15070-063
L-Glutamin 200mM	Invitrogen	25030-081
Albumin from bovine serum	Sigma	A4503
SureBlue TMB Microwell Peroxidase Substrate	KPL	52-00-03
Ovalbumin, Alexa Fluor® 647, Conjugate	Life Technologies	O34784
OVA peptide (SIINFEKL, aa 257-264)	AnaSpec Inc.	60193-1
OVA peptide (aa 323-339)	AnaSpec Inc.	62571-5
CD11c microbeads, mouse	Miltenyi Biotec	130-052-001
$CD8a^+$ T cell Isolation Kit II, mouse	Miltenyi Biotec	130-095-236
$CD4^+$ T cells isolation Kit II, mouse	Miltenyi Biotec	130-095-248
iScript™ Reverse Transcription Supermix for RT-qPCR	Bio-Rad	170-8841
SYBR® Select Master Mix	Applied Biosystems	4472920
NP-OVA	Biosearch Technologies Inc.	N-5051-10

RIPA Lysis Buffer System	Santa Cruz Biotechnologies	sc-24948
Protease Inhibitor Cocktail	Roche	11697498001
Phosphatase Inhibitor Cocktail B	Santa Cruz	sc-45045
Fix & Perm Medium A	Invitrogen	GAS001S100
Running buffer 10x	Santa Cruz Biotechnologies	sc-24949
10x Transfer buffer	National Diagnostics	EC-880
OptiPrep density gradient medium	Sigma	D1556
Recombinant murine IL-3	Peprotech	213-13
Stem cell factor	provided by Dr. M. F. Gurish (Brigham and Woman`s Hospital, Boston, MA)	
Cell lines	**Medium**	**Company**
Jw 8/5/13 (clone JW8/1)	RPMI, 10% FBS, 1% Pen/Strep, 1% L-Glut	provided by Dr. D. Maurer (Medical University of Vienna, Vienna, Austria)
B16 GM-CSF	DMEM, 10% FBS, 1% Pen/Strep, 1% L-Glut	provided by Dr. S. Turley (Dana-Farber Cancer Institute, Boston, MA)
Mice		
CD11c-αTG (C57BL/6N)	received from Dr. D. Maurer (Medical University of Vienna, Vienna, Austria)	
mu_{α}-KO	received from Dr. JP. Kinet (Laboratory of Allergy and Immunology, Beth Israel Deaconess Medical Center, Boston, MA)	
HP-αTG	received from Dr. JP Kinet (Laboratory of Allergy and Immunology, Beth Israel Deaconess Medical Center, Boston,	

	MA)	
OT-I (C57BL/6-Tg (TcraTcrb)1100Mjb/J)	The Jackson Laboratory	003831
OT-II (B6.Cg-Tg (TcraTcrb)425Cbn/J)	The Jackson Laboratory	004194
Caveolin knockout (C57BL/6N)	The Jackson Laboratory	004585
MyD88 knockout (C57BL/6N)	received from the Blumberg Laboratory (Brigham and Women´s Hospital, Boston, MA)	
WASP KO	received from Snapper Laboratory (Boston Children`s Hospital, Boston, MA)	

Primer #	**Primer**	**Sequence 5` to 3`**
Cav-/- #1 IgE_R-TG #3	oIMR 1972	GTG TAT GAC GCG CAC ACC AAG
Cav-/- #2	oIMR 1973	CTA GTG AGA CGT GCT ACT TCC
Cav-/- #3 IgE_R-TG #4	oIMR 1974	CTT GAG TTC TGT TAG CCC AG
IgE_R-TG #1	EGFP#5	CAC ATG AAG CAG CAC GAC TT
IgE_R-TG #2	EGFP#6	ACT GGG TGC TCA GGT AGT GG
MyD88 #1	MyD88 forward	TGG CAT GCC TCC ATC ATA GTT AAC C
MyD88 #2	MyD88 reverse	GTC AGA AAC AAC CAC CAC CAT GC
MyD88 #3	MyD88 neo	ATC GCC TTC TAT CGC CTT CTT GAC G
OT-I Tcra #1	oIMR 1321	CAG CAG CAG GTG AGA CAA AGT
OT-I Tcra #2	oIMR 1322	GGC TTT ATA ATT AGC TTG GTC C
OT-I Tcra #3	oIMR 8744	CAA ATG TTG CTT GTC TGG TG
OT-I Tcra #4	oIMR 8745	GTC AGT CGA GTG CAC AGT TT
OT-I Tcrb #1	oIMR 0675	AAG GTG GAG AGA GAC AAA GGA TTC
OT-I Tcrb #2	oIMR 0676	TTG AGA GCT GTC TCC
OT-I Tcrb #3	oIMR 8744	CAA ATG TTG CTT GTC TGG TG
OT-I Tcrb #4	oIMR 8745	GTC AGT CGA GTG CAC AGT TT
mu_α-KO #1	FcεRIα FOR2	TCC GTA TCC CCA ATG TAG TGA
mu_α-KO #2	FcεRIα REV3	TAG ATC ACC TTG CGG ACA TTC
mu_α-KO #3	PGK Neo	GGG CCA GCT CAT TCC TCC GAC TCA
HP-αTG #1	H.P. Alpha FOR	GCT CCA GAT GGC GTG TTA GC
HP-αTG #2	H.P. Alpha REV	TCC AGA AAG TAG TGA GAG GC
WASP #1	WASP Neo	ACC GCT TCC TCG TGC TTT AC
WASP #2	WASP FOR	ATC ACC TGC GCG TTC ATT CTT CA
WASP #3	WASP REV	CAC CGC TCT GTA GGC CTT GTT TAG
OT-II Tcra #1	oIMR1880	AAA GGG AGA AAA AGC TCT CC
OT-II Tcra #2	oIMR1881	ACA CAG CAG GTT CTG GGT TC

OT-II Tcrb#1	oIMR1825	GCT GCT GCA CAG ACC TAC T
OT-II Tcrb#2	oIMR1826	CAG CTC ACC TAA CAC GAG GA
Hu FcεRI forward		GTT CTT CGC TCC AGA TGG C
Hu FcεRI reverse		TTG TGG AAC CAT TTG GTG GAA

B: List of Buffers

Digestion buffer
5 ml 1 M Tris pH8
40 µl 5 M NaCl
2 ml 0.5 M EDTA pH8
10 ml 10% SDS
82.96 ml millipure H_2O

50x TAE buffer (for 1 L)
252 g Tris base
57.1 ml Glacial Acetic Acid
100 ml 0.5 M EDTA

10x TBS buffer (for 1L)
60.75 g Tris base
87.80 g NaCl
adjust pH to 7.4

10x PBS (for 2L)
4 g KCl
160 g NaCl
23 g Na_2HPO_4 * $7H_2O$
1.14 g KH_2PO_4
adjust pH to 7.4

MACS buffer
500 ml PBS sterile
2.5 ml FBS
2 mM EDTA

DC buffer pH 7.2 (for 200 ml, sterile filter)
1.76 g NaCl
0.4 ml 0.5 M EDTA
2 ml 1 M Hepes
1 ml FBS
adjust pH to 7.2